DEPARTMENT OF MATHEMATICS

SHOCK FITTING FOR THE 2D EULER EQUATIONS

Peter D. Arnold

Numerical Analysis Report 16/91

UNIVERSITY OF READING

SHOCK FITTING FOR THE 2D EULER EQUATIONS

Peter D. Arnold

Numerical Analysis Report No. 16/91

The work reported here forms part of the research programme of the Institute for Computational Fluid Dynamics at Oxford and Reading, and was carried out with the support of R.A.E. Farnborough under Contract Number DER/1/9/4/2035/065//XR/AERO.

CONTENTS

		Page Number
	INTRODUCTION	1
	CHAPTER 1 THE RANKINE HUGONIOT EQUATIONS	
1.1	Derivation of Rankine Hugoniot equations	3
1.2	Simplification of the Rankine Hugoniot equations	5
1.3	A case of mistaken shock speed	7
1.4	Calculation of the shock speed	10
	CHAPTER 2 SHOCK FITTING METHODS	
2.1	Capturing a fitted shock	13
2.2	Flux splitting via Roe's scheme in one direction, next to shock	19
2.3	Residual calculation on a moving grid	20
2.4	Driving the shock speeds to zero	21
2.5	The addition of real viscosity to the shock tip region	22
2.6	Methods for approximating the shock shape and/or angle	25
	CHAPTER 3 RESULTS AND DISCUSSION	
3.1	Assessment of real viscosity around shock tip	29
3.2	Assessment of driving the shock speeds to zero	29
3.3	Assessment of use of 1D flux splitting via Roe's scheme around shock, and methods of capturing a fitted shock	30
3.4	Assessment of use of residual calculation on a moving grid	34
3.5	Assessment of methods for approximating shock angles	35
3.6	Assessment of the effect of grid refinement on shock captured and fitted solutions	38

CHAPTER 4
CONCLUSIONS 43

Acknowledgements 46

References 47

Appendix 1 48

Appendix 2 54

Figures

Tables

Plots

INTRODUCTION

In the early 1980's a need was identified at R.A.E. Farnborough for a method capable of dealing with embedded shocks which was free of emperical tunning parameters, and could accurately confine a shock on an aerofoil to within a very narrow region as opposed to smearing shocks over a few mesh cells as was the case with shock capturing methods. Shock fitting was then earmarked for research and development work, and the first codes were produced by Albone [1] in about 1985. Morton and Paisley [2] then continued this work up to 1987 resulting in a code which was tested against a fine grid captured solution produced by Pulliam and Barton [3] and compared with Hall's [4] shock capturing code. The shock fitting code however was not and is still (in 1991) not entirely robust, and artificial restraints were required to prevent instability. For two years since 1987 analytical work was carried out on shock tip structure by Samuels [5] under an R.A.E. contract, and the contract was then extended for a further two years in which further research and development work was carried out by myself. This, the second in this series of reports, gives details of the work done since October 1990.

Within the aerospace community, shock fitting is unfashionable at present, the emphasis being directed at conservative finite volume and flux splitting shock capturing schemes. Whilst good results have been obtained with these methods, they are not capable of capturing a shock over the very narrow regions (typical shock width is 10^{-5}mm) required to predict shockwave/boundary layer interactions, and it is here that shock fitting holds the most promise.

This report is divided up into 4 chapters. The first deals with the

Rankine Hugoniot equations, their derivation, simplification and solution, and is probably the best starting point for the reader, as the concept of conservation of mass, and momentum through stationary and moving cells is a theme which is carried right through this work. The second chapter deals with the shock fitting methods which have been tried. Some of them were successful, others not. The failures are logged here to prevent other researchers repeating the same work. The most important sections of Chapter 2 are Section [2.1] which formulates an internal flux splitting method based on Roe's approximate Riemann solver for a moving cell of zero width across which conservation is ensured, i.e. a shock. Also Section [2.6] looks at various methods of approximating the shocks shape and/or angle which influence the stability of shock fitting. Section [2.4] is also important, not for the method used, but because of the implications that the differential forms of the Rankine Hugoniot conditions have for shock fitting schemes. Chapter 3 contains all the results obtained by using the methods described in Chapter 2 and discusses them, including plots of residuals obtained using shock capturing and fitting on three increasingly finer grids for the captured solution and two for the fitted. Chapter 4 draws conclusions and summarizes the state the work is in at present.

CHAPTER 1

THE RANKINE HUGONIOT EQUATIONS

1.1 DERIVATION OF RANKINE HUGONIOT (R-H) EQUATIONS

Let us begin by assuming our fluid obeys the 2D conservation law.

$$\frac{\partial \underline{u}}{\partial t} + \frac{\partial \underline{F}}{\partial x} + \frac{\partial \underline{G}}{\partial y} = \underline{0}$$

where $\underline{u}$, $\underline{F}$, and $\underline{G}$ are all vector differentiable functions of x, y and t.

Consider an infinitesimal volume moving through the fluid in a direction aligned to the x axis with velocity S.

Then
$$\frac{d\underline{u}}{dt} + \frac{\partial \underline{F}}{\partial x} + \frac{\partial \underline{G}}{\partial y} - S\frac{\partial \underline{u}}{\partial x} = \underline{0}$$

and therefore
$$\int_{y_1}^{y_2}\int_{x_1}^{x_2}\left[\frac{d\underline{u}}{dt} + \frac{\partial \underline{F}}{\partial x} + \frac{\partial \underline{G}}{\partial y} - S\frac{\partial \underline{u}}{\partial x}\right]dxdy = \underline{0}$$

over any volume

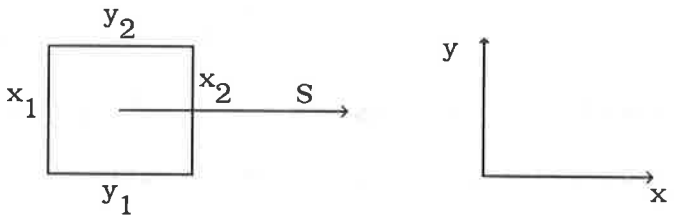

Now if we compress our volume so that $\Delta x \longrightarrow 0$ then

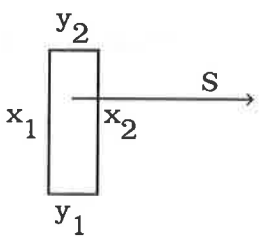

$$\int_{x_1}^{x_2}\int_{y_1}^{y_2}\frac{\partial \underline{G}}{\partial y}\,dydx = \int_{x_1}^{x_2}\left[G(x,y_2,t) - G(x,y_1,t)\right]dx \longrightarrow 0$$

leaving $$\int_{y_1}^{y_2}\int_{x_1}^{x_2}\left[\frac{d\underline{u}}{dt}+\frac{\partial \underline{F}}{\partial x}-S\frac{\partial \underline{u}}{\partial x}\right]dxdy = \underline{0}\ .$$

If the motion is locally steady in the moving frame $\frac{d\underline{u}}{dt}=\underline{0}$ over the entire volume, and then integrating with respect to x gives

$$\int_{y_1}^{y_2}\left[\underline{F}(x_2,y,t)-\underline{F}(x_1,y,t)-S\left[\underline{u}(x_2,y,t)-\underline{u}(x_1,y,t)\right]\right]dy = \underline{0}\ .$$

Since this must hold for any interval (y_1,y_2) then

$$\Rightarrow \quad \underline{F}(x_2,y,t)-F(x_1,y,t)-S\left[u(x_2,y,t)-u(x_1,y,t)\right] = 0$$

where $\underline{F}$ and $\underline{u}$ are no longer required to be differentiable with respect to x.

Hence

$$[\underline{u}]S = [\underline{F}] \qquad \text{where} \quad \underline{u} = \begin{vmatrix}\rho\\ \rho q^N\\ \rho q^T\end{vmatrix}\ ,\quad \underline{F} = \begin{vmatrix}\rho q^N\\ \rho q^{N^2}+P\\ \rho q^N q^T\end{vmatrix}$$

ρ is the density, P is pressure, and q^N, q^T are the velocities normal and tangential (previously the x and y directions) to the cell with speed S.

A shock in the flow field can be thought of as an infinitely compressed cell, across which $\underline{F}$ and $\underline{u}$ may be discontinuous, and within it $\frac{d\underline{u}}{dt}=\underline{0}$, so that the imbalance in the fluxes ($\underline{F}$ vector) is exactly off-set by the shock's movement through the fluid, and the shock speed S obeys

$$[\underline{u}]S = [\underline{F}]\ .$$

1.2 SIMPLIFICATION OF THE RANKINE HUGONIOT (R-H) EQUATIONS

Written in full, the Rankine Hugoniot (R-H) equations are:

$$S = \left[\rho^R q^{NR} - \rho^L q^{NL}\right] / \left[\rho^R - \rho^L\right] \tag{1}$$

$$S = \left[(\rho^R q^{NR^2} + P^R) - (\rho^L q^{NL^2} + P^L)\right] / \left[\rho^R q^{NR} - \rho^L q^{NL}\right] \tag{2}$$

$$S = \left[\rho^R q^{NR} q^{TR} - \rho^L q^{NL} q^{TL}\right] / \left[\rho^R q^{TR} - \rho^L q^{TL}\right] \tag{3}$$

where $$P = \frac{\rho}{\gamma}\left[1 - \frac{(\gamma-1)}{2}\left[q^{N^2} + q^{T^2}\right]\right]$$

and the superfixes L and R refer to the states immediately to the left and to the right of the shock. The denominators in each case are assumed to be non-zero. Equation (3) can be simplified as follows. Since

$$(1) \implies S(\rho^R - \rho^L) = \rho^R q^{NR} - \rho^L q^{NL}$$

$$(2) \implies S(\rho^R q^{TR} - \rho^L q^{TL}) = \rho^R q^{NR} q^{TR} - \rho^L q^{NL} q^{TL}$$

then

$$(3) - (1) \times q^{TR} = S\rho^R q^{TR} - S\rho^L q^{TL} - S\rho^R q^{TR} + S\rho^L q^{TR}$$

$$= \rho^R q^{NR} q^{TR} - \rho^L q^{NL} q^{TL} - \rho^R q^{NR} q^{TR} + \rho^L q^{NL} q^{TR}$$

So $$S\rho^L(q^{TR} - q^{TL}) = \rho^L q^{NL}(q^{TR} - q^{TL}) .$$

Therefore $S(q^{TR} - q^{TL}) = q^{NL}(q^{TR} - q^{TL})$.

Thus if $S \neq q^{NL}$ $\underset{\sim}{q^{TR} = q^{TL}}$.

If $S = q^{NL}$, then, using equations (1), (2) and (3), it can be shown that either $\underline{u}^L = \underline{u}^R \Longrightarrow q^{TR} = q^{TL}$ or $q^{NL} = q^{NR}$, $P^R = P^L$, $\rho^R \neq \rho^L$ and $q^{TR} \neq q^{TL}$. The last case is in fact a contact discontinuity, where there is no flow across the discontinuity. If $\underline{u}^L = \underline{u}^R$, then no discontinuity is present.

If we are not concerned with contact discontinuities, then we can safely assume that the tangential component of the flow is conserved across the shock, i.e. $q^{TR} = q^{TL}$ can be used to replace equation (3).

1.3 A CASE OF MISTAKEN SHOCK SPEED

The calculation of the shock speed S was based upon the Rankine Hugoniot (R-H) equations for two-dimensional inviscid flow, including an energy equation.

Hence $\frac{\partial \underline{u}}{\partial t} + \frac{\partial \underline{F}}{\partial x} + \frac{\partial \underline{G}}{\partial y} = 0$, where

$$\underline{u} = \begin{vmatrix} \rho \\ \rho u \\ \rho v \\ \rho E \end{vmatrix} , \quad \underline{F} = \begin{vmatrix} \rho u \\ \rho u^2 + P \\ \rho uv \\ \rho u[E+P/e] \end{vmatrix} , \quad \underline{G} = \begin{vmatrix} \rho v \\ \rho uv \\ \rho v^2 + P \\ \rho v[E+P/e] \end{vmatrix}$$

and an equation of state

$$E = \frac{P}{\rho(\gamma-1)} + \frac{1}{2}(u^2 + v^2) .$$

We also have

$$[\underline{u}]S = [\underline{F}]$$

(the R-H equations, where u, v are velocity components normal and tangential to the shock respectively).

These equations can be manipulated to give an alternative form of the R-H equations (see Appendix 1) which are identical to those found in Paisley [Ref 2].

$$v_1 = v_2$$

$$\rho_2/\rho_1 = \frac{(\gamma+1)M_1^2}{(\gamma-1)M_1^2 + 2}$$

$$\rho_2/\rho_1 = \frac{u_1 - S}{u_2 - S}$$

where $M_1 = \frac{u_1 - S}{C_1}$ and $C_1^2 = \frac{\gamma P_1}{\rho_1}$, and $1 \equiv L$, $2 \equiv R$.

However, the model we are using in the present work is based upon the Euler H system [8], which assumes that the enthalpy H is constant throughout the entire flow field, where

$$H = E + P/\rho \ .$$

Now the fourth component of the R-H equations for the full Euler system is

$$S = \frac{\rho_1 u_1 [E_1 + P_1/\rho_1] - \rho_2 u_2 [E_2 + P_2/\rho_2]}{\rho_1 E_1 - \rho_2 E_2}$$

$$\Rightarrow \qquad \rho_1 E_1 [u_1 - S] + \rho_1 u_1 \, P_1/\rho_1 = \rho_2 E_2 [u_2 - S] + \rho_2 u_2 \, P_2/\rho_2$$

$$\Rightarrow \qquad E_1 + \frac{\rho_1 u_1 \, P_1/\rho_1}{\rho_1 (u_1 - S)} = E_2 + \frac{\rho_2 u_2 \, P_2/\rho_2}{\rho_1 (u_1 - S)}$$

$$\Rightarrow \qquad E_1 + P_{1/\rho_1} = E_2 + \frac{\rho_2 u_2 \, P_2/\rho_2 - \rho_1 u_1 \, P_1/\rho_1}{\rho_1 (u_1 - S)} + P_{1/\rho_1}$$

$$\Rightarrow \qquad E_1 + P_{1/\rho_1} = E_2 + \frac{\rho_2 u_2 \, P_2/\rho_2 - \rho_1 \, S \, P_1/\rho_1}{\rho_1 (u_1 - S)} \ .$$

Hence $E_1 + P_1/\rho_1$ can only equal $E_2 + P_2/\rho_2$ if

$$\rho_1 S \, P_1/\rho_1 = \rho_2 \, S \, P_2/\rho_2 \quad \Rightarrow \quad S = 0 \quad \text{or} \quad P_1 = P_2 \ .$$

Therefore, we deduce that enthalpy is equal on either side of a shock when $S = 0$, or $P_1 = P_2$. But our model ensures that enthalpy is constant everywhere.

The two viewpoints are inconsistent, and the result is a shock speed which is inconsistent with all of the R-H equations. In fact, the value of S given above is used to calculate the normal velocity on the downstream side of the shock, u_2, via the mass R-H equation. When this value of u_2 is put into the momentum R-H equation a completely different shock speed is produced.

A correct formulation of the shock speed calculation which is consistent with all three R-H equations is given in Section [1.4].

1.4 CALCULATION OF THE SHOCK SPEED

In order to calculate the shock speed we must satisfy our simplified R-H equations (1), (2) and (3) (see §1.2). These can be considered as three nonlinear equations in seven unknowns, ρ^L, q^{NL}, q^{TL}, ρ^R, q^{NR}, q^{TR} and S. To match the number of unknowns with the number of equations it is necessary to specify four of the unknowns. Using the eigenvalues of the matrix $\partial \underline{F}'/\partial \underline{u}'$ (where $\underline{u}'$ is orientated with the shock) as a guide, we update all three quantities on the upstream side, ρ^L, q^{NL}, q^{TL}, and one quantity on the downstream side ρ^R. Here we must now arrange the R-H equations so that we can solve explicitly for S using these known quantities.

Firstly, in equation (2) we expand $\left[\rho^R q^{NR^2} + P^R\right] - \left[\rho^L q^{NL^2} + P^L\right]$ to form

$$\frac{1}{\gamma}\left[\rho^R - \rho^L\right] + \left[\frac{\gamma+1}{2\gamma}\right]\left[\rho^R q^{NR^2} - \rho^L q^{NL^2}\right] + \left[\frac{1-\gamma}{2\gamma}\right]\left[\rho^R q^{TR^2} - \rho^L q^{TL^2}\right]$$

so that equation (2) now becomes

$$S = \frac{\frac{1}{\gamma}\left[\rho^R - \rho^L\right) + \left[\frac{\gamma+1}{2\gamma}\right]\left[\rho^R q^{NR^2} - \rho^L q^{NL^2}\right] + \left[\frac{1-\gamma}{2\gamma}\right]\left[\rho^R q^{TR^2} - \rho^L q^{TL^2}\right]}{\rho^R q^{NR} - \rho^L q^{NL}}$$

Now, if we substitute for the denominator from equation (1), we get

$$S = \frac{\frac{1}{\gamma}\left[\rho^R - \rho^L\right) + \left[\frac{\gamma+1}{2\gamma}\right]\left[\rho^R q^{NR^2} - \rho^L q^{NL^2}\right] + \left[\frac{1-\gamma}{2\gamma}\right]\left[\rho^R q^{TR^2} - \rho^L q^{TL^2}\right]}{S\left[\rho^R - \rho^L\right]}.$$

Multiplying through by S and using equation (3) to eliminate q^{TR} gives

$$S^2 = \frac{1}{\gamma} + \left[\frac{1-\gamma}{2\gamma}\right] q^{TL^2} + \frac{\left[\frac{\gamma+1}{2\gamma}\right]\left[\rho^R q^{NR^2} - \rho^L q^{NL^2}\right]}{\left[\rho^R - \rho^L\right]} .$$

and again using equation (1) to eliminate q^{NR} as
$q^{NR} = \left[S(\rho^R - \rho^L) + \rho^L q^{NL}\right] / \rho^R$ gives the term

$$\rho^R q^{NR^2} - \rho^L q^{NL^2} = \left[S^2\left[\rho^R - \rho^L\right]^2 + 2\rho^L q^{NL}\, S\left[\rho^R - \rho^L\right]\right] / \rho^R + \frac{\rho^{L^2} q^{NL^2}}{\rho^R} - \rho^L q^{NL^2} .$$

Substituting this into the new equation (2) gives

$$S^2 = \frac{1}{\gamma} + \left[\frac{1-\gamma}{2\gamma}\right] q^{TL^2} + \left[\frac{\gamma+1}{2\gamma}\right]\left[\rho^R - \rho^L\right] S^2/\rho^R + \left[\frac{\gamma+1}{2\gamma}\right] 2\rho^L q^{NL} S / \rho^R - \left[\frac{\gamma+1}{2\gamma}\right] q^{NL^2} \rho^L/\rho^R$$

and collecting terms in powers of S gives

$$S^2\left[\left[\frac{\gamma+1}{2\gamma}\right]\left[\frac{\rho^R - \rho^L}{\rho^R}\right] - 1\right] + S\left[\left[\frac{\gamma+1}{2\gamma}\right]\frac{2\rho^L q^{NL}}{\rho^R}\right] + \left[\frac{1}{\gamma} + \left[\frac{1-\gamma}{2\gamma}\right] q^{TL} - \left[\frac{\gamma+1}{2\gamma}\right] q^{NL^2} \rho^L/\rho^R\right] = 0$$

which can now be solved as a quadratic $\quad S = \dfrac{-\,b \pm \sqrt{b^2 - 4ac}}{2a}$

where $\quad a = \left[\left[\frac{\gamma+1}{2\gamma}\right]\left[\frac{\rho^R - \rho^L}{\rho^R}\right] - 1\right] \qquad b = \left[\left[\frac{\gamma+1}{2\gamma}\right]\frac{2\rho^L q^{NL}}{\rho^R}\right]$

and $\quad c = \left[\frac{1}{\gamma} + \left[\frac{1-\gamma}{2\gamma}\right] q^{TL^2} - \left[\frac{\gamma+1}{2\gamma}\right] q^{NL^2} \rho^L/\rho^R\right] .$

Both roots of this quadratic will satisfy the R-H equations where q^{TR} and q^{NR} are calculated as $q^{TR} = q^{TL}$ and $q^{NR} = \frac{\rho^L}{\rho^R}[q^{NL}-S] + S$, i.e. conservation of tangential velocity and mass. However the positive root corresponds to $q^{NL}, q^{NR} < S$, so that the fluid enters from the left-hand side and exits on the right-hand side. The negative root corresponds to the exact reverse, i.e. the shock speed is $> q^{NL}, q^{NR}$ such that the relative velocities of the fluid to the shock are in the opposite direction, and so conservation of mass and momentum still holds. In the problem we are dealing with, we expect to find a steady shock where fluid enters through the left-hand side, consequently the positive root is selected.

CHAPTER 2

SHOCK FITTING METHODS

2.1 CAPTURING A FITTED SHOCK

So far, when updating the shocked nodes, the upstream vector of unknowns $\underline{u}^L$ has been updated using a one-sided form of the finite volume scheme, equivalent to assuming that the boundary is non-reflective. The downstream vector of unknowns $\underline{u}^R$ is updated by specifying one of the unknowns, usually density ρ^R, and then solving the R-H equations to find q^{NR}, q^{TR} and S. If we were to use a flux-splitting scheme then we could split the fluxes in one direction perpendicular to the shock, or ideally perpendicular and tangentially. In both cases the eigenvectors, the wavespeeds and the α coefficients are used to update the shock. However, this would essentially involve mixing a finite volume scheme and a flux splitting scheme around the shock.

An alternative procedure is described here which does not split the fluxes around the shock, but rather across the shock itself, and is used as a correction to the updating of all components upstream and downstream of the shock by the one-sided, non-reflecting finite volume update.

Consider Roe's scheme [6], [10] applied to a stationary cell for 1D flow

$$\underline{u}^{n+1} - \underline{u}^{n} = \frac{\partial \underline{u}}{\partial t}\Delta t = -\frac{\partial \underline{F}}{\partial \underline{u}}\frac{\partial \underline{u}}{\partial x}\Delta t \simeq -\frac{\tilde{\tilde{\partial}}\underline{\tilde{\tilde{F}}}}{\partial \underline{u}}\frac{\Delta \underline{u}}{\Delta x}\Delta t \ .$$

Δt is restricted by the maximum wavespeed crossing the cell so

$$\Delta t = \frac{\Delta x}{MAX|\lambda_i|} \quad \text{where } \lambda_i \text{ are eigenvalues of matrix } \frac{\tilde{\tilde{\partial}}\underline{\tilde{\tilde{F}}}}{\partial \underline{u}} = \tilde{A} \ .$$

So $$\underline{u}^{n+1} - \underline{u}^{n} = - \tilde{A} \frac{\Delta \underline{u}}{\Delta x} \frac{\Delta x}{\max|\lambda_i|} = \frac{- \tilde{A}\, \Delta \underline{u}}{\max|\lambda_i|}$$

and $$\Delta \underline{u} = \tilde{\alpha}_1 \underline{\tilde{e}_1} + \tilde{\alpha}_2 \underline{\tilde{e}_2} + \tilde{\alpha}_3 \underline{e_3}$$

where $\tilde{\alpha}_i$, $\tilde{e}_i$ and $\frac{\tilde{\partial F}}{\partial u}$ are all composed of Roe averaged values of $\tilde{\rho}$, $\tilde{u}$ and $\tilde{v}$, i.e.

$$\tilde{\rho} = \sqrt{\rho^R}\sqrt{\rho^L}$$

$$\tilde{u} = \frac{\sqrt{\rho^R}\, u^R + \sqrt{\rho^L}\, u^L}{\sqrt{\rho^R} + \sqrt{\rho^L}}$$

$$\tilde{V} = \frac{\sqrt{\rho^R}\, V^R + \sqrt{\rho^L}\, V^L}{\sqrt{\rho^R} + \sqrt{\rho^L}}$$

We now extend this to a cell moving with speed S. Firstly, the differential equation becomes $\frac{d\underline{u}}{dt} = \frac{\partial \underline{u}}{\partial t} + S \frac{\partial \underline{u}}{\partial x}$, and Roe's scheme becomes,

$$\underline{u}^{n+1} - \underline{u}^{n} = \frac{- \tilde{A}\, \Delta \underline{u}}{\max|\lambda_i - S|} + \frac{S\, \Delta \underline{u}}{\max|\lambda_i - S|}$$

so $$\underline{u}^{n+1} - \underline{u}^{n} = \frac{-1}{\max|\lambda_i - S|} \left[\tilde{A} - SI \right] \Delta \underline{u} \ .$$

$$\text{RHS} = \frac{-1}{\max|\lambda_i - S|} \left[\tilde{\alpha}_1 \tilde{\lambda}_1 \underline{\tilde{e}_1} + \tilde{\alpha}_2 \tilde{\lambda}_2 \underline{\tilde{e}_2} + \tilde{\alpha}_3 \tilde{\lambda}_3 \underline{\tilde{e}_3} - \tilde{\alpha}_1 S \underline{\tilde{e}_1} - \tilde{\alpha}_2 S \underline{\tilde{e}_2} - \tilde{\alpha}_3 S \underline{\tilde{e}_3} \right] .$$

So $$\underline{u}^{n+1} - \underline{u}^{n} = \frac{-1}{\text{MAX}|\lambda_i - S|} \left[\tilde{\alpha}_1 \left[\tilde{\lambda}_1 - S\right] \underline{\tilde{e}_1} + \tilde{\alpha}_2 \left[\tilde{\lambda}_2 - S\right] \underline{\tilde{e}_2} + \tilde{\alpha}_3 \left[\tilde{\lambda}_3 - S\right] \underline{\tilde{e}_3} \right] .$$

The direction in which the fluxes are then distributed depends on the sign of $\lambda_i - S$, hence the wavespeeds are now relative to the moving cell. Notice that the update is independent of the cell width Δx. But of course if the flow is smooth then as $\Delta x \longrightarrow 0$ so does $\Delta \underline{u} \longrightarrow \underline{0}$ and the update $\longrightarrow \underline{0}$. However, if our cell contains a shock then $\Delta \underline{u} \not\longrightarrow \underline{0}$ as $\Delta x \longrightarrow 0$, and the update may be non zero.

The Roe averaged matrix $\tilde{A} = \dfrac{\tilde{\partial} \underline{F}}{\partial \underline{u}}$ has the following three properties [6]

(A) $\tilde{A}\, \Delta \underline{u} = \Delta \underline{F}$

(B) $\tilde{A}$ is diagonalizable with real eigenvalues

(C) $\tilde{A} \rightarrow \dfrac{\partial \underline{F}}{\partial \underline{u}}$ smoothly as $\underline{u}^L, \underline{u}^R \longrightarrow \underline{u}$.

Also the Rankine Hugoniot conditions for a shock are $S\, \Delta \underline{u} = \Delta \underline{F}$, where S is the shock speed,

$$\Delta \underline{u} = \begin{vmatrix} \rho^R - \rho^L \\ \rho^R q^{NR} - \rho^L q^{NL} \\ \rho^R q^{TR} - \rho^L q^{TL} \end{vmatrix}, \quad \Delta \underline{F} = \begin{vmatrix} \rho^R q^{NR} - \rho^L q^{NL} \\ \left[\rho^R q^{NR^2} + P^R\right] - \left[\rho^L q^{NL^2} + P^L\right] \\ \rho^R q^{NR} q^{TR} - \rho^L q^{NL} q^{TL} \end{vmatrix}.$$

Consequently, property A implies that $\tilde{A}\, \Delta \underline{u} = S\, \Delta \underline{u}$, i.e. the shock speed S and the jump in $\underline{u}$, $\Delta \underline{u}$, are an eigenvalue, eigenvector pair of the $\tilde{A}$ matrix.

To find which eigenvalue, eigenvector pair is appropriate we notice that

$$\underset{\sim}{\tilde{e}_2} = \begin{vmatrix} 1 \\ \tilde{\lambda}_2 \\ \tilde{q}^T \end{vmatrix} \quad \text{and} \quad \underset{\sim}{\tilde{e}_3} = \begin{vmatrix} 1 \\ \tilde{\lambda}_3 \\ \tilde{q}^T \end{vmatrix}$$

where $$\tilde{\lambda}_2 = \left[\frac{1+\gamma}{2\gamma}\right]\tilde{q}^N + \sqrt{\left[\frac{1-\gamma}{2\gamma}\right]\tilde{q}^{N^2} + \tilde{a}^2/\gamma}$$

and $$\tilde{\lambda}_3 = \left[\frac{1+\gamma}{2\gamma}\right]\tilde{q}^N - \sqrt{\left[\frac{\gamma-1}{2\gamma}\right]\tilde{q}^{N^2} + \tilde{a}^2/\gamma} \ .$$

If either of these eigenvectors is the one with an eigenvalue equal to S, then it must be a multiple of $\Delta\underline{u}$, i.e. $\Delta\underline{u} = \alpha\underset{\sim}{\tilde{e}_2}$ or $\Delta\underline{u} = \alpha\underset{\sim}{\tilde{e}_3}$.

The R-H equations imply that $q^{TL} = q^{TR} = \tilde{\tilde{q}}^T$ so if $\alpha = \rho^R - \rho^L$ then

$$\rho^R - \rho^L = (\rho^R - \rho^L)\ 1$$
$$\rho^R q^{NR} - \rho^L q^{NL} = (\rho^R - \rho^L)\ \tilde{\lambda}$$
$$\rho^R q^{TR} - \rho^L q^{TL} = (\rho^R - \rho^L)\ q^T \ .$$

Clearly the 1st and 3rd components are satisfied by either eigenvector, and from the R-H equations the 1st component gives

$$S(\rho^R - \rho^L) = \rho^R q^{NR} - \rho^L q^{NL}$$

$\Rightarrow$ λ_2 or λ_3 must equal S .

In Section [1.4] we found that the R-H equations have two possible solutions for S for a given $\underline{u}^L$ and ρ^R corresponding to two roots of a quadratic. One root corresponds to fluid entering the shock from the left hand side (positive root), the other root corresponds to fluid

entering the shock from the right-hand side (negative root). Numerical experimentation shows that the shock speed of a shock using the positive root is equal the eigenvalue $\tilde{\lambda}_3$ of $\frac{\partial \underline{F}}{\partial \underline{u}}$, whilst the shock speed of a shock using the negative root is equal to the $\tilde{\lambda}_2$ of $\frac{\tilde{\partial}\tilde{\underline{F}}}{\partial \underline{u}}$, where $\frac{\tilde{\partial}\tilde{\underline{F}}}{\partial \underline{u}}$ is the Roe averaged Jacobian matrix for each shock.

Since we choose the positive root shock speed (the negative root is physically inappropriate), this implies that our eigenvector, eigenvalue pair is $\tilde{\lambda}_3$ and $\tilde{\underline{e}}_3$. Hence we see that $\Delta \underline{u} = \alpha\, \tilde{\underline{e}}_3$ and $\tilde{\lambda}_3 = S$. (Property (B) ensures that the eigenvectors are linearly independent so that $\Delta \underline{u}$ has no components of $\underline{e}_1$ or $\underline{e}_2$)

Implementation

In practice this one-dimensional flux-splitting scheme can be applied to a shock, since the shock is essentially a cell of zero width, provided the fluxes are split perpendicular to the shock orientation.

Firstly the one sided finite volume scheme is used to update all three components of $\underline{u}$ on both sides of the shock. Invariably the R-H conditions will now not be satisfied, and so the fluxes are split and distributed to either side, and the $\underline{u}$ vectors updated. Usually this last step needs to be repeated about 100 times using the most recently updated values of $\underline{u}_{L,R}$ to recalculate the fluxes to be split. After a sufficient number of iterations we find $\Delta \underline{u} = \alpha_3 \underline{e}_3$, $\lambda_3 = S$ and $\alpha_1 = \alpha_2 = 0$ [in reality α_1 α_2 start at $\simeq 10^{-7}$ after the finite volume update, and decrease to $\simeq 10^{-17}$ after 100 iterations]. So by satisfying the R-H equations the update is automatically zero.

An undesirable feature of this procedure is the estimation of the shock speed S when the R-H conditions have not yet been satisfied (This is required for the flux splitting calculation). The value of S is calculated by specifying $\underline{u}^L$ and ρ^R and solving the R-H equations. However, we find that the value of S changes as the fluxes are being split, until it is equal to λ_3.

2.2 FLUX SPLITTING VIA ROE'S SCHEME IN ONE DIRECTION, NEXT TO SHOCK

Roe's approximate Riemann solver was used to split the fluxes in the cells immediately adjoining the shock. (The eigenvalues, eigenvectors, α coefficients, and form of the Roe averaged variables can be found in Appendix 2.) The flux splitting was applied only to the $\underline{F}$ vector whilst a 1st order cell vertex method was used to calculate the contribution to the update from the $\underline{G}$ vector.

The algorithm is as follows:-

1) Calculate $\underline{u}$ in the rotated coordinate frame such that the x axis is aligned along edge 1-2, i.e. $\underline{u}'$ for points 1,2,3,4,5 and 6 (see Fig. 1).

2) Calculate Roe averages eigenvalues, eigenvectors and α's for edge 1-2, where $\underline{u}'_L = \underline{u}'_1$, and $\underline{u}'_R = \underline{u}'_2$.

3) Sum the terms of $\Delta\underline{F}' = \sum_{j=1}^{3} \lambda_j \alpha_j \underline{e}_j$, those corresponding to positive eigenvalues, multiply by $-\Delta t/\Delta x$ and put equal to $\delta\underline{u}'_R$.

4) Calculate X', Y' and $\underline{G}'$ in the rotated frame.

5) Calculate $\partial\underline{G}'/\partial y'$ in cells A and B using a cell centred finite volume method, then calculate the area weighted average over cells A and B, multiply by $-\Delta t$ and add to $\delta\underline{u}'_R$.

6) Resolve $\delta\underline{u}'_R$ back into X, Y coordinates and update the $\underline{u}$ vector on the shock.

A similar process is applied to the downstream side of the shock, but selecting instead the backward travelling waves in the splitting method. All non shock nodes are updated using the usual cell vertex method.

2.3 RESIDUAL CALCULATION ON A MOVING GRID

It was realised that, during our shock fitting process, all nodes but particularly those closest to the shock were being moved as the solution was updated, and therefore to be more accurate the calculation of $\frac{\partial \underline{u}}{\partial t}$ should be replaced by a calculation of $\frac{d\underline{u}}{dt}$, where

$$\frac{d\underline{u}}{dt} = \frac{\partial \underline{u}}{\partial t} + S_x \frac{\partial \underline{u}}{\partial x} + S_y \frac{\partial \underline{u}}{\partial y},$$

S_x, S_y being the velocities in x and y directions respectively.

In order to fit in with the rest of the program, $\frac{d\underline{u}}{dt}$ was calculated in a cell, where S_x, S_y were taken to be the average of the velocities of the four cell corners, so that

S_x = average distance moved in x direction / time step

S_y = average distance moved in y direction / time step

and global time stepping was used.

The values of $\frac{\partial \underline{u}}{\partial x}$ and $\frac{\partial \underline{u}}{\partial y}$ were calculated at each cell centre using a finite volume approach, and the new cell-based values of $\frac{d\underline{u}}{dt}$ were then used as usual to calculate the 1st and 2nd order updates. The magnitude of the additional terms $S_x \frac{\partial \underline{u}}{\partial x}$ and $S_y \frac{\partial \underline{u}}{\partial y}$ were assessed and compared with the magnitude of the $\frac{\partial \underline{u}}{\partial t}$ term.

2.4 DRIVING THE SHOCK SPEEDS TO ZERO

The Rankine Hugoniot (R-H) equations may be written

$$\Delta \underline{F} = S\Delta \underline{u} \qquad \text{where} \quad \underline{u} = \begin{vmatrix} \rho \\ \rho q^N \\ \rho q^T \end{vmatrix}, \quad \underline{F} = \begin{vmatrix} \rho q^N \\ \rho q^{N^2} + P \\ \rho q^N q^T \end{vmatrix}.$$

$$\text{or} \quad \underline{F}^R - \underline{F}^L = S(\underline{u}^R - \underline{u}^L)$$

If we now differentiate this equation partially with respect to time, we get

$$\frac{\partial \underline{F}^R}{\partial t} - \frac{\partial \underline{F}^L}{\partial t} = S\left[\frac{\partial \underline{u}^R}{\partial t} - \frac{\partial \underline{u}^L}{\partial t}\right] + \left[\underline{u}^R - \underline{u}^L\right]\frac{\partial s}{\partial t}$$

and since $\dfrac{\partial \underline{F}}{\partial t} = \dfrac{\partial \underline{F}}{\partial \underline{u}}\dfrac{\partial \underline{u}}{\partial t}$ then

$$\frac{\partial \underline{F}^R}{\partial \underline{u}^R}\frac{\partial \underline{u}^R}{\partial t} - \frac{\partial \underline{F}^L}{\partial \underline{u}^L}\frac{\partial \underline{u}^L}{\partial t} = S\left[\frac{\partial \underline{u}^R}{\partial t} - \frac{\partial \underline{u}^L}{\partial t}\right] + \left[\underline{u}^R - \underline{u}^L\right]\frac{\partial s}{\partial t}.$$

Rearranging gives

$$\left[\frac{\partial \underline{F}^R}{\partial \underline{u}^R} - S\right]\frac{\partial \underline{u}^R}{\partial t} = \left[\frac{\partial \underline{F}^L}{\partial \underline{u}^L} - S\right]\frac{\partial \underline{u}^L}{\partial t} + (\underline{u}^R - \underline{u}^L)\frac{\partial s}{\partial t}.$$

Now assuming that at some time $\underline{u}^L$ and $\underline{u}^R$ are known such that the R-H equations are satisfied, then S, $\dfrac{\partial \underline{F}^R}{\partial \underline{u}^R}$ and $\dfrac{\partial \underline{F}^L}{\partial \underline{u}^L}$ will also be known.

Let us now specify $\dfrac{\partial s}{\partial t}$ so that if $S > 0$ then $\dfrac{\partial s}{\partial t} < 0$ and if $S < 0$ then $\dfrac{\partial s}{\partial t} > 0$. For example, we could use $\dfrac{\partial s}{\partial t} = -\alpha S \quad (\alpha > 0)$.

It is now possible to solve a linear system of equations for $\frac{\partial \underline{u}^R}{\partial t}$, provided that we supply $\frac{\partial \underline{u}^L}{\partial t}$ or vice versa. In effect we are specifying one of $\frac{\partial \underline{u}^L}{\partial t}$ or $\frac{\partial \underline{u}^R}{\partial t}$ and solving for the other under the condition that the magnitude of the shock speed is decreasing. In fact, if the shock is not moved, then $\frac{\partial s}{\partial t} = \frac{ds}{dt} = -\alpha S$

$$\Rightarrow S = S_o e^{-\alpha t} ,$$

i.e. the shock speed's magnitude will decrease exponentially with time.

In practice the procedure used is to calculate $\frac{\partial \underline{u}^L}{\partial t}$ using our finite volume scheme on the upstream side of the shock, and to solve the linear system for $\frac{\partial \underline{u}^R}{\partial t}$. Then the upstream shock nodes are updated using the usual one-sided cell vertex method, whilst the downstream nodes are updated as $\underline{u}^{n+1} - \underline{u}^n = \frac{\partial \underline{u}^R}{\partial t} \Delta t$, i.e. a first order update only. A correction method is then applied to the updated values of $\underline{u}^L$ and $\underline{u}^R$ on either side of the shock to ensure that the R-H equations are satisfied, and to calculate the new reduced shock speed.

2.5 THE ADDITION OF REAL VISCOSITY TO THE SHOCK TIP REGION

The general approach here is to apply the Navier-Stokes equations to the region around the shock tip in order to smear out any large flow gradients or discontinuities which might cause erratic convergence in the shock tip area.

In the first of this series of reports [8], artificial viscosity was applied in the shock tip region, without success. It was hoped that real viscosity would produce the desired smearing and a more stable shock tip.

The Navier Stokes equations for the H system can be written in conservation form as $\frac{\partial \underline{u}}{\partial t} + \frac{\partial \underline{F}}{\partial x} + \frac{\partial \underline{G}}{\partial y} = \underline{0}$, where the $\underline{F}$ and $\underline{G}$ vectors can be decomposed into inviscid and viscous parts, i.e.

$$\underline{F} = \underline{F}_i + \underline{F}_v \quad \text{where} \quad \underline{F}_i = \begin{vmatrix} \rho u \\ \rho u^2 + P \\ \rho uv \end{vmatrix} \quad \text{and} \quad \underline{F}_v = \begin{vmatrix} 0 \\ -T_{xx} \\ -T_{xy} \end{vmatrix}$$

and $$\underline{G} = \underline{G}_i + \underline{G}_v \quad \text{where} \quad \underline{G}_i = \begin{vmatrix} \rho v \\ \rho uv \\ \rho v^2 + P \end{vmatrix} \quad \text{and} \quad \underline{G}_v = \begin{vmatrix} 0 \\ -T_{xy} \\ -T_{yy} \end{vmatrix}$$

where $$T_{xx} = \frac{2}{3\ Re_L}\left[2\frac{\partial u}{\partial x} - \frac{\partial v}{\partial y}\right]$$

$$T_{xy} = \frac{1}{Re_L}\left[\frac{\partial u}{\partial y} + \frac{\partial v}{\partial x}\right]$$

and $$T_{yy} = \frac{2}{3\ Re_L}\left[2\frac{\partial v}{\partial y} - \frac{\partial u}{\partial x}\right] .$$

Re_L, the Reynolds number, was varied between 10^1 and 10^7, though for this problem it is typically 10^6 to 10^7.

The viscous fluxes T_{xx}, T_{xy} and T_{yy}, were calculated using a finite volume approach as proposed by Mackenzie (Ref 7). These were then simply added to the inviscid flux vectors and the cell vertex method was then applied as usual.

The viscous fluxes were calculated at the points marked * on the diagram in Fig. [2]. If the stencil touched on a shocked node then the upstream or downstream value of $\underline{u}$ was used in the calculation, depending on whether the central node in Fig. [2] was upstream or downstream of the shock. If the point was on the same vertical grid line as the shock then the average of the shock tip values was used.

2.6 METHODS FOR APPROXIMATING THE SHOCK SHAPE AND/OR ANGLE

In order to model the shock's behaviour in the flow field, it is necessary to know the precise location of the shock and the angle which the shock makes with the coordinate axes. To do this a curve of some kind is fitted through the shocked nodes, and the angle that the curve makes with the coordinate axes is then used to calculate the velocity components normal and tangential to the shock, so that the Rankine Hugoniot (R-H) equations can then be satisfied.

Clearly there are many different curves which could be used to fit the shocked nodes, each giving a slightly different orientation angle. All of the curves however must be constrained to be normal to the solid wall boundary to satisfy the R-H equations, since the flow is tangential to the solid wall.

When this work was first begun, the curve used was a weighted least squares (L-S) polynomial of degree three, which was weighted to fit the points closest to the shock foot. The shocked nodes were then moved so that they lay along the line of the fitted curve. Other methods of curve fitting tried during the course of the contract were as follows.

Least Squares (L-S) Polynomials

These were L-S polynomials of varying degrees but different from the above, in that the curves were not weighted at all, and they were used merely to obtain the shock angles. That is, the shock nodes were no longer moved onto the curve, so that the shock was constrained to be the shape of the polynomial. Instead the points were allowed to move freely. Polynomials from degree 2 to a degree equal to the number of shocked

nodes were tried. These curves were of the form

$$x = C_1 + C_2(y-y_0) + C_3(y-y_0)^2 + \ldots C_n(y-y_0)^{n-1}$$

where $y_0 = y$ at shock foot.

Exponential Least Squares

These curves were of the form

$$x' = C_1 + C_2e^{(y'-y_0')} + C_3e^{2(y'-y_0')} + \ldots C_ne^{n-1(y'-y_0')}$$

where x' and y' and y_0' were the x and y coordinates in a frame slightly rotated so that the orientation of the shock foot was aligned to the y' axis. These curves can also be considered as L-S polynomials in the variable $e^{(y'-y_0)}$.

Cubic Spline

This was a straightforward cubic spline, with the boundary conditions required at each end being $\frac{dx}{dy}$ supplied at the shock foot, such that the spline was normal to the boundary, and $\frac{d^2x}{dy^2} = 0$ at the shock tip (natural spline), or $\frac{d^2x}{dy^2}$ (JMS) = $\frac{d^2x}{dy^2}$ (JMS-1), where JMS corresponds to the shock tip and JMS-1 the node below it.

Three Point Angle Approximation

This method is a continuation of some of the methods used in the first report in this series, ref [8]. The shock angle is approximated by

the expression $x = f(y)$ and expanded in a Taylor series about the node in question for the two nodes immediately below it. The expansion is up to and including the 2nd order derivatives, and the two equations found are solved simultaneously for $\frac{dx}{dy}$.

Hence

$$x_{J-1} = x_J - \left[\frac{dx}{dy}\right]_J \Delta y_{J-1} + \left[\frac{d^2X}{dY^2}\right]_J (\Delta y_{J-1})^2$$

$$x_{J-2} = x_J - \left[\frac{dx}{dy}\right]_J (\Delta y_{J-1}+\Delta y_{J-2}) + \left[\frac{d^2x}{dy^2}\right]_J (\Delta y_{J-1}+\Delta y_{J-2})^2$$

where $\Delta y_{J-1} = y_J - y_{J-1}$.

Note that the angle at point J is approximated by the relative positions of the two nodes immediately below it. This has the advantage that movement of the more volatile shock tip will not alter the angles of the points below it. (At the first node up from the shock foot, it is necessary to use a centrally expanded difference to obtain 2nd order accuracy.)

Tangential Velocity Conservation

The R-H equations imply that the tangential velocity components on either side of a shock are equal. This fact can then be used to approximate the shock angle.

Assume at some time the R-H equations are satisfied and the tangential component is conserved. Now if both sides of the shock are updated using the finite volume scheme by an amount $\delta\underline{u}^L$ and $\delta\underline{u}^R$ then we choose our angle α such that $qT^L = qT^R$, where qT is the tangential velocity component equal to $qT = u\cos\alpha + v\sin\alpha$

$$\Rightarrow \quad (u^L + \delta u^L)\cos\alpha + (v^L + \delta v^L)\sin\alpha = (u^R + \delta u^R)\cos\alpha + (v^R + \delta v^R)\sin\alpha$$

$$\Rightarrow \quad \tan\alpha \left[(v^L + \delta V^L) - (v^R + \delta v^R)\right] = \left[(u^R + \delta u^R) - (u^L + \delta u^L)\right]$$

$$\Rightarrow \quad \alpha = \tan^{-1}\left[\frac{(u^R + \delta u^R) - (u^L + \delta u^L)}{(v^L + \delta v^L) - (v^R + \delta v^R)}\right] .$$

Notice that this technique is different from all the others described so far in that no account is taken of the positions of the other shocked nodes.

CHAPTER 3

RESULTS AND DISCUSSION

3.1 Assessment of Real Viscosity around Shock Tip

These results relate to the addition of real viscosity around the shock tip area, as described in Section [2.5].

The additional viscous terms, added to the inviscid flux vectors $\underline{F}$ and $\underline{G}$, proved to be of approximately the same magnitude as the value of $1/Re_L$. The lower Reynolds numbers (Re_L) between 1 and 10^3 gave the worst results, i.e. large residuals around the shock tip and large shock tip speeds, where the residuals were those calculated including the viscous terms. It is possible that these might have been reduced, had the viscous terms been applied over a larger area, so that the influence of the larger derivatives near the shock would have been faded into the inviscid area more smoothly. For Reynolds numbers greater than 10^3 the effect of the additional terms was negligible, and the results resembled the inviscid case.

A typical Reynolds number for this problem is $10^6 - 10^7$, hence realistic amounts of viscosity have a negligible effect, whilst unrealistically large amounts of viscosity produce poor results when the application is restricted to a few points immediately around the shock tip.

3.2 Assessment of Driving the Shock Speeds to Zero

This technique, as described in Section [2.4], was investigated using various values of the damping factor α, where $\frac{\partial s}{\partial t} = - \alpha S$, and different values of the frequency at which the shock was moved.

By increasing the damping factor, the rate at which the shock speeds decayed was increased successfully, and the shock speeds could be decreased indefinitely. However, if too large a value of α was used, the shock speed would decay to almost zero before the shock had a chance to manoeuvre itself into the correct position. To compensate for this, the frequency with which the shock was moved could be increased. In effect the shock could be made to settle virtually anywhere by adjusting the damping and frequency parameters.

The best results were obtained using $\alpha = 1.0$ and frequency of movement = 5 iterations. This gave shock speeds of $< 10^{-5}$ after only 1,000 iterations, but the residuals on the downstream side of the shock were much larger than was usually encountered. This method was thought to be unusual in that it was the only technique used throughout this contract that has been able to reduce the magnitude of the shock speed to any required size. However it is unacceptable because of the arbitrary use of the damping and frequency parameters, and also because the residual equations were far from satisfied.

The formulation of the method however raises important points, namely that not only must the Rankine Hugoniot equations be satisfied across a shock but so must the time and space differential forms. This has implications for the vectors $\frac{\partial \underline{u}}{\partial t}$, $\frac{\partial \underline{u}}{\partial x}$ and $\frac{\partial \underline{u}}{\partial y}$ on either side of the shock.

3.3 Assessment of Use of 1D Flux Splitting via Roe's Scheme around Shock, and Method of Capturing a Fitted Shock

The technique of 1D Flux splitting was performed as described in Section [2.2], and shall be abbreviated here to external flux splitting.

The method of capturing a fitted shock was used as described in Section [2.1], and is abbreviated here as internal flux splitting.

The external flux splitting method was used as an initial guess to the updates on either side of the shock, and was compared to the usual one sided cell vertex method. The internal flux splitting was used as a correction procedure to satisfy the R-H equations, and was compared with the method of specifying three variables from upstream, density from downstream, and then solving the R-H equations. The latter shall be known as characteristic solving.

The method of external flux splitting was compared with the one sided cell vertex method, using both characteristic solving and internal flux splitting as the correction procedure. Using the same results, characteristic solving and internal flux splitting were compared with each other using both external flux splitting and one sided cell vertex to calculate the initial guess, i.e.

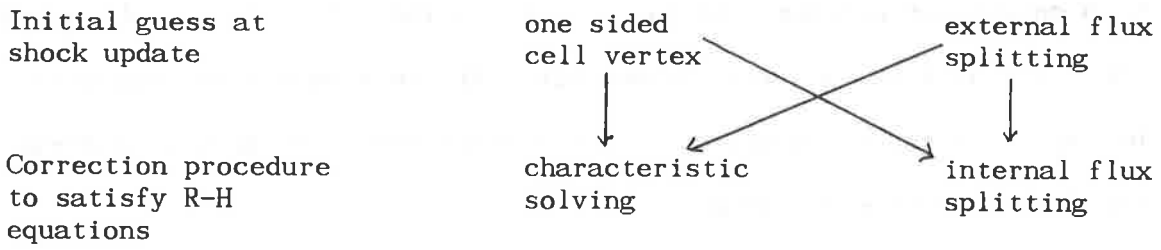

Each of the four combinations above was carried out using three different values of the shock movement frequency parameter, chosen as 5, 20 and 50 iterations, and the effect was assessed.

Result of Comparison between One Sided Cell Vertex and External Flux Splitting

The shock speeds generated using external flux splitting were slightly larger than those generated by the one sided cell vertex method, particularly at the shock foot, resulting in a shock that moved further upstream as the iteration progressed. Comparing external flux splitting with the one sided cell vertex method when both use characteristic solving, we found the residuals are approximately twice as large and the updates 100 times as large in favour of one sided cell vertex. However when we did the same comparison replacing characteristic solving with internal flux splitting, we found that the residuals were now twice as large in favour of external flux splitting, and the updates were thirty times as large in favour of one sided cell vertex.

Hence, in terms of residuals, external flux splitting works better only if it is combined with the internal flux splitting routine, but in terms of updates the one sided cell vertex method is far superior for both correction methods. In fact there was thought to be a problem with the external flux splitting method since the updates did not converge, but actually increased slightly as the iteration progressed regardless of the frequency of shock movement.

Result of Comparison of Characteristic Solving and Internal Flux Splitting

Internal flux splitting showed a significant improvement over characteristic solving in terms of updates and residuals which were both consistently half the size, provided external flux splitting was used to calculate the initial update. If however the one sided cell vertex

method was used to calculate the initial update, then the results were very similar in all respects during the earlier period of the calculation. However later on differences began to emerge, namely the shock foot using characteristic solving departed from the rest of the shock by moving too far upstream. This in turn caused the shock angles to change and then the shock speeds and updates became larger than for the internal flux splitting case. The residuals of both methods were comparable over the entire calculation.

Result of Varying Shock Movement Frequency

Identical methods were compared after the same number of shock movements for different values of the shock movement frequency parameter. It was found that the shock positions, shock speeds and residuals for each case were very similar. The updates however were smaller for the shocks that were moved less frequently, since this allowed the iteration to converge (provided external flux splitting was not used). In effect then there would seem to be little point in allowing too large an interval between shock movements since the residuals, shock speeds and consequently shock positions are sufficiently insensitive to this parameter. A movement frequency of between 5 and 10 iterations was found to be sufficiently robust to allow the solution to develop readily.

3.4 ASSESSMENT OF USE OF RESIDUAL CALCULATED ON A MOVING GRID

The cell based residual approximation was supplemented with additional terms to take account of the movement of the grid (see Section 2.3).

These additional terms were found to vary in magnitude, depending mainly upon how much grid movement was taking place locally. Consequently these terms were largest at the beginning of the calculation when the shock speeds were highest. They also became larger in the areas nearest the shock where the most movement was taking place.

Typically the magnitudes found varied from 1,000 times smaller than the stationary residuals, in the areas well away from the shock, to the same size in the areas around the shock. However, although the movement of the grid was clearly significant in the residual calculation, the inclusion of these terms was found to increase the instability of the code, and the procedure was therefore not permanently incorporated into the program. The reason for this increased instability is not known.

3.5 ASSESSMENT OF METHODS FOR APPROXIMATING SHOCK ANGLES

Least squares polynomials of varying degrees were used to approximate the shock angle as in section [2.6]. The best results were obtained by the use of a polynomial of degree 3, i.e. a cubic. The L-S curve of degree 2 was found to be too inflexible, since after taking up one degree of freedom to ensure that the curve was normal to the wall and another for the shock to pass through the given foot position, only one degree of freedom was left. The polynomials of degree 5 and above steadily became too oscillatory giving rise to sawtooth shaped shocks, see Fig. [3]. The polynomial of degree 4 gave reasonable results, but the tip tended to fall backwards, producing large shock angles which then caused the shock length to shorten because the shock existence criterion was no longer satisfied. The shock would then move back downstream and lengthen again, only to repeat a similar action a few hundred iterations later.

In this problem, with the grid used, the shock was 7 nodes long. A cubic with 4 degrees of freedom gives a plausible shock shape, but also has an inflection point near the tip, which keeps the shock angles from becoming too large and prevents the shock tip from falling backwards as described above for the least squares quadratic. This phenomenon of the shock tip falling backwards (upstream) when the shock angle became greater than about 1.6 radians at the tip was observed frequently when using other methods. The reason why it occurs is not clear. However in the more stable cases the phenomenon is almost oscillatory in the way the shock length shortens and then relengthens, suggesting that an intermediate shock length would be less oscillatory. Various attempts were made to alter the shock's length but none met with success.

A significant difference in the speed and level to which the shock speeds decreased was observed when using the least squares cubic to approximate the shock angles only, as opposed to then moving the shocked nodes so that they lay on the cubic (as was done in the original method when this work was started). A comparison of the new and original methods can be found in Tables 1 and 2, where all except the curve fitting routines are identical.

In Table 3 there is a history of a much longer run employing this new method of curve fitting. One can see that the shock speeds decay rapidly at the beginning of the calculation and reach a minimum after approximately 3,500 iterations where the shock is virtually motionless and the updates are tending towards zero. However, after this point the speed at the shock foot goes through zero and starts to become increasingly negative; the same thing occurs at the shock tip and then all the shock speeds start to increase in magnitude again. This type of instability after an initial period of apparent convergence is not understood.

An exponential least squares curve of degree 3, where the x and y coordinates were rotated so that the shock foot aligned with the y axis, were less convergent in terms of shock speeds than the least squares cubic, and no other advantages were seen in favour of adopting this method.

A cubic spline was tried with two different boundary conditions for the shock tip end, as described in Section [2.6]. Both conditions resulted in a shock shape whose angles gradually became more oscillatory

as the iteration progressed, until they resembled the curves formed using the higher degree least squares polynomials.

The three point angle approximation suggested by Moretti [Ref 9] and described in Section [2.6] resulted in the same type of sawtooth shaped shocks that were observed using the first order backward differencing and central differencing described in the first report in this series (see [8], Chapter [4]).

The conservation of tangential velocity method of approximating the shock angle as described in Section [2.6], resulted in a shock whose foot moved further downstream and a tip which moved further upstream as the iteration progressed. The shape of the shock would, by comparison with all methods which are vaguely stable, be regarded as incorrect. However the shock speeds slowly decreased for all the shocked nodes as the iteration progressed and the updates around the shock also decreased. Consequently the method is something of a curiosity. The convergence history is logged in Table 4. The shock shape and angles are similar to the result obtained using the assumption that the flow is normal to the shock (see first report, Table 2).

3.6 ASSESSMENT OF THE EFFECT OF GRID REFINEMENT ON THE SHOCK CAPTURED AND FITTED SOLUTIONS

The effect of refining the grid was assessed on 3 increasingly finer grids for shock capturing, and 2 grids for shock fitting. We were unable to obtain a fitted result on the 257×65 grid, presumably because adjustments to the background smoothing were necessary. No adjustments were required to the smoothing parameters for the shock capturing cases. The smoothing used was of the form

$$\left[\mu_0 + \mu_1\left[|R_A(\rho)| + |R_B(\rho)| + |R_C(\rho)| + |R_D(\rho)|\right]\right]\left[u_A + u_B + u_C + u_D - u_1\right]$$

where $u_{A,B,C,D}$ are the relevant components of the surrounding cell centred values of $\underline{u}$, and u_1 is the vertex value. $R_{A,B,C,D(\rho)}$ are the density cell residuals.

$\mu_0 = 0.006$ and $\mu_1 = 0.02$ for shock capturing

or $\mu_1 = 0$ for shock fitting .

The results can be found in the plots at the back of this report (in colour in the master copies). Plots were made of all three components for

(i) the cell residuals

(ii) the absolute values of the cell residuals

(iii) the LOG_{10} of the absolute values of the cell residuals.

Shock Captured Results

It was observed on all the grids that around the shock area the residuals were much larger than in the smoother parts of the flow. Also counterbalancing of large positive and negative residuals was taking place between groups of four cells situated on either side of the shock.

Comparison of the absolute values of the residuals on each grid around the shock area showed that the density residuals were largest, followed by the y momentum and then the x momentum. The largest gap was a factor of 5 to 10 between density and y momentum residuals. Refinement of the grid caused both the density and x momentum residuals to approximately double each time, whilst the y momentum residuals increased only slightly. Far away from the shock all residuals decrease with grid refinement.

Compared to the other large residuals which occurred at the leading and trailing edge of the bump, we find the density residuals around the shock are 5 to 10 times larger on the 65×17 grid, and 10 to 15 times larger on both the 129×33 and 257×65 grids. The x and y momentum residuals are 2 to 3 times larger on all grids. Also the difference between the largest and smallest residuals of the same type is about a factor of 1 to 10,000 on the 65×17 grid and 1 to 100,000 on the 129×33 grid.

Shock Captured Bottom Wall Plots

Density, pressure and Mach number were plotted along the bottom wall for all three grids.

Refinement of the grid shows the shock resolution improving. The Zierup singularity is only a slight kink in all three curves after the

shock on the 65 x 17 grid, but turns into a complete reverse of direction on the 129 x 33 and 257 x 65 grids.

Shock Fitted Results

These results were obtained using the usual one sided cell vertex method to obtain an initial guess to the shock updates, then correcting this using the technique of internal flux splitting described in Section [2.1] in order to satisfy the R-H conditions. The curve fitting method was an unweighted least squares cubic as described in Section [2.6]. The movement of the shock was ceased after 3,000 iterations, and the calculation was continued to drive the updates towards zero for a further 1,000 iterations.

Examination of the plots of the absolute values of the residuals shows that on the 65 x 17 grid the density and y momentum residuals are comparable whilst both are approximately twice the size of the x momentum residuals. On the finer 129 x 33 grid all three are approximately equal.

The effect of refining the grid is to double the size of the density and x momentum residuals around the shock area, whilst the y momentum residuals only show a slight increase. Away from the shock all three residuals appear to be approximately the same as the grid is refined. Compared to the other large residuals which occur around the leading and trailing edges on the 65 x 17 grid, the density residuals are comparable, whilst the x momentum residuals are approximately half the size and the y momentum residuals are approximately double the size. On the 129 x 33 grid all three residuals are comparable to those at the leading and trailing edges.

A comparison of the largest and smallest residuals shows that on the

65 x 17 grid the difference is a factor of approximately 10,000 for all components, whilst on the 129 x 33 the grid factor is about 100,000.

Bottom Wall Plots

The finer grid solution shows slightly better resolution of the Zierup singularity. Also the density and pressure are slightly smaller immediately upstream of the shock, and slightly larger immediately downstream, whilst the Mach number displays the opposite result. This therefore implies that the shock is slightly stronger on the finer grid.

Comparison of Captured and Fitted Results

On both the 65 x 17 and 129 x 33 grids the density residuals around the shock are more than 10 times larger for the captured solution. The x and y momentum residuals are however only slightly larger than the fitted residuals. Also the residuals around the leading and trailing edges are comparable with each other for fitting and capturing as one would expect. In general the shock fitted residuals around the shock are comparable to those at the leading and trailing edges, whilst those produced by shock capturing are much larger in the case of the density and slightly larger for the x and y momenta.

This would appear to be because the residuals produced at the shock by capturing are largely a result of excessive amounts of smoothing used to smear the shock, whilst those produced by fitting are similar to those at the leading and trailing edges, and are due to the use of a one sided cell vertex stencil being applied to a boundary at points where the boundary is relatively highly curved, and so large truncation errors are incurred.

At both the edges and the shock there is the additional complication of choosing an angle to which the flow must be aligned (in the case of the leading and trailing edges) or an angle which is used to satisfy the R-H equations (this mainly affects the downstream side of the shock). Table 5 shows the size of all residual components immediately upstream and downstream of a fitted shock, those downstream being on average 3 times larger.

Comparison of the plots of density, pressure and Mach number for the fitted and captured solutions show that, apart from the shock being resolved better by fitting, it is also about 15% stronger on both grids.

CHAPTER 4

CONCLUSIONS

Shock fitting by the methods outlined in this report is now at the stage where it can be applied to a few specialised problems in which the shock is embedded and is not too oblique to the flow. An artificial restriction is however necessary in the form of some criterion to prevent the shock from moving once the calculation has reached a suitable stage. For example we could measure the sum of the magnitudes of the individual shock speeds and restrict the shock as soon as this measure started to increase. It is in the earlier parts of the calculation that most of the good work is done, and the shock speed can be reduced to less than 10^{-3}; after this point, instability may set in as described in Section [3.5].

The cell residuals give us a measure of how well the difference equations are being satisfied. In this respect, fitting is superior to shock capturing (particularly for the density residuals). However the final proof of a method is the validation. The lift coefficient on an AGARD test case was calculated using the 1987 version of this code by Morton and Paisley [2]. They found that the lift coefficient was about 2½% higher than the fine grid captured solution produced by Pulliam and Barton [3] for the $M_\infty = 0.8 \quad \alpha = 1.25$ case, and about 7% higher for the $M_\infty = 0.85 \quad \alpha = 1.0$ case, and that the captured solution produced by Hall [4] on an equivalent grid was in slightly better agreement with Pulliam and Barton's result.

However since 1987 various minor bugs have been found in the code, the formulation of the shock speed calculation has been found to be incorrect (although the error due to this diminishes as the shock speed

tends to zero), see Section [1.3], and the weighted least squares cubic by which the shocked nodes were restricted has been replaced by an unweighted least squares cubic which is only used to approximate the shock angles and allows the nodes to move freely, see Section [2.6]. Also the arbitrary specification of density from the downstream side of the shock to solve the R-H equations has been replaced by an internal flux splitting method, see Section [2.1]. Finally the remeshing procedure has been improved to minimise grid distortion due to shock movement.

The visible result of all this work is that the shock speeds can be reduced to an order of magnitude lower than was possible previously, and the robustness of the code in terms of constancy of shock position and length is greatly improved.

The present method can be criticised for the arbitary choice of a least squares cubic, since this curve might not do so well for other shocks. Ideally we require a method of approximating the shock angles which does so for each node independently, or fits a curve which uses all the degrees of freedom available to it but is not oscillatory. Attempts were made to find the former via the assumption of normal flow (see first report [8], Chapter 2), and the conservation of tangential velocity (see Section [2.6]). A cubic spline was also tried but found to give shock angles which gradually became more oscillatory. A tensioned spline may have worked better but then the amount of tension applied would be arbitrary.

There are also problems with grid distortion. The remeshing procedure was designed to keep the cells as near to parallelograms as possible, but in the region of the shock tip where the curvature of the

shock is greatest this inevitably leads to thin parallelograms adjoining ones which are not so thin. This problem could be largely overcome by the use of a grid specifically generated to take account of curved shock waves, or by the use of an unstructured grid.

Two areas which have not been addressed during this work are the analysis of the one sided cell vertex stencil on a distorted grid and the inflow and outflow boundary conditions.

Acknowledgements

The author wishes to thank R.A.E. Farnborough for the funding of this work, Dr. M.J. Baines for constructive supervision during the last two years, Dr. C.M. Albone for his advice and experience on the project and all members of the Oxford-Reading I.C.F.D. group for stimulating discussions and seminars. Also M. Aves who has provided practical help particularly with computational matters and finally Mrs. Brigitte Calderon for typing this report.

References

1. C.M. Albone (1986), *A shock fitting scheme for the Euler equations using dynamically overlying meshes.* Proc. Conf. on Num. Meth. for Fl. Dyn. - University of Reading, 1985 (Eds K.W. Morton and M.J. Baines), OUP pp 427-437.

2. K.W. Morton and M.F. Paisley (1987), *A finite volume scheme with shock fitting for the steady Euler equations.* Oxford University Computing Laboratory, Numerical Analysis Group Report No. 87/6.

3. T.H. Pulliam and J.T. Barton (1985), *Euler Computations* of AGARD Working Group 07 airfoil test cases. AIAA Paper 85-0018.

4. M.G. Hall (1986), *Cell vertex schemes for solution of the Euler equations.* Proc. Conf. on Num. Meth. for Fl. Dyn. University of Reading 1985 (Eds K.W. Morton and M.J. Baines), OUP pp. 303-345.

5. P.C. Samuels, Numerical Analysis Reports 4/88, 7/88, 10/89, 12/89 University of Reading, Mathematics Department.

6. P.L. Roe (1981), *Approximate Riemann solvers, parameter vectors and difference schemes.* J. Comput. Phys., 43: 357-72.

7. J. Mackenzie (1989), *The cell vertex method for viscous transport problems.* Oxford University Computing Laboratory, Numerical Analysis Group Report No. 89/4.

8. P.D. Arnold (1990), Numerical Analysis Report 18/90, University of Reading, Mathematics Department.

9. G. Moretti (1974), *Look Ma, no wiggles,* Polytechnic Institute of New York, Department of Aerospace Engineering and Applied Mechanics, Report No. 74-15.

10. P. Glaister (1985), *An approximate linearised Riemann solver for the Euler equations in one dimension with a general equation of state.* University of Reading, Mathematics Department, Report No. 7/85.

11. J.N. Hunt, Lecture Notes, *Shock waves in one dimensional flow I, II.* University of Reading, Mathematics Department.

APPENDIX 1

The full 2-D Euler equations are

$$\frac{\partial \underline{u}}{\partial t} + \frac{\partial \underline{F}}{\partial x} + \frac{\partial \underline{G}}{\partial y} = \underline{0}$$

where $\underline{u} = \begin{vmatrix} \rho \\ \rho u \\ \rho v \\ \rho E \end{vmatrix}$, $\underline{F} = \begin{vmatrix} \rho u \\ \rho u^2 + P \\ \rho uv \\ \rho u[E+P/e] \end{vmatrix}$, $\underline{G} = \begin{vmatrix} \rho v \\ \rho uv \\ \rho v^2 + P \\ \rho v[E+P/e] \end{vmatrix}$

with an equation of state

$$E = \frac{P}{\rho(\gamma-1)} + \frac{1}{2}(u^2 + v^2)$$

where E is the total energy per unit mass (kinetic + internal). The R-H equations are $[\underline{u}]S = [\underline{F}]$ where u and v now represent the velocity components normal and tangential to the shock.

The third component of the R-H equations simplifies to $v_1 = v_2$ (see Section 1.2). Written in full, the R-H equations are:

$$S = \left[\rho_1 u_1 - \rho_2 u_2\right] / \left[\rho_1 - \rho_2\right] \qquad (1)$$

$$S = \left[\left[\rho_1 u_1^2 + P_1\right] - \left[\rho_2 u_2^2 + P_2\right]\right] / \left[\rho_1 u_1 - \rho_2 u_2\right] \qquad (2)$$

$$S = \left[\rho_1 u_1 \left[E_1 + \frac{P_1}{\rho_1}\right] - \rho_2 u_2 \left[E_2 + \frac{P_2}{\rho_2}\right]\right] / \left[\rho_1 E_1 - \rho_2 E_2\right] \qquad (3)$$

$$v_1 = v_2 \tag{4}$$

where $1 \equiv L$, $2 \equiv R$.

Therefore, $(1) \Longrightarrow \rho_1(u_1-S) = \rho_2(u_2-S)$

$(2) \Longrightarrow \rho_1 u_1(u_1-S) + P_1 = \rho_2 u_2(u_2-S) + P_2$

$(3) \Longrightarrow \rho_1(u_1-S)E_1 + P_1u_1 = \rho_2(u_2-S)E_2 + P_2u_2$.

Now (1) and (2) $\Longrightarrow \rho_1(u_1-S)(u_1-S) + P_1 = \rho_2(u_2-S)(u_2-S) + P_2$ (5)

and since $$E = \frac{P}{\rho(\gamma-1)} + \frac{1}{2}(u^2 + v^2)$$

and $v_1^2 = v_2^2$ from (4), and $\rho_1(u_1-S) = \rho_2(u_2-S)$ from (1) ,

then this implies that the energy fluxes due to the tangential velocity on both sides of the shock are equal, i.e.

$$\rho_1(u_1-S)\ \frac{v_1^2}{2} = \rho_2(u_2-S)\ \frac{v_2^2}{2}$$

so that equation (3) becomes

$$\rho_1(u_1-S)\left[\frac{P_1}{\rho_1(\gamma-1)} + \frac{u_1^2}{2}\right] + P_1u_1 = \rho_2(u_2-S)\left[\frac{P_2}{\rho_2(\gamma-1)} + \frac{u_2^2}{2}\right] + P_2u_2$$

Also $$(u-S)^2 = u^2 + S^2 - 2uS$$

and $$P(u-S) = Pu - PS$$

so that (3) becomes

$$\rho_1(u_1-S)\left[\frac{P_1}{\rho_1(\gamma-1)} + \tfrac{1}{2}(u_1-S)^2 + u_1S - \frac{S^2}{2}\right] + P_1(u_1-S) + P_1S$$

$$= \rho_2(u_2-S)\left[\frac{P_2}{\rho_2(\gamma-1)} + \tfrac{1}{2}(u_2-S)^2 + u_2S - \frac{S^2}{2}\right] + P_2(u_2-S) + P_2S \ .$$

Now $$\rho_1(u_1-S)\left[u_1S - \frac{S^2}{2}\right] + P_1S = \rho_2(u_2-S)\left[u_2S - \frac{S^2}{2}\right] + P_2S$$

because from (1) $$\rho_1(u_1-S)\frac{S^2}{2} = \rho_2(u_2-S)\frac{S^2}{2}$$

and from (2) $$\rho_1(u_1-S)u_1 + P_1 = \rho_2(u_2-S)u_2 + P_2 \ .$$

Therefore (3) becomes

$$\rho_1(u_1-S)\left[\frac{P_1}{\rho_1(\gamma-1)} + \tfrac{1}{2}(u_1-S)^2\right] + P_1(u_1-S) =$$

$$\rho_2(u_2-S)\left[\frac{P_2}{\rho_2(\gamma-1)} + \tfrac{1}{2}(u_2-S)^2\right] + P_2(u_2-S)$$

and using a change of variable $u' = u-S$, the full R-H equations in 2-D become

$$\rho_1 u_1' = \rho_2 u_2' \qquad (1)$$

$$\rho_1 u_1'^2 + P_1 = \rho_2 u_2'^2 + P_2 \qquad (5)$$

$$\rho_1 u_1'\left[\frac{P_1}{\rho_1(\gamma-1)} + \frac{u_1'}{2}\right] + P_1 u_1' = \rho_2 u_2'\left[\frac{P_2}{\rho_2(\gamma-1)} + \frac{u_2'}{2}\right] + P_2 u_2' \qquad (6)$$

$$v_1 = v_2 \ . \qquad (4)$$

Equation (6) can now be divided through by equation (1) giving

$$\frac{P_1}{\rho_1}\left[\frac{\gamma}{\gamma-1}\right] + \frac{u_1'^2}{2} = \frac{P_2}{\rho_2}\left[\frac{\gamma}{\gamma-1}\right] + \frac{u_2'^2}{2} \qquad (7)$$

Also equation (1) and (5) can be manipulated to obtain u_1' and u_2' in terms of ρ_1, ρ_2, P_1 and P_2.

i.e. $u_1' = \sqrt{\frac{\rho_2}{\rho_1}\left[\frac{P_2-P_1}{\rho_2-\rho_1}\right]}$ (8) and $u_2' = \sqrt{\frac{\rho_1}{\rho_2}\left[\frac{P_2-P_1}{\rho_2-\rho_1}\right]}$ (9) .

Substituting for u_1' and u_2' in (7) from (8) and (9) gives after some algebra

$$\frac{P_2}{P_1} = \frac{1 - h^2\left[\rho^2/\rho_1\right]}{\rho^2/\rho_1 - h^2} \qquad (10)$$

where $$h^2 = \frac{\gamma+1}{\gamma-1} .$$

Now defining the relative normal Mach number by $M_N^2 = \frac{u'^2}{C^2}$, and defining $C^2 = \frac{\gamma P}{\rho}$

gives $$M_N^2 = \frac{\rho u'^2}{\gamma P} . \qquad (11)$$

Substituting (11) into the momentum equation (5) gives

$$P_2 - P_1 = \gamma P_1 M_1^2 - \gamma P_2 M_2^2 . \qquad (12)$$

Also the energy equation (7) can be rearranged as

$$u_1'^2 - u_2'^2 = (u_1' - u_2')(u_1' + u_2') = \frac{2\gamma}{\gamma-1}\left[\frac{P_2}{\rho_2} - \frac{P_1}{\rho_1}\right] \qquad (13)$$

and the mass equation (1) and the momentum equation (5) can be combined to give

$$P_2 - P_1 = \rho_1 u_1' (u_1' - u_2') \qquad (14)$$

and substituting from (14) for $(u_1' - u_2')$ into (13) gives

$$\frac{P_2 - P_1}{\rho_1 u_1'}(u_1' + u_2') = \frac{2\gamma}{\gamma-1}\left[\frac{P_2}{\rho_2} - \frac{P_1}{\rho_1}\right] = \frac{2\gamma}{\gamma-1}\left[\frac{P_2 u_2'}{\rho_2 u_1'} - \frac{P_1 u_1'}{\rho_1 u_1'}\right]. \qquad (15)$$

Multiplying through by $\rho_1 u_1' = \rho_2 u_2'$ and simplifying gives

$$P_2\left[u_1' - u_2' h^2\right] - P_1\left[u_2' - h^2 u_1'\right] = 0 .$$

Now substituting in for u_1' and u_2' from (11) gives

$$P_2\left[\frac{\gamma P_1 M_1^2}{\rho_1 u_1} - \frac{h^2 \gamma P_2 M_2^2}{\rho_2 u_2}\right] - P_1\left[\frac{\gamma P_2 M_2^2}{\rho_2 u_2} - \frac{h^2 \gamma P_1 M_1^2}{\rho_1 u_1}\right] = 0 .$$

Multiplying through again by $\rho_1 u_1 = \rho_2 u_2$ gives

$$P_1 M_1^2 \left[P_1 h^2 + P_2\right] - P_2 M_2^2 \left[P_2 h^2 + P_1\right] . \qquad (16)$$

Now equations (12) and (16) are simultaneous equation in M_1^2, M_2^2 . Solving eventually yields:

$$M_1^2 = \left[\frac{\gamma+1}{2\gamma}\right] \frac{P_2}{P_1} + \frac{\gamma-1}{2\gamma} \tag{17}$$

$$M_2^2 = \left[\frac{\gamma+1}{2\gamma}\right] \frac{P_1}{P_2} + \frac{\gamma-1}{2\gamma} \tag{18}$$

and substituting from (10) for P_2/P_1 into (17) after some algebra gives

$$\frac{\rho_2}{\rho_1} = \frac{(\gamma+1)M_1^2}{(\gamma-1)M_1^2 + 2} \tag{19}$$

as in Paisley [Ref 2],

where $$M_1^2 = \frac{u_1^{2\prime}}{C_1^2} \implies M_1 = \frac{u_1'}{C_1} = \frac{u_1 - S}{C_1}$$

and finally $$S = u_1 - M_1 C_1 \ . \tag{20}$$

APPENDIX 2

Eigenvalues, Eigenvectors and Roe Averages of 2D H System

$$\frac{\partial \underline{u}}{\partial t} + \frac{\partial \underline{F}}{\partial x} + \frac{\partial \underline{G}}{\partial y} = \underline{0}$$

$$\Rightarrow \quad \frac{\partial \underline{u}}{\partial t} + \frac{\partial \underline{F}}{\partial \underline{u}} \frac{\partial \underline{u}}{\partial x} + \frac{\partial \underline{G}}{\partial \underline{u}} \frac{\partial \underline{u}}{\partial y} = \underline{0}$$

where $\underline{u} = \begin{vmatrix} \rho \\ \rho u \\ \rho v \end{vmatrix}$ $\underline{F} = \begin{vmatrix} \rho u \\ \rho u^2 + P \\ puv \end{vmatrix}$ $\underline{G} = \begin{vmatrix} \rho v \\ \rho uv \\ \rho v^2 + P \end{vmatrix}$

$$\frac{\partial \underline{F}}{\partial \underline{u}} = \begin{bmatrix} 0 & 1 & 0 \\ \frac{1}{\gamma} - \left[\frac{1+\gamma}{2\gamma}\right]u^2 + \left[\frac{\gamma-1}{2\gamma}\right]v^2 & \left[\frac{1+\gamma}{\gamma}\right]u & \left[\frac{1-\gamma}{\gamma}\right]v \\ -uv & v & u \end{bmatrix}$$

and $$\frac{\partial \underline{G}}{\partial \underline{u}} = \begin{bmatrix} 0 & 0 & 1 \\ -uv & v & u \\ \frac{1}{\gamma} + \left[\frac{1-\gamma}{2\gamma}\right]u^2 - \left[\frac{\gamma+1}{2\gamma}\right]v^2 & \left[\frac{1-\gamma}{\gamma}\right]u & \left[\frac{\gamma+1}{\gamma}\right]v \end{bmatrix}$$

The eigenvalues of $\frac{\partial \underline{F}}{\partial \underline{u}}$ are

$$\lambda_1 = u, \quad \lambda_2, \lambda_3 = \left[\frac{1+\gamma}{2\gamma}\right]u \pm \sqrt{\left[\frac{\gamma-1}{2\gamma}\right]^2 u^2 + \frac{a^2}{\gamma}}$$

and the corresponding eigenvectors of $\frac{\partial \underline{F}}{\partial \underline{u}}$ are

$$\underline{e}_1 = \begin{vmatrix} v \\ uv \\ \frac{1}{\gamma-1} - \frac{u^2}{2} + \frac{v^2}{2} \end{vmatrix}, \quad \underline{e}_2 = \begin{vmatrix} 1 \\ \lambda_2 \\ v \end{vmatrix}, \quad \underline{e}_3 = \begin{vmatrix} 1 \\ \lambda_3 \\ v \end{vmatrix}.$$

The eigenvalues of $\frac{\partial \underline{G}}{\partial \underline{u}}$ are

$$\lambda_1 = v, \quad \lambda_2, \lambda_3 = \left[\frac{1+\gamma}{2\gamma}\right]v \pm \sqrt{\left[\frac{\gamma-1}{2\gamma}\right]^2 v^2 + \frac{a^2}{\gamma}}$$

and the corresponding eigenvectors of $\frac{\partial \underline{G}}{\partial \underline{u}}$ are

$$\underline{e}_1 = \begin{vmatrix} u \\ \frac{1}{\gamma-1} + \frac{u^2}{2} - \frac{v^2}{2} \\ uv \end{vmatrix}, \quad \underline{e}_2 = \begin{vmatrix} 1 \\ u \\ \lambda_2 \end{vmatrix}, \quad \underline{e}_3 = \begin{vmatrix} 1 \\ u \\ \lambda_3 \end{vmatrix}.$$

When splitting the $\underline{F}$ fluxes, the α coefficients in the expansion of $\Delta \underline{u} = \sum_{i=1}^{3} \tilde{\alpha}_i \tilde{\underline{e}}_i$ are:

$$\tilde{\alpha}_1 = \frac{\tilde{\rho}\, \Delta v}{\frac{1}{\gamma-1} - \tfrac{1}{2}(\tilde{u}^2+\tilde{v}^2)}$$

$$\tilde{\alpha}_2 = \frac{\tilde{\lambda}_3(\tilde{\alpha}_1\tilde{v}-\Delta\rho) + \Delta(\rho u) - \tilde{\alpha}_1\tilde{u}\tilde{v}}{2\sqrt{\left[\frac{\gamma-1}{2\gamma}\right]^2\tilde{u}^2 + \tilde{a}^2/\gamma}}$$

$$\tilde{\alpha}_3 = \frac{\tilde{\alpha}_1\tilde{u}\tilde{v} - \Delta(\rho u) + \tilde{\lambda}_2(\Delta\rho - \tilde{\alpha}_1\tilde{v})}{2\sqrt{\left[\frac{\gamma-1}{2\gamma}\right]^2\tilde{u}^2 + \tilde{a}^2/\gamma}}$$

where $\tilde{\rho}$, $\tilde{u}$, $\tilde{v}$ are the Roe averaged values, and $\tilde{a}^2 = 1 - \frac{(\gamma-1)}{2}(\tilde{u}^2+\tilde{v}^2)$ i.e. the Roe averaged sound speed, and $\Delta(\cdot) = \cdot R - \cdot L$.

N.B. $\tilde{\lambda}_2$ and $\tilde{\lambda}_3$ are the eigenvalues of $\partial\tilde{F}/\partial\tilde{u}$ chosen so that $\tilde{\lambda}_2$ corresponds to the positive root, whilst $\tilde{\lambda}_3$ corresponds to the negative root. If reversed then the sign of $\tilde{\alpha}_2$ and $\tilde{\alpha}_3$ are also reversed.

Also the Roe averaged values of ρ, u and v used in the eigenvalues, eigenvectors and α's are

$$\tilde{\rho} = \sqrt{\rho^R}\sqrt{\rho^L}$$

$$\tilde{u} = \frac{\sqrt{\rho^R}\,u^R + \sqrt{\rho^L}\,u^L}{\sqrt{\rho^R} + \sqrt{\rho^L}}$$

$$\tilde{v} = \frac{\sqrt{\rho^R}\,v^R + \sqrt{\rho^L}\,v^L}{\sqrt{\rho^R} + \sqrt{\rho^L}} .$$

FIG. 1

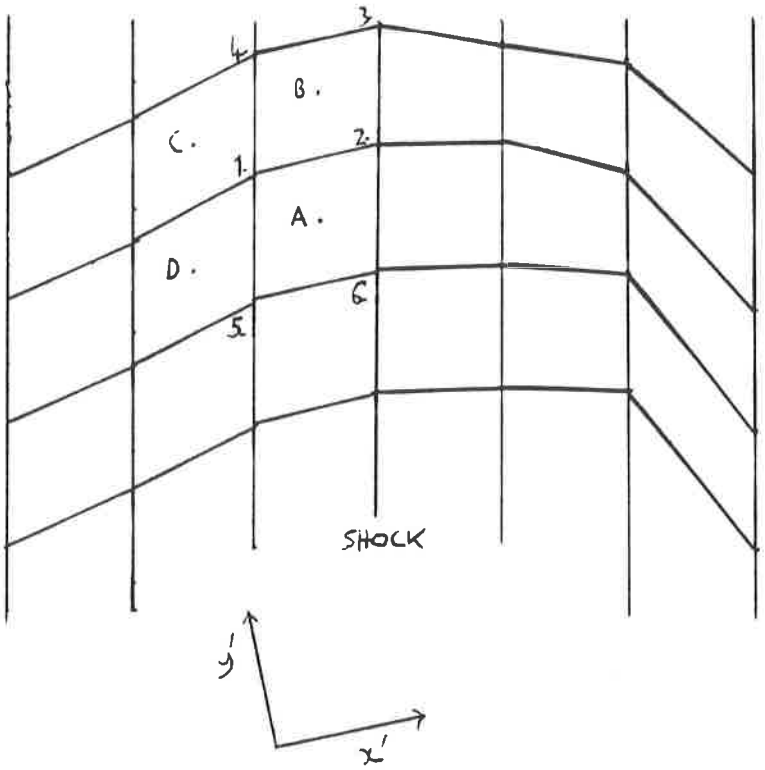

FIG. 2

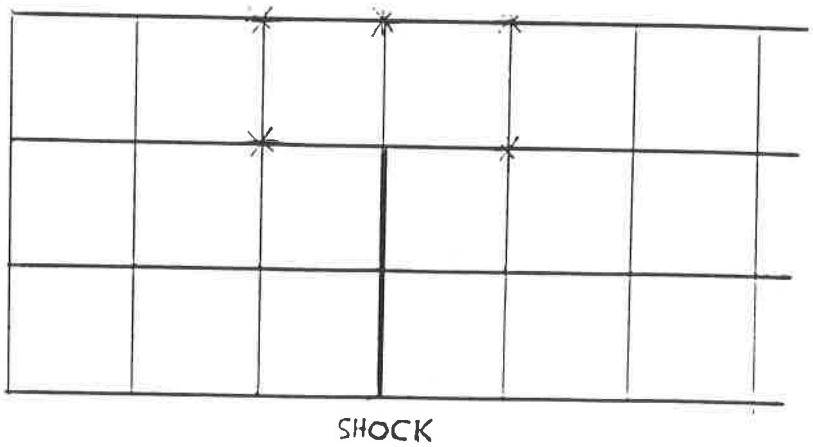

* VISCOSITY ADDED

FIG.3

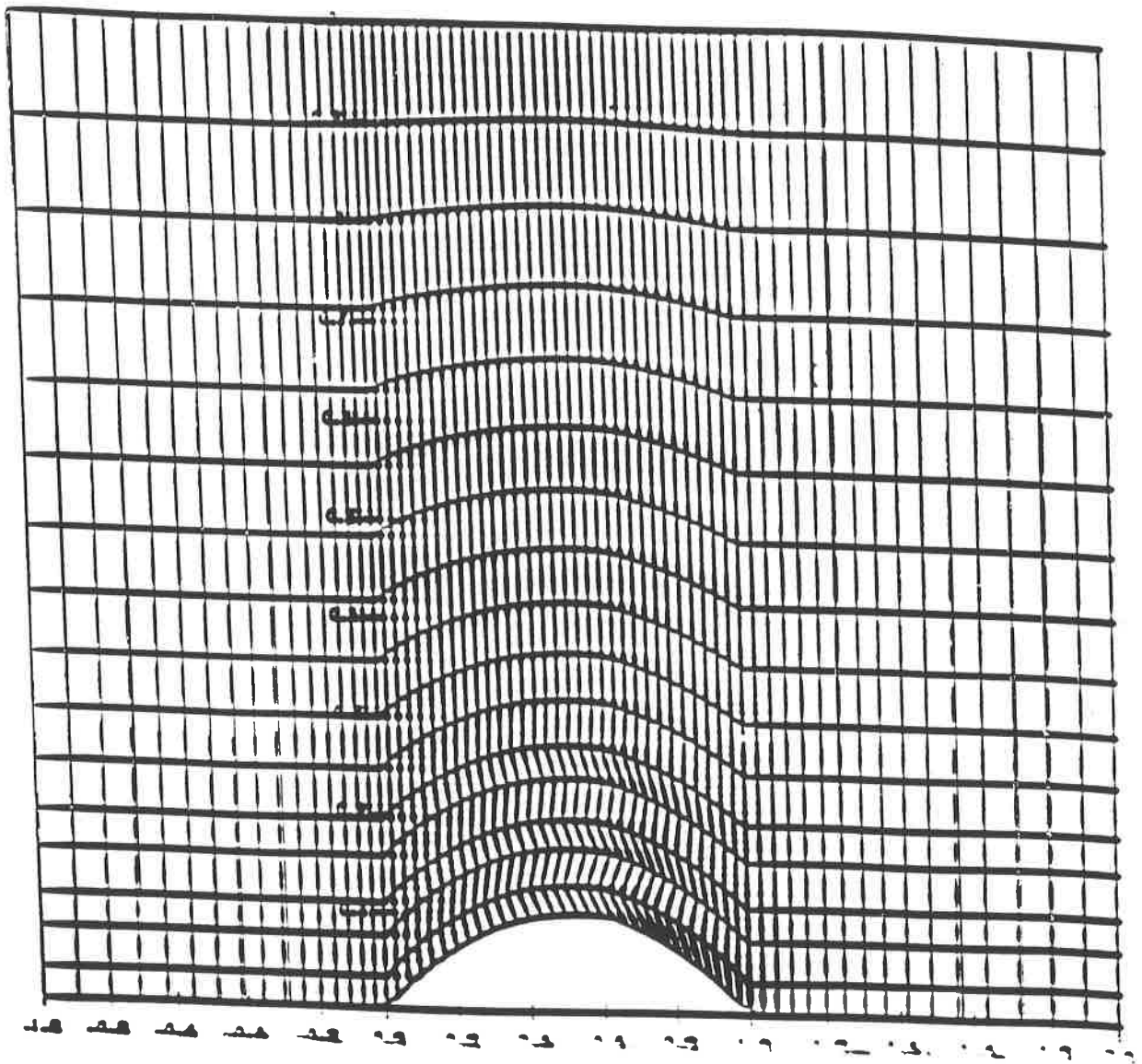

RESULT USING ORIGINAL L.S CUBIC TO APPROXIMATE SHOCK ANGLES AND SHOCK SHAPE.

TABLE.1

```
   ixs is  39 jms is   7
   1  0.6364  0.7358 -0.1057 alfa= 1.428 s=0.045146  ml= 1.317  xs=0.685
   1  0.9633  0.7504 -0.1078 alfa= 1.428 s=0.045146  ml= 1.317  xs=0.685
   2  0.6648  0.7464 -0.1007 alfa= 1.495 s=0.024561  ml= 1.283  xs=0.688
   2  0.9775  0.7525 -0.1218 alfa= 1.495 s=0.024561  ml= 1.283  xs=0.688
   3  0.6937  0.7584 -0.0906 alfa= 1.542 s=0.021218  ml= 1.236  xs=0.690
   3  0.9647  0.7634 -0.1178 alfa= 1.542 s=0.021218  ml= 1.236  xs=0.690
   4  0.7277  0.7764 -0.0842 alfa= 1.564 s=0.023568  ml= 1.190  xs=0.690
   4  0.9545  0.7816 -0.1087 alfa= 1.564 s=0.023568  ml= 1.190  xs=0.690
   5  0.7554  0.7831 -0.0788 alfa= 1.552 s=0.016957  ml= 1.154  xs=0.691
   5  0.9473  0.7861 -0.0951 alfa= 1.552 s=0.016957  ml= 1.154  xs=0.691
   6  0.7955  0.7977 -0.0795 alfa= 1.500 s=0.007544  ml= 1.120  xs=0.692
   6  0.9543  0.7986 -0.0841 alfa= 1.500 s=0.007544  ml= 1.120  xs=0.692
   7  0.8436  0.8074 -0.1045 alfa= 1.399 s=-.013871  ml= 1.084  xs=0.698
   7  0.9688  0.8066 -0.0991 alfa= 1.399 s=-.013871  ml= 1.084  xs=0.698
iteration     20
    ixs is  39 jms is   7
   1  0.6347  0.7289 -0.1109 alfa= 1.420 s=0.000969  ml= 1.358  xs=0.696
   1  1.0259  0.7292 -0.1109 alfa= 1.420 s=0.000969  ml= 1.358  xs=0.696
   2  0.6642  0.7449 -0.1058 alfa= 1.531 s=-.000467  ml= 1.307  xs=0.699
   2  1.0156  0.7431 -0.1461 alfa= 1.531 s=-.000467  ml= 1.307  xs=0.699
   3  0.6999  0.7613 -0.1017 alfa= 1.623 s=-.000169  ml= 1.238  xs=0.698
   3  0.9853  0.7643 -0.1594 alfa= 1.623 s=-.000169  ml= 1.238  xs=0.698
   4  0.7387  0.7774 -0.0953 alfa= 1.689 s=0.000753  ml= 1.169  xs=0.695
   4  0.9507  0.7838 -0.1484 alfa= 1.689 s=0.000753  ml= 1.169  xs=0.695
   5  0.7777  0.7895 -0.0906 alfa= 1.723 s=-.004071  ml= 1.113  xs=0.690
   5  0.9281  0.7950 -0.1306 alfa= 1.723 s=-.004071  ml= 1.113  xs=0.690
   6  0.8183  0.7983 -0.0826 alfa= 1.719 s=-.011856  ml= 1.070  xs=0.683
   6  0.9194  0.8008 -0.1072 alfa= 1.719 s=-.011856  ml= 1.070  xs=0.683
   7  0.8617  0.8057 -0.0798 alfa= 1.666 s=-.020239  ml= 1.038  xs=0.678
   7  0.9242  0.8056 -0.0912 alfa= 1.666 s=-.020239  ml= 1.038  xs=0.678
iteration     480
rms shock density residual = 0.050852942149
rms shock density update = 0.005579649329
i=  39 j=   7 iu=   1 max d  update= 0.009523285607
rms density update =  0.001168375324
i=  39 j=   5 iu=   1 max d resid= 0.101608033139
rms density residual =  0.008755097991
     ixs is  39 jms is   6
   1  0.6373  0.7322 -0.1117 alfa= 1.419 s=0.004082  ml= 1.356  xs=0.696
   1  1.0257  0.7337 -0.1120 alfa= 1.419 s=0.004082  ml= 1.356  xs=0.696
   2  0.6656  0.7472 -0.1056 alfa= 1.530 s=0.004103  ml= 1.304  xs=0.699
   2  1.0115  0.7470 -0.1447 alfa= 1.530 s=0.004103  ml= 1.304  xs=0.699
   3  0.7010  0.7637 -0.1002 alfa= 1.646 s=0.006472  ml= 1.228  xs=0.699
   3  0.9713  0.7701 -0.1607 alfa= 1.646 s=0.006472  ml= 1.228  xs=0.699
   4  0.7374  0.7790 -0.0926 alfa= 1.764 s=0.006566  ml= 1.144  xs=0.694
   4  0.9152  0.7912 -0.1492 alfa= 1.764 s=0.006566  ml= 1.144  xs=0.694
   5  0.7742  0.7921 -0.0833 alfa= 1.874 s=-.008469  ml= 1.073  xs=0.684
   5  0.8723  0.8032 -0.1218 alfa= 1.874 s=-.008469  ml= 1.073  xs=0.684
   6  0.8083  0.8010 -0.0729 alfa= 1.977 s=-.041193  ml= 1.023  xs=0.670
   6  0.8520  0.8076 -0.0927 alfa= 1.977 s=-.041193  ml= 1.023  xs=0.670
iteration    1000
rms shock density residual = 0.089625217221
rms shock density update = 0.029451717574
i=  43 j=   1 iu=   1 max d  update= 0.090948536752
rms density update =  0.010457636296
i=  40 j=   4 iu=   1 max d resid= 0.236212594318
```

RESULT USING NEW L.S CUBIC TO APPROXIMATE SHOCK ANGLES ONLY.

TABLE.2

```
 ixs is  39 jms is   7
  1  0.6345  0.7333 -0.1070 alfa= 1.426 s=0.042662  ml= 1.319  xs=0.688
  1  0.9644  0.7472 -0.1090 alfa= 1.426 s=0.042662  ml= 1.319  xs=0.688
  2  0.6654  0.7470 -0.0996 alfa= 1.514 s=0.022437  ml= 1.284  xs=0.688
  2  0.9799  0.7525 -0.1271 alfa= 1.514 s=0.022437  ml= 1.284  xs=0.688
  3  0.6956  0.7608 -0.0895 alfa= 1.574 s=0.018989  ml= 1.234  xs=0.688
  3  0.9669  0.7661 -0.1254 alfa= 1.574 s=0.018989  ml= 1.234  xs=0.688
  4  0.7281  0.7769 -0.0837 alfa= 1.596 s=0.020963  ml= 1.189  xs=0.689
  4  0.9541  0.7825 -0.1157 alfa= 1.596 s=0.020963  ml= 1.189  xs=0.689
  5  0.7545  0.7819 -0.0798 alfa= 1.573 s=0.015833  ml= 1.153  xs=0.691
  5  0.9446  0.7849 -0.1003 alfa= 1.573 s=0.015833  ml= 1.153  xs=0.691
  6  0.7956  0.7975 -0.0806 alfa= 1.492 s=0.008661  ml= 1.119  xs=0.694
  6  0.9522  0.7986 -0.0842 alfa= 1.492 s=0.008661  ml= 1.119  xs=0.694
  7  0.8443  0.8081 -0.1045 alfa= 1.345 s=-.016893  ml= 1.083  xs=0.697
  7  0.9696  0.8087 -0.0926 alfa= 1.345 s=-.016893  ml= 1.083  xs=0.697
iteration      20
 ixs is  39 jms is   7
  1  0.6336  0.7274 -0.1121 alfa= 1.418 s=0.000952  ml= 1.358  xs=0.698
  1  1.0242  0.7278 -0.1122 alfa= 1.418 s=0.000952  ml= 1.358  xs=0.698
  2  0.6652  0.7465 -0.1034 alfa= 1.557 s=-.000488  ml= 1.305  xs=0.694
  2  1.0138  0.7456 -0.1520 alfa= 1.557 s=-.000488  ml= 1.305  xs=0.694
  3  0.7004  0.7626 -0.0977 alfa= 1.658 s=-.001513  ml= 1.233  xs=0.692
  3  0.9802  0.7679 -0.1630 alfa= 1.658 s=-.001513  ml= 1.233  xs=0.692
  4  0.7383  0.7779 -0.0926 alfa= 1.717 s=-.001578  ml= 1.165  xs=0.692
  4  0.9468  0.7860 -0.1498 alfa= 1.717 s=-.001578  ml= 1.165  xs=0.692
  5  0.7775  0.7888 -0.0915 alfa= 1.724 s=-.004175  ml= 1.112  xs=0.691
  5  0.9260  0.7944 -0.1314 alfa= 1.724 s=-.004175  ml= 1.112  xs=0.691
  6  0.8203  0.7977 -0.0862 alfa= 1.669 s=-.005023  ml= 1.070  xs=0.689
  6  0.9192  0.7991 -0.1059 alfa= 1.669 s=-.005023  ml= 1.070  xs=0.689
  7  0.8641  0.8058 -0.0822 alfa= 1.524 s=-.010317  ml= 1.042  xs=0.680
  7  0.9289  0.8050 -0.0855 alfa= 1.524 s=-.010317  ml= 1.042  xs=0.680
iteration     480
rms shock density residual = 0.050318992270
rms shock density update = 0.003893393168
i=  39 j=   7 iu=   1 max d  update= 0.005701700411
rms density update =  0.001004170375
i=  39 j=   5 iu=   1 max d resid= 0.093673418141
rms density residual =  0.008949692526
 ixs is  39 jms is   7
  1  0.6307  0.7257 -0.1127 alfa= 1.417 s=0.000617  ml= 1.363  xs=0.700
  1  1.0250  0.7259 -0.1128 alfa= 1.417 s=0.000617  ml= 1.363  xs=0.700
  2  0.6628  0.7456 -0.1030 alfa= 1.568 s=0.000568  ml= 1.306  xs=0.695
  2  1.0109  0.7456 -0.1559 alfa= 1.568 s=0.000568  ml= 1.306  xs=0.695
  3  0.6977  0.7618 -0.0960 alfa= 1.679 s=0.000090  ml= 1.230  xs=0.692
  3  0.9722  0.7693 -0.1654 alfa= 1.679 s=0.000090  ml= 1.230  xs=0.692
  4  0.7346  0.7771 -0.0904 alfa= 1.743 s=0.000782  ml= 1.160  xs=0.692
  4  0.9347  0.7876 -0.1500 alfa= 1.743 s=0.000782  ml= 1.160  xs=0.692
  5  0.7721  0.7880 -0.0876 alfa= 1.754 s=-.000655  ml= 1.107  xs=0.689
  5  0.9122  0.7956 -0.1286 alfa= 1.754 s=-.000655  ml= 1.107  xs=0.689
  6  0.8136  0.7972 -0.0818 alfa= 1.701 s=-.000621  ml= 1.068  xs=0.687
  6  0.9074  0.7998 -0.1029 alfa= 1.701 s=-.000621  ml= 1.068  xs=0.687
  7  0.8570  0.8063 -0.0768 alfa= 1.551 s=-.001417  ml= 1.041  xs=0.675
  7  0.9171  0.8061 -0.0811 alfa= 1.551 s=-.001417  ml= 1.041  xs=0.675
iteration    1000
rms shock density residual = 0.051741004135
rms shock density update = 0.000491599775
i=  37 j=  17 iu=   1 max d  update= 0.001728132211
rms density update =  0.000306846902
i=  40 j=   1 iu=   1 max d resid= 0.092021579401
rms density residual =  0.000750251317
```

TABLE 3

```
 ixs is  39 jms is
   1  0.6230  0.7222  -0.1566  alfa=  1.[illegible]  s=2.[illegible]45715  ml=  1.316  xs=0.687
   1  1.7577  0.7485  -0.1257  alfa=  [illegible]  s=0.[illegible]437[illegible]  ml=  1.31[illegible]  xs=0.687
   2  2.5855  0.7472  -0.0994  alfa=  1.[illegible]  s=0.[illegible]  ml=  1.[illegible]  xs=0.687
   2  0.9765  0.7536  -0.1178  alfa=  1.394  s=0.[illegible]  ml=  1.[illegible]  xs=0.687
   3  0.6985  0.7607  -0.0695  alfa=  1.[illegible]  s=0.[illegible]  ml=  1.[illegible]  xs=0.687
   3  0.9662  0.7660  -0.1157  alfa=  1.542  s=0.022277  ml=  1.[illegible]  xs=0.687
   4  2.7280  0.7769  -0.0837  alfa=  1.563  s=0.023461  ml=  1.191  xs=0.689
   4  0.9556  0.7820  -0.1077  alfa=  1.563  s=0.023461  ml=  1.191  xs=0.689
   5  2.7543  0.7819  -0.0797  alfa=  1.551  s=0.016145  ml=  1.155  xs=0.691
   5  0.9475  0.7847  -0.0958  alfa=  1.551  s=0.016145  ml=  1.155  xs=0.691
   6  0.7953  0.7973  -0.0806  alfa=  1.498  s=0.006993  ml=  1.120  xs=0.694
   6  0.9550  0.7901  -0.0848  alfa=  1.498  s=0.006993  ml=  1.120  xs=0.694
   7  0.8441  0.8030  -0.1043  alfa=  1.396  s=-.014086  ml=  1.084  xs=0.697
   7  0.9693  0.8073  -0.0980  alfa=  1.396  s=-.014088  ml=  1.084  xs=0.697
iteration     20
     ixs is  39 jms is   7
   1  0.6309  0.7236  -0.1141  alfa=  1.415  s=0.008249  ml=  1.354  xs=0.702
   1  1.0116  0.7257  -0.1146  alfa=  1.415  s=0.008247  ml=  1.354  xs=0.702
   2  0.6627  0.7447  -0.1048  alfa=  1.533  s=0.005189  ml=  1.304  xs=0.698
   2  1.0066  0.7453  -0.1465  alfa=  1.533  s=0.005189  ml=  1.304  xs=0.698
   3  0.5966  0.7620  -0.0973  alfa=  1.641  s=0.002750  ml=  1.235  xs=0.694
   3  0.9790  0.7669  -0.1579  alfa=  1.641  s=0.002750  ml=  1.235  xs=0.694
   4  0.7362  0.7772  -0.0916  alfa=  1.705  s=0.001555  ml=  1.169  xs=0.693
   4  0.9474  0.7850  -0.1467  alfa=  1.705  s=0.001555  ml=  1.169  xs=0.693
   5  0.7748  0.7888  -0.0890  alfa=  1.724  s=-.002153  ml=  1.113  xs=0.690
   5  0.9263  0.7947  -0.1292  alfa=  1.724  s=-.002153  ml=  1.113  xs=0.690
   6  0.8165  0.7978  -0.0825  alfa=  1.691  s=-.008540  ml=  1.073  xs=0.686
   6  0.9186  0.7999  -0.1046  alfa=  1.691  s=-.008540  ml=  1.073  xs=0.686
   7  0.8606  0.8062  -0.0892  alfa=  1.664  s=-.010795  ml=  1.047  xs=0.679
   7  0.9265  0.8084  -0.0971  alfa=  1.664  s=-.[illegible]  ml=  1.047  xs=0.677
```

```
 ixs is  37 jms is   7
   1  0.6230  0.7222  -0.1172  alfa=  1.410  s=0.021382  ml=  1.371  xs=0.708
   1  1.0116  0.7244  -0.1171  alfa=  1.410  s=0.021382  ml=  1.371  xs=0.708
   2  0.6562  0.7433  -0.1364  alfa=  1.526  s=0.011704  ml=  1.316  xs=0.702
   2  1.0027  0.7439  -0.1377  alfa=  1.526  s=0.011704  ml=  1.316  xs=0.702
   3  0.6792  0.7606  -0.0978  alfa=  1.[illegible]  s=0.[illegible]  ml=  1.[illegible]  xs=0.697
   3  0.9662  0.7660  -0.1157  alfa=  1.[illegible]  s=0.[illegible]  ml=  1.[illegible]  xs=0.697
   4  0.7280  0.7769  -0.0837  alfa=  1.[illegible]  s=0.[illegible]  ml=  1.[illegible]  xs=0.693
   4  0.9556  0.7820  -0.1077  alfa=  1.[illegible]  s=0.[illegible]  ml=  1.[illegible]  xs=0.693
   5  0.7543  0.7819  -0.0797  alfa=  1.[illegible]  s=0.[illegible]  ml=  1.[illegible]  xs=0.691
   5  0.9475  0.7847  -0.0958  alfa=  1.[illegible]  s=0.[illegible]  ml=  1.[illegible]  xs=0.691
   6  0.7953  0.7973  -0.0806  alfa=  1.[illegible]  s=0.[illegible]  ml=  1.[illegible]  xs=0.694
   6  0.9550  0.7901  -0.0848  alfa=  1.[illegible]  s=0.[illegible]  ml=  1.[illegible]  xs=0.694
   7  0.8441  0.8030  -0.1043  alfa=  1.[illegible]  s=0.[illegible]  ml=  1.[illegible]  xs=0.697
   7  0.9693  0.8073  -0.0980  alfa=  1.[illegible]  s=0.[illegible]  ml=  1.[illegible]  xs=0.697
```

```
    ixs is  39 jms is   7
  1  0.6227  0.7205 -0.1175 alfa= 1.409 s=0.000561  ml= 1.376  xs=0.709
  1  1.0259  0.7207 -0.1176 alfa= 1.409 s=0.000561  ml= 1.376  xs=0.709
  2  0.6562  0.7416 -0.1071 alfa= 1.553 s=0.001025  ml= 1.316  xs=0.704
  2  1.0129  0.7410 -0.1562 alfa= 1.553 s=0.001025  ml= 1.316  xs=0.704
  3  0.6929  0.7597 -0.0980 alfa= 1.675 s=0.000376  ml= 1.237  xs=0.698
  3  0.9742  0.7672 -0.1692 alfa= 1.675 s=0.000376  ml= 1.237  xs=0.698
  4  0.7299  0.7751 -0.0917 alfa= 1.751 s=0.000647  ml= 1.163  xs=0.697
  4  0.9323  0.7866 -0.1542 alfa= 1.751 s=0.000647  ml= 1.163  xs=0.697
  5  0.7672  0.7870 -0.0866 alfa= 1.776 s=0.001006  ml= 1.105  xs=0.692
  5  0.9034  0.7960 -0.1292 alfa= 1.776 s=0.001006  ml= 1.105  xs=0.692
  6  0.8068  0.7966 -0.0782 alfa= 1.742 s=0.000896  ml= 1.066  xs=0.685
  6  0.8965  0.8007 -0.1015 alfa= 1.742 s=0.000896  ml= 1.066  xs=0.685
  7  0.8495  0.8059 -0.0744 alfa= 1.625 s=0.000897  ml= 1.041  xs=0.676
  7  0.9072  0.8063 -0.0824 alfa= 1.625 s=0.000897  ml= 1.041  xs=0.676
iteration =  2880
rms shock density residual = 0.053380414356
rms shock density update = 0.000205327174
i=  39 j=   4 iu=   1 max d update= 0.000271189583
rms density update = 0.000045570252
i=  40 j=   4 iu=   1 max d resid= 0.104641625399
rms density residual =  0.009634351070
    ixs is  39 jms is   7
  1  0.6218  0.7202 -0.1176 alfa= 1.409 s=-.000472  ml= 1.379  xs=0.709
  1  1.0285  0.7200 -0.1176 alfa= 1.409 s=-.000472  ml= 1.379  xs=0.709
  2  0.6550  0.7407 -0.1077 alfa= 1.551 s=0.000715  ml= 1.318  xs=0.706
  2  1.0135  0.7400 -0.1586 alfa= 1.551 s=0.000715  ml= 1.318  xs=0.706
  3  0.6920  0.7593 -0.0982 alfa= 1.672 s=0.000551  ml= 1.239  xs=0.699
  3  0.9753  0.7666 -0.1691 alfa= 1.672 s=0.000551  ml= 1.239  xs=0.699
  4  0.7293  0.7749 -0.0919 alfa= 1.747 s=0.000392  ml= 1.166  xs=0.698
  4  0.9349  0.7862 -0.1548 alfa= 1.747 s=0.000392  ml= 1.166  xs=0.698
  5  0.7667  0.7868 -0.0872 alfa= 1.772 s=0.000392  ml= 1.107  xs=0.693
  5  0.9060  0.7957 -0.1304 alfa= 1.772 s=0.000392  ml= 1.107  xs=0.693
  6  0.8065  0.7966 -0.0789 alfa= 1.740 s=0.000353  ml= 1.068  xs=0.686
  6  0.8983  0.8006 -0.1026 alfa= 1.740 s=0.000353  ml= 1.068  xs=0.686
  7  0.8493  0.8057 -0.0751 alfa= 1.627 s=0.000265  ml= 1.041  xs=0.677
  7  0.9081  0.8062 -0.0834 alfa= 1.627 s=0.000265  ml= 1.041  xs=0.677
iteration =  3980
rms shock density residual = 0.053034306666
rms shock density update = 0.000151863634
i=  39 j=   1 iu=   1 max d update= 0.000156253526
rms density update =  0.000022945044
i=  40 j=   4 iu=   1 max d resid= 0.101315340710
rms density residual =  0.009598232011
    ixs is  39 jms is   7
  1  0.6221  0.7208 -0.1163 alfa= 1.410 s=-.001457  ml= 1.381  xs=0.700
  1  1.0210  0.7202 -0.1167 alfa= 1.410 s=-.001457  ml= 1.381  xs=0.700
  2  0.6546  0.7403 -0.1050 alfa= 1.547 s=0.000125  ml= 1.320  xs=0.706
  2  1.0146  0.7392 -0.1577 alfa= 1.547 s=0.000125  ml= 1.320  xs=0.706
  3  0.6917  0.7590 -0.0966 alfa= 1.666 s=0.000417  ml= 1.241  xs=0.700
  3  0.9770  0.7659 -0.1686 alfa= 1.666 s=0.000417  ml= 1.241  xs=0.700
  4  0.7291  0.7749 -0.0922 alfa= 1.744 s=0.000337  ml= 1.167  xs=0.699
  4  0.9364  0.7859 -0.1551 alfa= 1.744 s=0.000337  ml= 1.167  xs=0.699
  5  0.7664  0.7868 -0.0871 alfa= 1.775 s=-.000252  ml= 1.108  xs=0.693
  5  0.9052  0.7958 -0.1309 alfa= 1.775 s=-.000252  ml= 1.108  xs=0.693
  6  0.8057  0.7966 -0.0792 alfa= 1.736 s=-.000311  ml= 1.067  xs=0.686
  6  0.8974  0.8007 -0.1027 alfa= 1.736 s=-.000311  ml= 1.067  xs=0.686
  7  0.8491  0.8058 -0.0752 alfa= 1.627 s=-.000231  ml= 1.040  xs=0.676
  7  0.9081  0.8062 -0.0836 alfa= 1.627 s=-.000231  ml= 1.040  xs=0.676
iteration =  4980
rms shock density residual = 0.052963377227
rms shock density update = 0.000077776744
i=  39 j=   2 iu=   1 max d update= 0.000080201225
rms density update =  0.000022945044
i=  40 j=   4 iu=   1 max d resid= 0.100235161571
rms density residual =  0.009583742575
    ixs is  39 jms is   7
  1  0.6217  0.7214 -0.1161 alfa= 1.411 s=-.001707  ml= 1.381  xs=0.707
  1  1.0284  0.7206 -0.1160 alfa= 1.411 s=-.001707  ml= 1.381  xs=0.707
```

```
i=  [illegible] j=   7 iu=   1 max d  update= 0.200622201956
rms density update =  0.000860674683
i=  40 j=   4 iu=   1 max d resid= 0.103335654591
rms density residual =  0.009659407576
     ixs is  39 jms is   7
  1  0.6227  0.7214 -0.1161 alfa= 1.411 s=-.001929  ml= 1.381  xs=0.707
  1  1.0323  0.7206 -0.1160 alfa= 1.411 s=-.001929  ml= 1.381  xs=0.707
  2  0.6547  0.7402 -0.1079 alfa= 1.545 s=-.000246  ml= 1.320  xs=0.706
  2  1.0153  0.7389 -0.1569 alfa= 1.545 s=-.000246  ml= 1.320  xs=0.706
  3  0.6917  0.7590 -0.0987 alfa= 1.664 s=0.000153  ml= 1.242  xs=0.700
  3  0.9730  0.7655 -0.1684 alfa= 1.664 s=0.000153  ml= 1.242  xs=0.700
  4  0.7291  0.7748 -0.0924 alfa= 1.746 s=0.000055  ml= 1.167  xs=0.699
  4  0.9361  0.7860 -0.1555 alfa= 1.746 s=0.000055  ml= 1.167  xs=0.699
  5  0.7661  0.7863 -0.0866 alfa= 1.794 s=-.001002  ml= 1.106  xs=0.693
  5  0.9037  0.7962 -0.1307 alfa= 1.794 s=-.001002  ml= 1.106  xs=0.693
  6  0.8047  0.7966 -0.0767 alfa= 1.777 s=-.003314  ml= 1.064  xs=0.684
  6  0.8922  0.8016 -0.1023 alfa= 1.777 s=-.003314  ml= 1.064  xs=0.684
  7  0.8466  0.8059 -0.0716 alfa= 1.706 s=-.004647  ml= 1.036  xs=0.674
  7  0.8994  0.8072 -0.0827 alfa= 1.706 s=-.004647  ml= 1.036  xs=0.674
iteration   5480
rms shock density residual = 0.055493669964
rms shock density update = 0.000882225743
i=  40 j=   7 iu=   1 max d  update= 0.001478990860
rms density update = 0.000136775441
i=  40 j=   4 iu=   1 max d resid= 0.110074853467
rms density residual =  0.009892912247
     ixs is  39 jms is   7
  1  0.6229  0.7216 -0.1160 alfa= 1.411 s=-.002045  ml= 1.381  xs=0.706
  1  1.0326  0.7208 -0.1158 alfa= 1.411 s=-.002045  ml= 1.381  xs=0.706
  2  0.6548  0.7402 -0.1077 alfa= 1.545 s=-.000338  ml= 1.320  xs=0.706
  2  1.0154  0.7388 -0.1568 alfa= 1.545 s=-.000338  ml= 1.320  xs=0.706
  3  0.6918  0.7590 -0.0988 alfa= 1.664 s=0.000073  ml= 1.242  xs=0.700
  3  0.9731  0.7655 -0.1684 alfa= 1.664 s=0.000073  ml= 1.242  xs=0.700
  4  0.7291  0.7748 -0.0924 alfa= 1.747 s=-.000051  ml= 1.166  xs=0.699
  4  0.9358  0.7860 -0.1556 alfa= 1.747 s=-.000051  ml= 1.166  xs=0.699
  5  0.7660  0.7868 -0.0864 alfa= 1.788 s=-.001272  ml= 1.105  xs=0.692
  5  0.9027  0.7963 -0.1307 alfa= 1.788 s=-.001272  ml= 1.105  xs=0.692
  6  0.8045  0.7966 -0.0765 alfa= 1.784 s=-.003925  ml= 1.063  xs=0.683
  6  0.8906  0.8019 -0.1020 alfa= 1.784 s=-.003925  ml= 1.063  xs=0.683
  7  0.8461  0.8060 -0.0703 alfa= 1.719 s=-.005165  ml= 1.033  xs=0.673
  7  0.8977  0.8074 -0.0823 alfa= 1.719 s=-.005165  ml= 1.033  xs=0.673
iteration   5562
rms shock density residual = 0.23[illegible]
rms shock density update = [illegible]
i=  [illegible] j=  [illegible] iu=   1 max d  update= 0.0013[illegible]
rms density update = 0.[illegible]
i=  40 j=  [illegible] iu=   1 max d resid= 0.1122799[illegible]
rms density residual =  0.[illegible]
     ixs is  39 jms is   7
  1  0.6241  0.7228 -0.1153 alfa= 1.413 s=-.[illegible]  ml= 1.380  xs=0.705
  1  1.0342  0.7214 -0.1151 alfa= 1.413 s=-.[illegible]  ml= 1.380  xs=0.705
  2  0.6554  0.7404 -0.1075 alfa= 1.544 s=-.000736  ml= 1.320  xs=0.706
  2  1.0167  0.7383 -0.1562 alfa= 1.544 s=-.000756  ml= 1.320  xs=0.706
  3  0.6922  0.7591 -0.0990 alfa= 1.660 s=-.000341  ml= 1.241  xs=0.700
  3  [illegible]
  [illegible]
```

TABLE 4

```
 ixs is  39 jms is   7
 1  0.6331  0.7282 -0.1076 alfa= 1.424 s=0.052375  ml= 1.300  xs=0.690
 1  0.9370  0.7439 -0.1099 alfa= 1.424 s=0.052375  ml= 1.300  xs=0.690
 2  0.6646  0.7462 -0.0993 alfa= 1.482 s=0.039782  ml= 1.266  xs=0.689
 2  0.9515  0.7563 -0.1144 alfa= 1.482 s=0.039782  ml= 1.266  xs=0.689
 3  0.6967  0.7617 -0.0936 alfa= 1.520 s=0.027522  ml= 1.231  xs=0.689
 3  0.9606  0.7679 -0.1147 alfa= 1.520 s=0.027522  ml= 1.231  xs=0.689
 4  0.7341  0.7766 -0.0871 alfa= 1.569 s=0.013759  ml= 1.187  xs=0.690
 4  0.9633  0.7797 -0.1139 alfa= 1.569 s=0.013759  ml= 1.187  xs=0.690
 5  0.7726  0.7896 -0.0902 alfa= 1.539 s=0.003008  ml= 1.151  xs=0.691
 5  0.9701  0.7896 -0.1068 alfa= 1.539 s=0.003008  ml= 1.151  xs=0.691
 6  0.8193  0.7964 -0.0860 alfa= 1.589 s=-.020298  ml= 1.101  xs=0.693
 6  0.9672  0.7938 -0.1043 alfa= 1.589 s=-.020298  ml= 1.101  xs=0.693
 7  0.8735  0.8064 -0.0995 alfa= 1.360 s=-.038031  ml= 1.061  xs=0.695
 7  0.9770  0.8043 -0.0904 alfa= 1.360 s=-.038031  ml= 1.061  xs=0.695
iteration    100
rms shock density residual = 0.050351069269
rms shock density update = 0.032026283357
i=  41 j=   8 iu=   1 max d  update= 0.060461378460
rms density update =  0.005819235053
i=  39 j=   7 iu=   1 max d resid= 0.137059219799
rms density residual =  0.009668365068
 ixs is  39 jms is   6
 1  0.6755  0.7445 -0.1406 alfa= 1.385 s=0.041793  ml= 1.248  xs=0.741
 1  0.9455  0.7556 -0.1427 alfa= 1.385 s=0.041793  ml= 1.248  xs=0.741
 2  0.6910  0.7500 -0.1382 alfa= 1.348 s=0.032602  ml= 1.231  xs=0.728
 2  0.9503  0.7609 -0.1287 alfa= 1.348 s=0.032602  ml= 1.231  xs=0.728
 3  0.7320  0.7692 -0.1319 alfa= 1.341 s=0.024350  ml= 1.183  xs=0.718
 3  0.9508  0.7776 -0.1195 alfa= 1.341 s=0.024350  ml= 1.183  xs=0.718
 4  0.7721  0.7839 -0.1199 alfa= 1.335 s=0.010222  ml= 1.141  xs=0.702
 4  0.9526  0.7893 -0.1051 alfa= 1.335 s=0.010222  ml= 1.141  xs=0.702
 5  0.8168  0.7955 -0.1014 alfa= 1.409 s=-.000180  ml= 1.092  xs=0.687
 6  0.9443  0.7962 -0.0972 alfa= 1.409 s=-.000180  ml= 1.092  xs=0.687
 6  0.8578  0.8069 -0.0887 alfa= 1.368 s=-.014523  ml= 1.056  xs=0.666
 6  0.9437  0.8072 -0.0810 alfa= 1.368 s=-.014523  ml= 1.056  xs=0.666
iteration   1500
 ixs is  39 jms is   6
 1  0.7081  0.7520 -0.1747 alfa= 1.346 s=0.016735  ml= 1.230  xs=0.794
 1  0.9794  0.7564 -0.1757 alfa= 1.346 s=0.016735  ml= 1.230  xs=0.794
 2  0.7223  0.7585 -0.1586 alfa= 1.327 s=0.013949  ml= 1.206  xs=0.771
 2  0.9707  0.7643 -0.1496 alfa= 1.327 s=0.013949  ml= 1.206  xs=0.771
 3  0.7394  0.7647 -0.1528 alfa= 1.263 s=0.009892  ml= 1.177  xs=0.753
 3  0.9592  0.7745 -0.1291 alfa= 1.263 s=0.009892  ml= 1.177  xs=0.753
 4  0.7698  0.7811 -0.1317 alfa= 1.241 s=0.003072  ml= 1.140  xs=0.717
 4  0.9521  0.7914 -0.1032 alfa= 1.241 s=0.003072  ml= 1.140  xs=0.717
 5  0.8175  0.7972 -0.1020 alfa= 1.306 s=-.002066  ml= 1.087  xs=0.686
 5  0.9577  0.8012 -0.0863 alfa= 1.306 s=-.002066  ml= 1.087  xs=0.686
 6  0.8571  0.8103 -0.0728 alfa= 1.383 s=-.006378  ml= 1.050  xs=0.646
 6  0.9518  0.8112 -0.0658 alfa= 1.383 s=-.006378  ml= 1.050  xs=0.646
iteration   3000
rms shock density residual = 0.040242415052
rms shock density update = 0.000735955479
i=  37 j=   1 iu=   1 max d  update= 0.001891897882
rms density update =  0.000169220153
```

TABLE. 5

j= 1 iu= 1 RESIDUALS EITHER SIDE OF FITTED SHOCK

dul= -2.9164558895913D-02 dur= 6.4381387398691D-02

j= 1 iu= 2

dul= -1.7963894071497D-02 dur= 3.6285747123105D-02

j= 1 iu= 3

dul= -1.4933145023818D-02 dur= 9.8327629612926D-02

j= 2 iu= 1

dul= -8.0727250795596D-04 dur= 1.0147430238152D-02

j= 2 iu= 2

dul= 6.7625633359951D-03 dur= -1.4903655649105D-02

j= 2 iu= 3

dul= -1.9746369360248D-02 dur= -3.5225995555314D-02

j= 3 iu= 1

dul= -2.6789779340115D-02 dur= -7.1166276929829D-02

j= 3 iu= 2

dul= -1.8743030445949D-02 dur= 1.2051071838907D-02

j= 3 iu= 3

dul= -2.4824718526312D-02 dur= 4.0887178531127D-02

j= 4 iu= 1

dul= 1.2292804252997D-02 dur= -7.5091524050377D-02

j= 4 iu= 2

dul= 1.7517283626303D-02 dur= 1.7033448223670D-02

j= 4 iu= 3

dul= -1.2288099544232D-02 dur= -1.2082272994482D-02

j= 5 iu= 1

dul= -2.9134562895589D-02 dur= -9.3673418141294D-02

j= 5 iu= 2

dul= -2.5209463157303D-02 dur= -1.7576931681779D-03

TABLE. 5

```
j=  6 iu=   1
dul=     3.6056524707296D-02 dur=    -7.8882488087415D-02
j=  6 iu=   2
dul=     2.7588697108403D-02 dur=     1.1656649461098D-02
j=  6 iu=   3
dul=    -2.0772741202216D-03 dur=    -3.2389777835299D-02
j=  7 iu=   1
dul=    -3.3556579588130D-02 dur=    -2.2462857555534D-02
j=  7 iu=   2
dul=    -2.4329489083349D-02 dur=     1.4085422e80037D-02
j=  7 iu=   3
dul=    -5.7925351149404D-02 dur=     7.2538033044502D-02
```

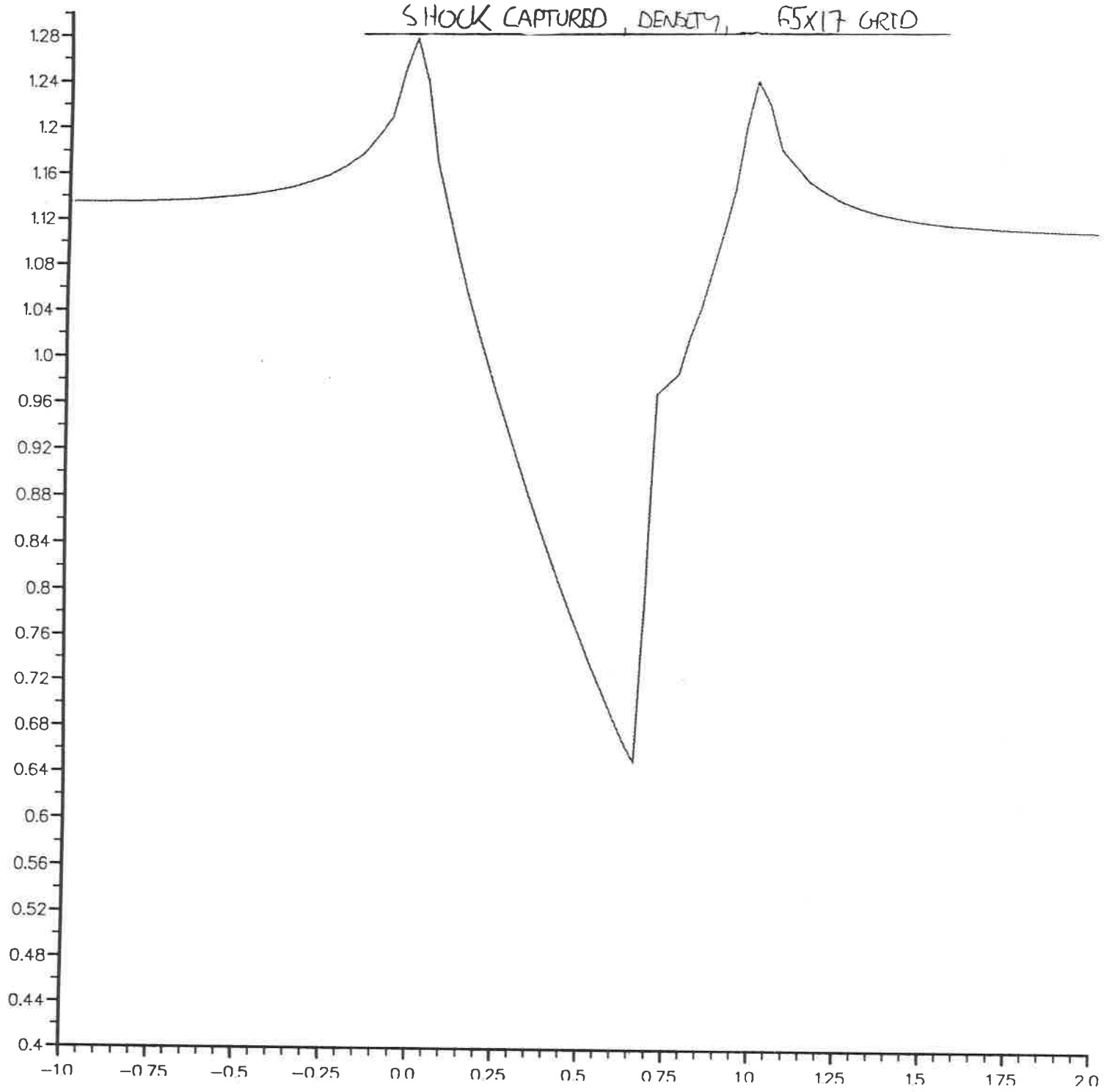
SHOCK CAPTURED, DENSITY, 65X17 GRID
1.28
1.24
1.2
1.16
1.12
1.08
1.04
1.0
0.96
0.92
0.88
0.84
0.8
0.76
0.72
0.68
0.64
0.6
0.56
0.52
0.48
0.44
0.4
−1.0
−0.75
−0.5
−0.25
0.0
0.25
0.5
0.75
1.0
1.25
1.5
1.75
2.0

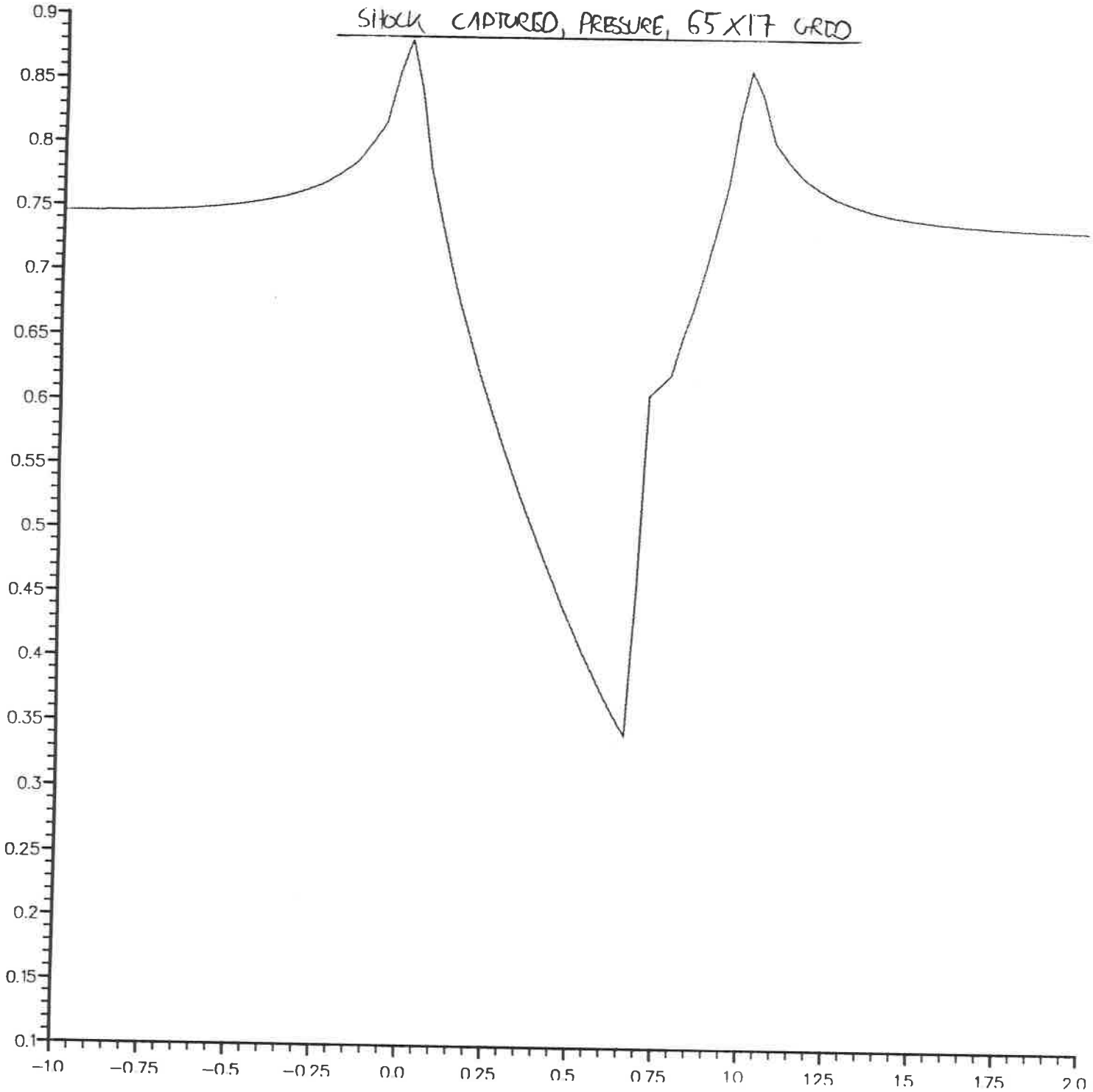
SHOCK CAPTURED, PRESSURE, 65 X 17 GRID
0.9
0.85
0.8
0.75
0.7
0.65
0.6
0.55
0.5
0.45
0.4
0.35
0.3
0.25
0.2
0.15
0.1
−1.0
−0.75
−0.5
−0.25
0.0
0.25
0.5
0.75
1.0
1.25
1.5
1.75
2.0

SHOCK CAPTURED, MACH NO., 65 X 17 GRID

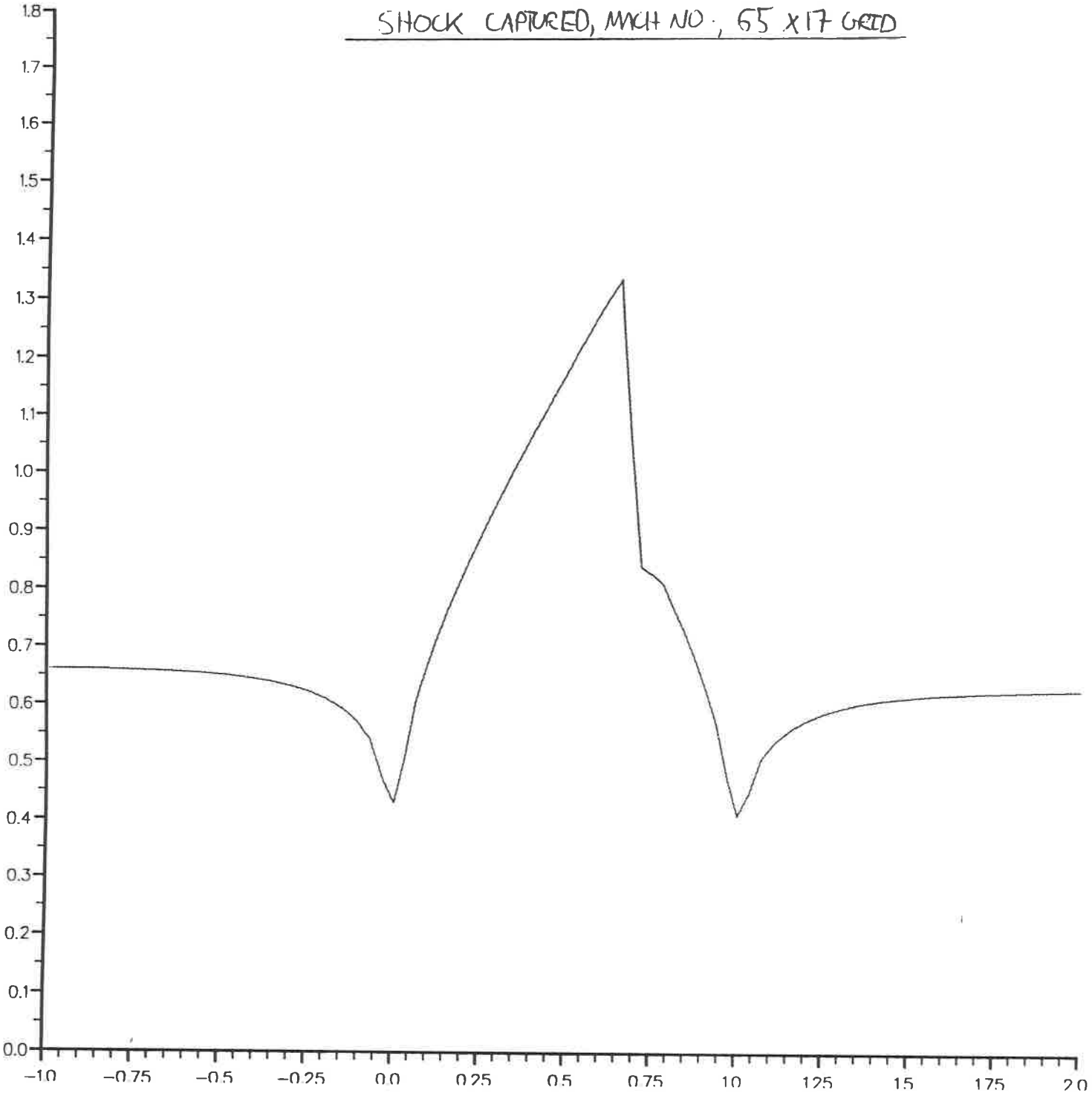

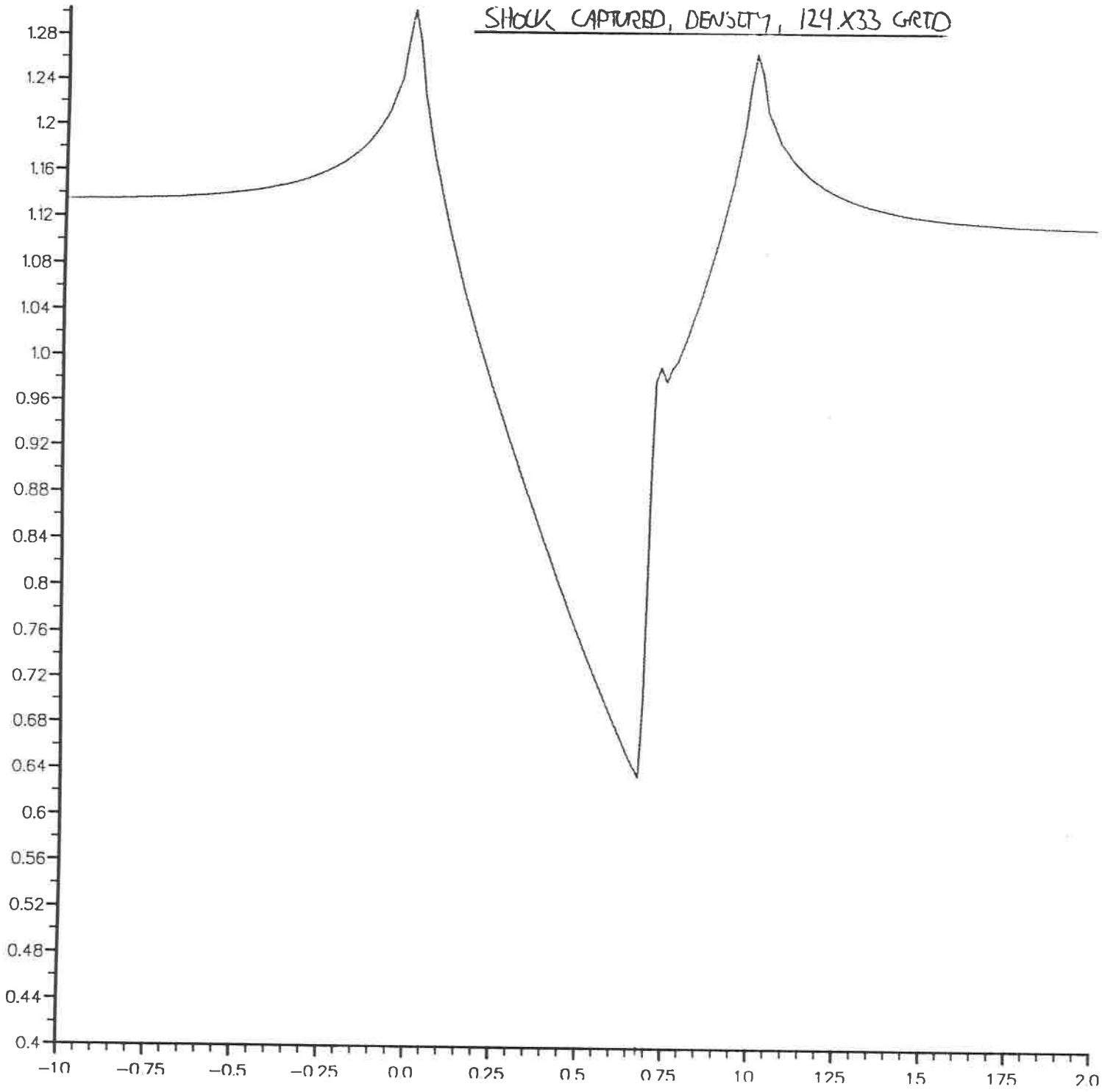
SHOCK CAPTURED, DENSITY, 129 X 33 GRID
1.28
1.24
1.2
1.16
1.12
1.08
1.04
1.0
0.96
0.92
0.88
0.84
0.8
0.76
0.72
0.68
0.64
0.6
0.56
0.52
0.48
0.44
0.4
-1.0
-0.75
-0.5
-0.25
0.0
0.25
0.5
0.75
1.0
1.25
1.5
1.75
2.0

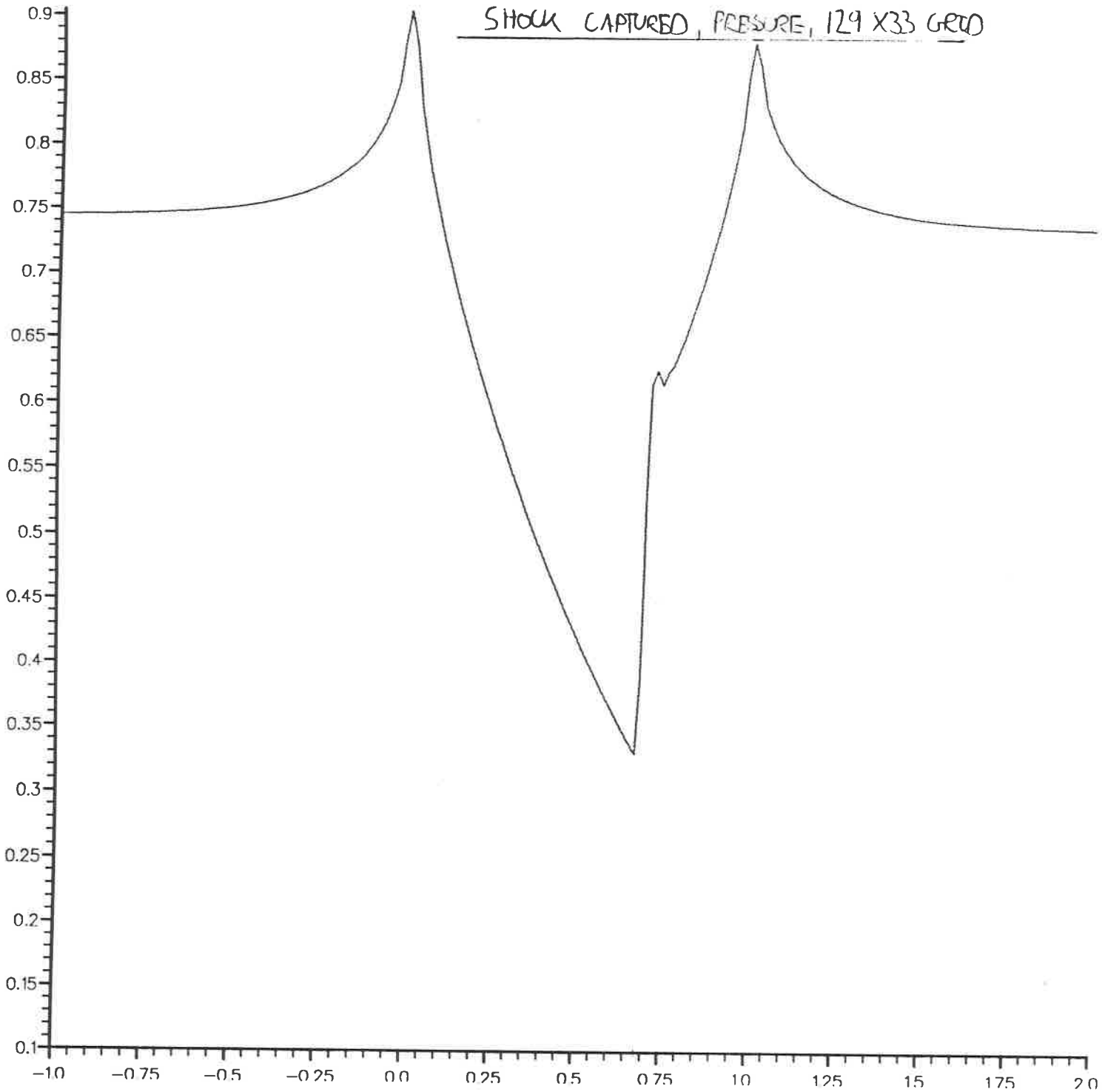
SHOCK CAPTURED, PRESSURE, 129 X33 GRID
0.9
0.85
0.8
0.75
0.7
0.65
0.6
0.55
0.5
0.45
0.4
0.35
0.3
0.25
0.2
0.15
0.1
-1.0
-0.75
-0.5
-0.25
0.0
0.25
0.5
0.75
1.0
1.25
1.5
1.75
2.0

SHOCK CAPTURED, MACH NO. 129 X 33 GRID

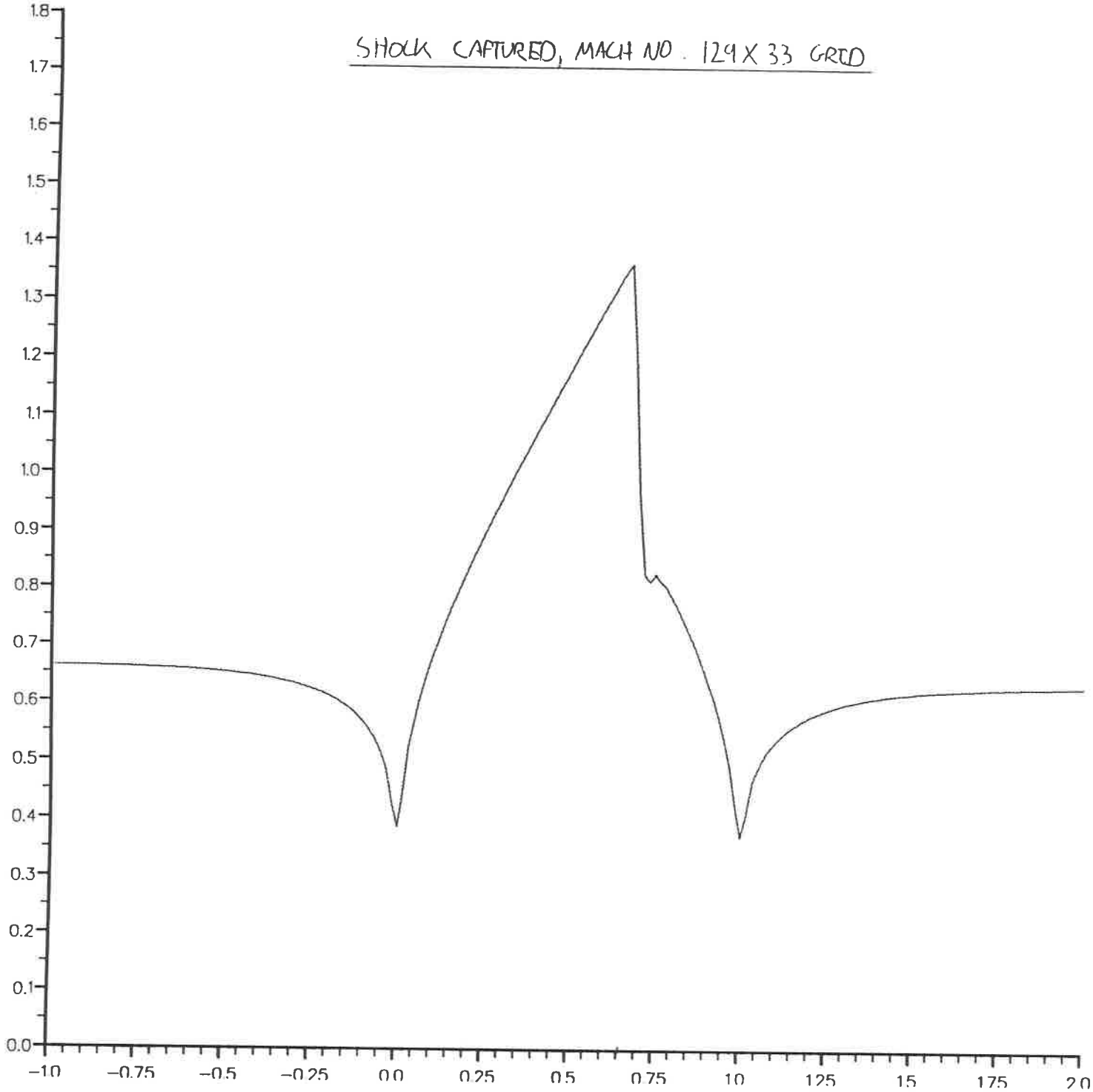

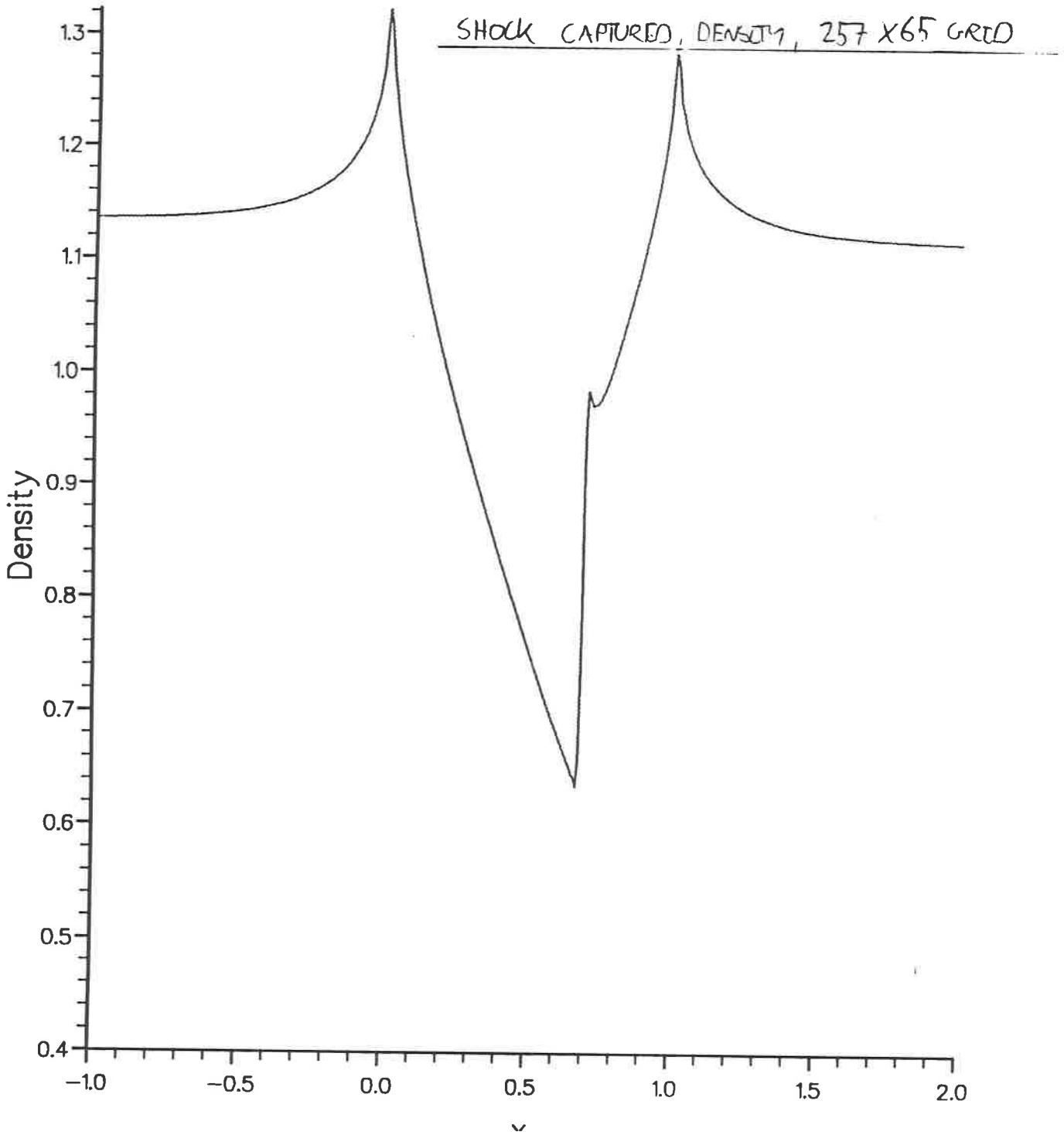
SHOCK CAPTURED, DENSITY, 257 X65 GRID
Density
1.3
1.2
1.1
1.0
0.9
0.8
0.7
0.6
0.5
0.4
−1.0
−0.5
0.0
0.5
1.0
1.5
2.0
x

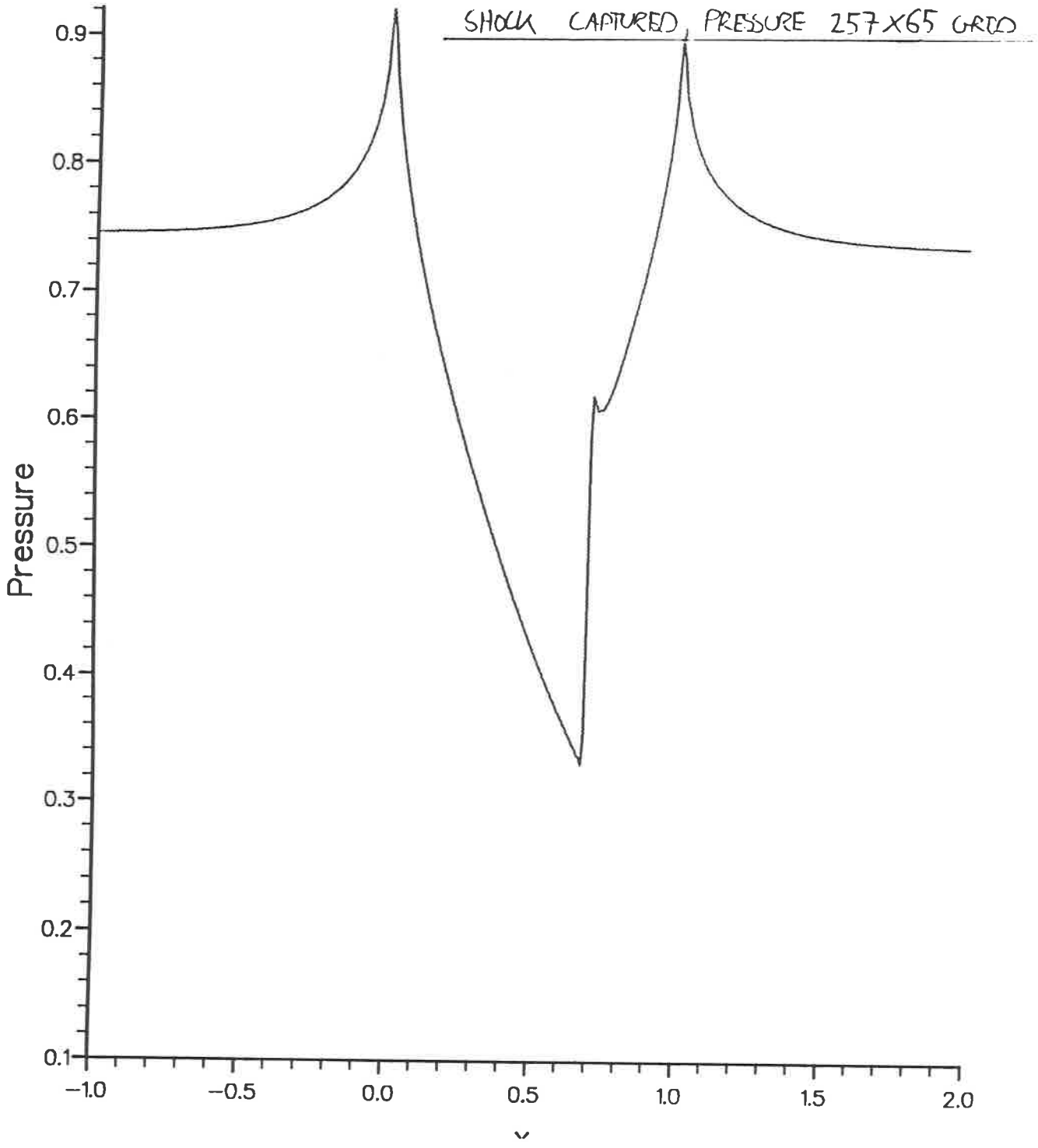
SHOCK CAPTURED PRESSURE 257x65 GRID
Pressure
0.9
0.8
0.7
0.6
0.5
0.4
0.3
0.2
0.1
−1.0
−0.5
0.0
0.5
1.0
1.5
2.0
x

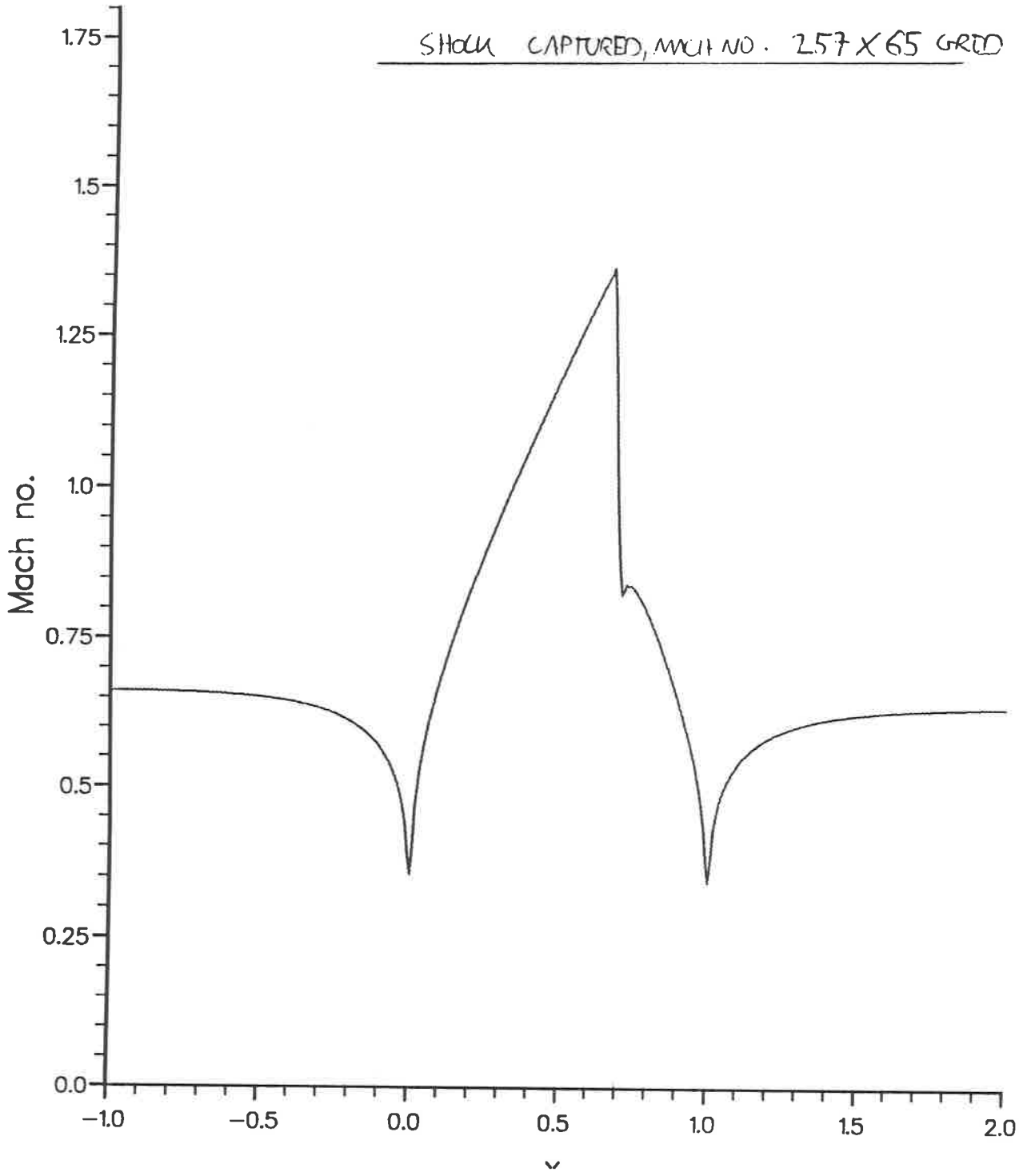
SHOCK CAPTURED, MACH NO. 2.57 X 65 GRID
Mach no.
1.75
1.5
1.25
1.0
0.75
0.5
0.25
0.0
−1.0
−0.5
0.0
0.5
1.0
1.5
2.0
X

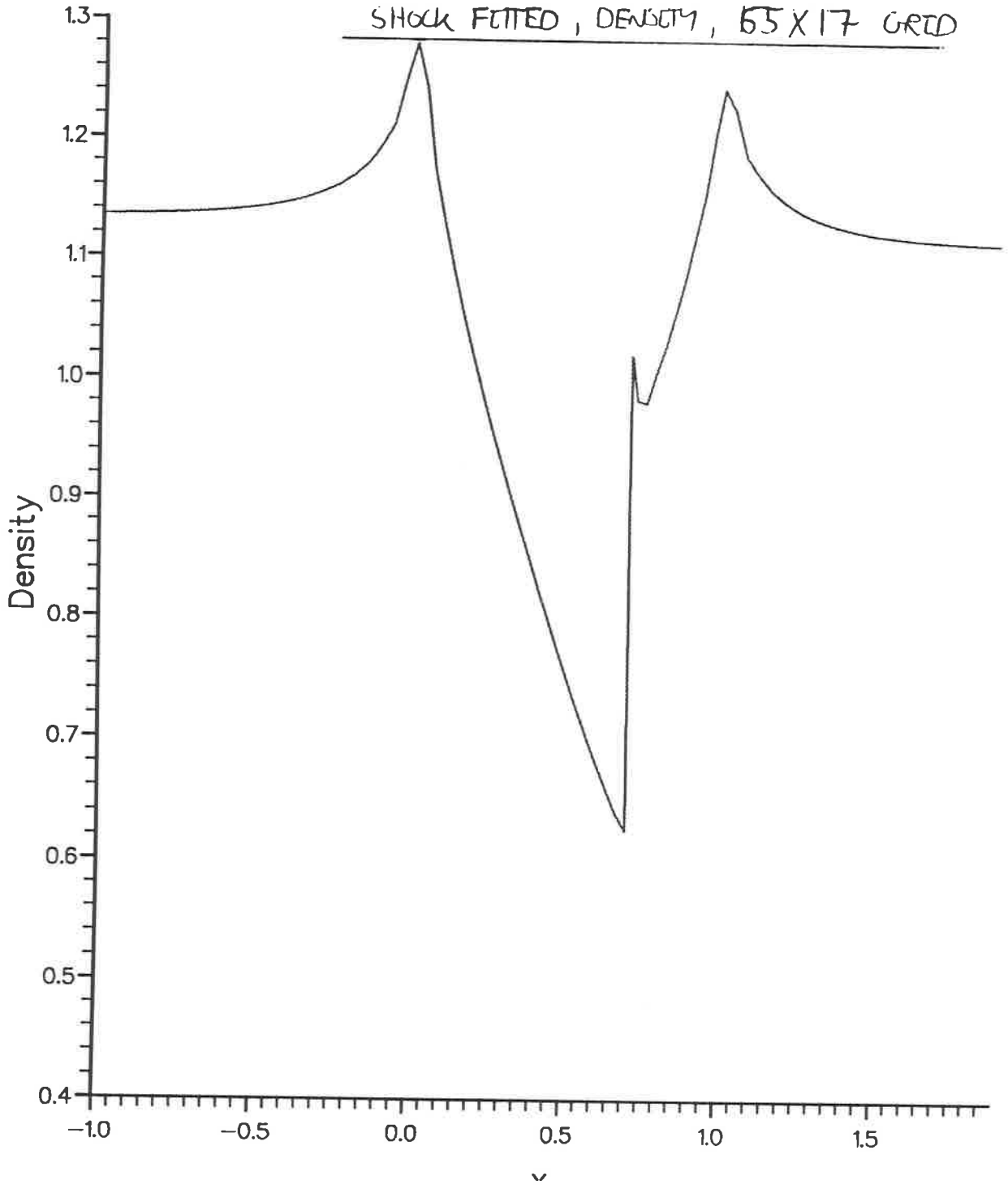
SHOCK FITTED, DENSITY, 65X17 GRID
Density
1.3
1.2
1.1
1.0
0.9
0.8
0.7
0.6
0.5
0.4
−1.0
−0.5
0.0
0.5
1.0
1.5
X

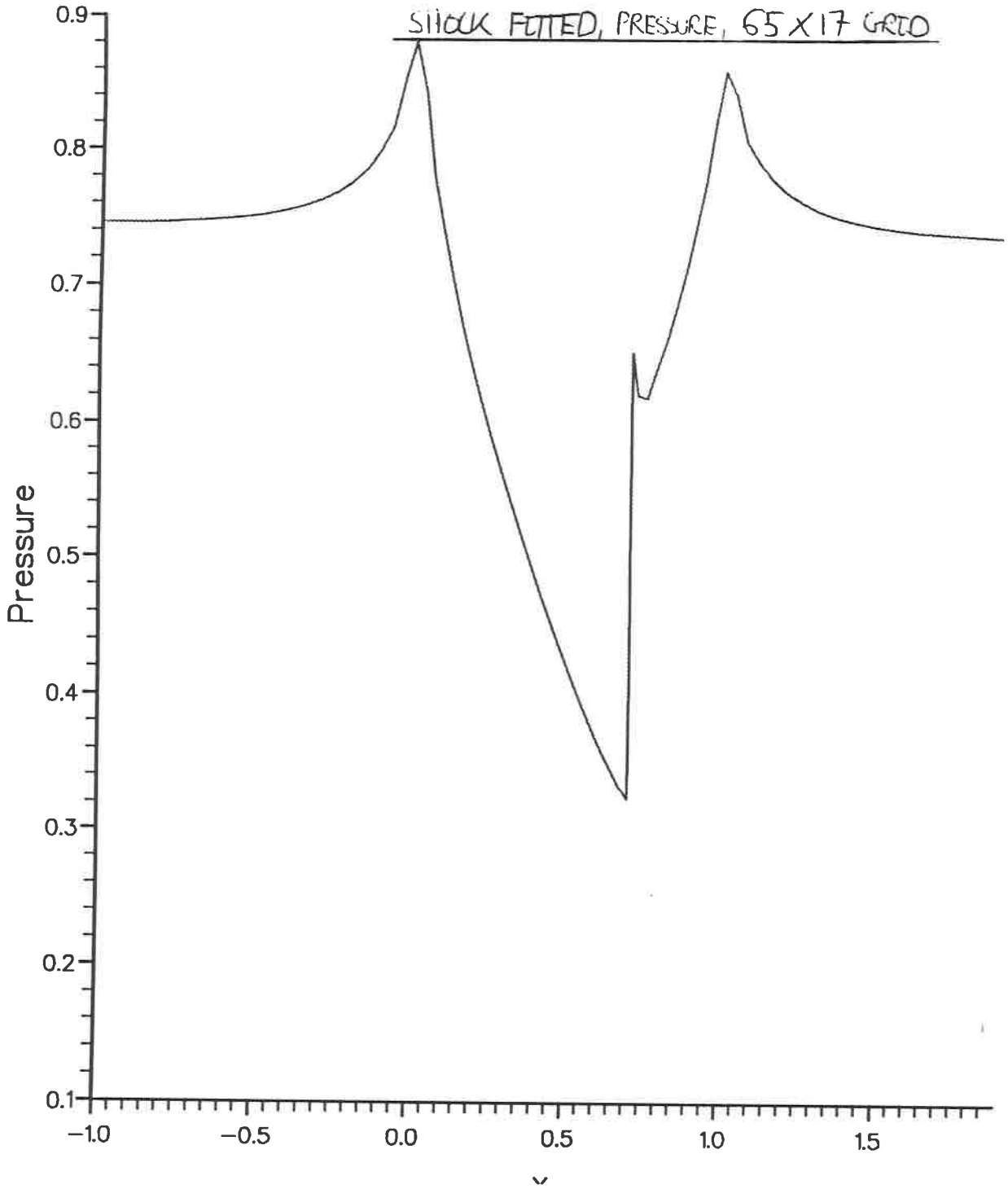
SHOCK FITTED, PRESSURE, 65 X 17 GRID
Pressure
0.9
0.8
0.7
0.6
0.5
0.4
0.3
0.2
0.1
−1.0
−0.5
0.0
0.5
1.0
1.5
x

SHOCK FITTED, MACH NO. 65 X 17 GRID

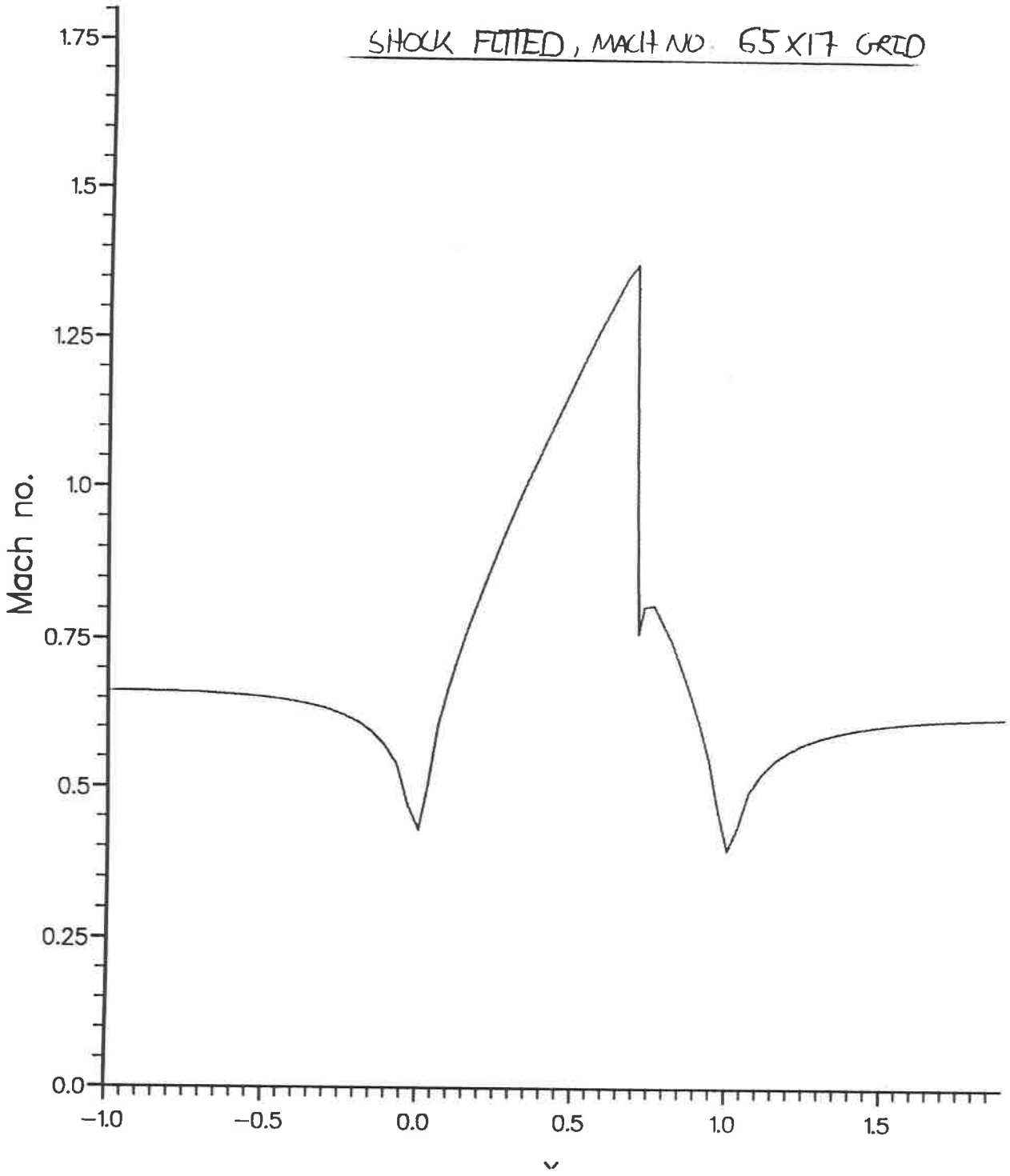

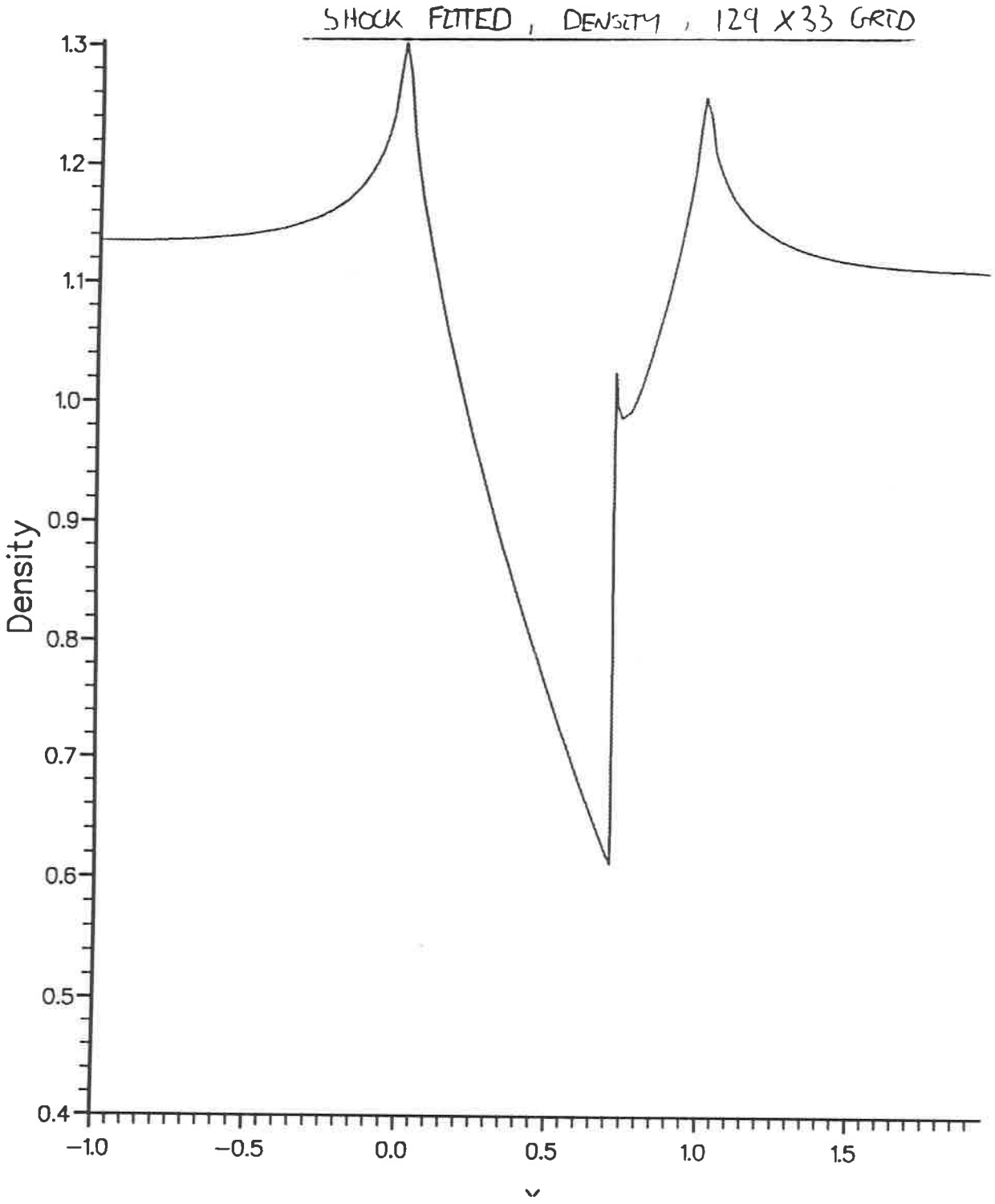
SHOCK FITTED, DENSITY, 129 X 33 GRID
Density
1.3
1.2
1.1
1.0
0.9
0.8
0.7
0.6
0.5
0.4
−1.0
−0.5
0.0
0.5
1.0
1.5
X

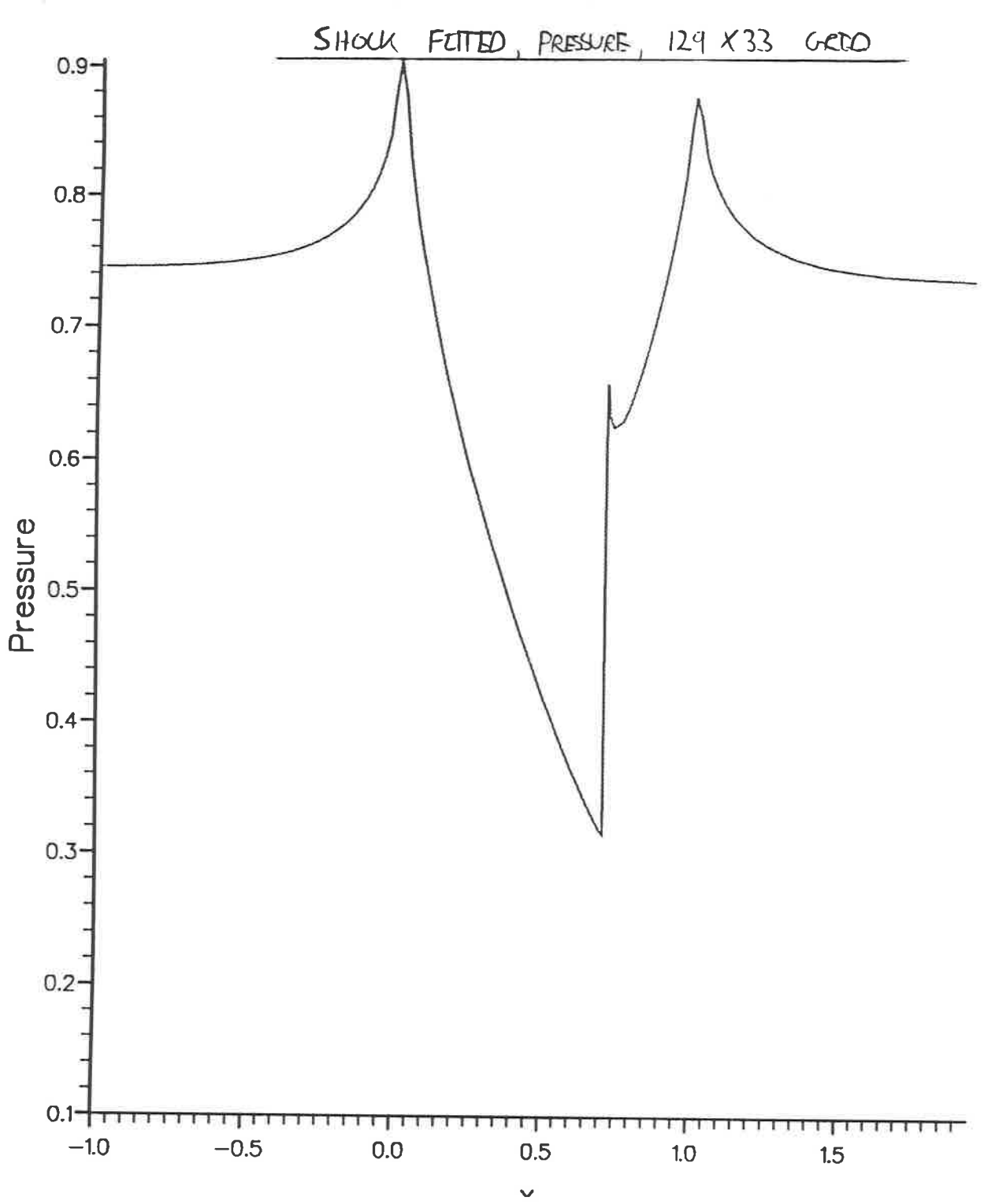
SHOCK FITTED, PRESSURE, 129 X 33 GRID
0.9
0.8
0.7
0.6
0.5
0.4
0.3
0.2
0.1
Pressure
−1.0
−0.5
0.0
0.5
1.0
1.5
x

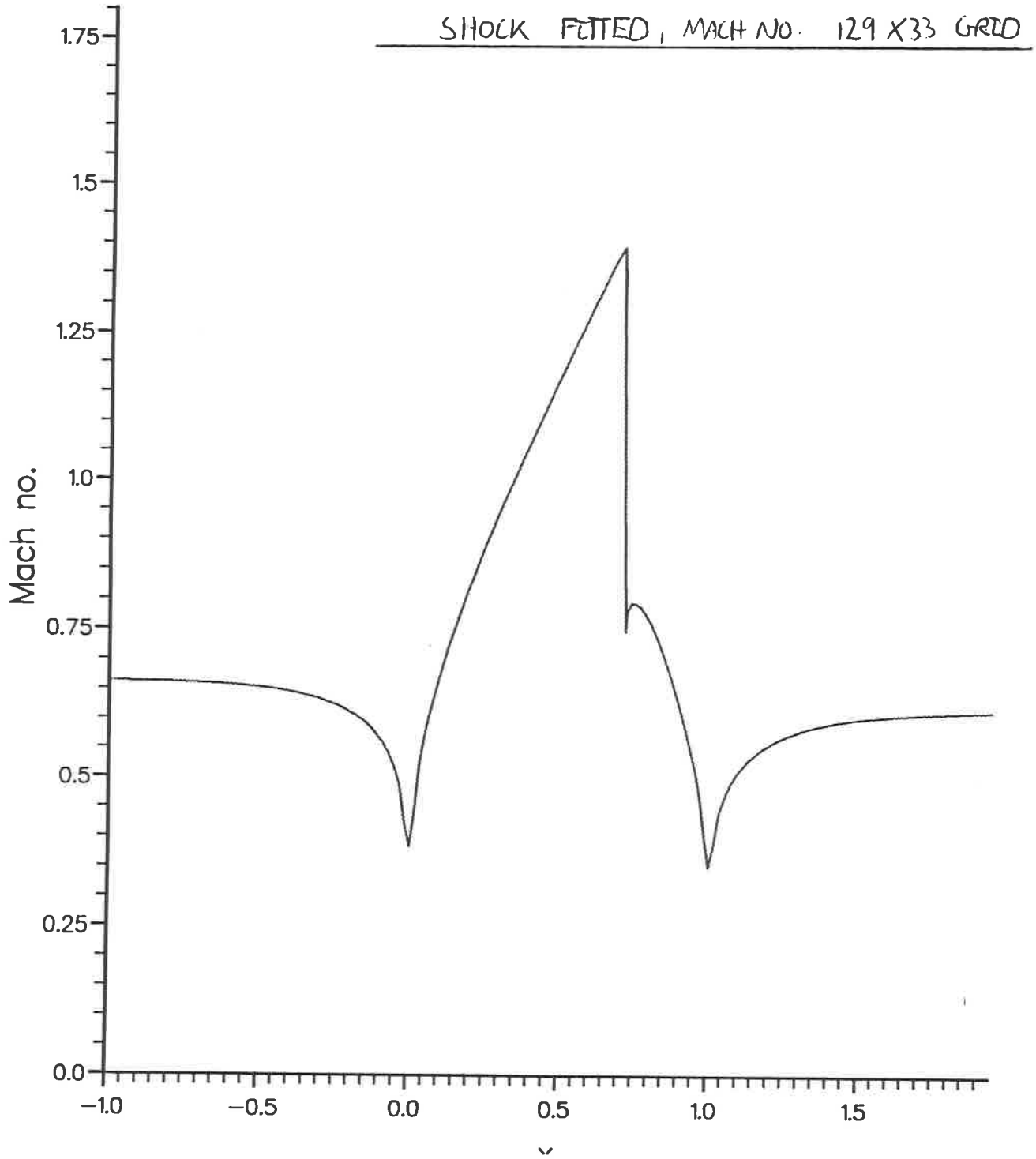
SHOCK FITTED, MACH NO. 129 X 33 GRID
Mach no.
1.75
1.5
1.25
1.0
0.75
0.5
0.25
0.0
−1.0
−0.5
0.0
0.5
1.0
1.5
X

Shock Captured, density x 10

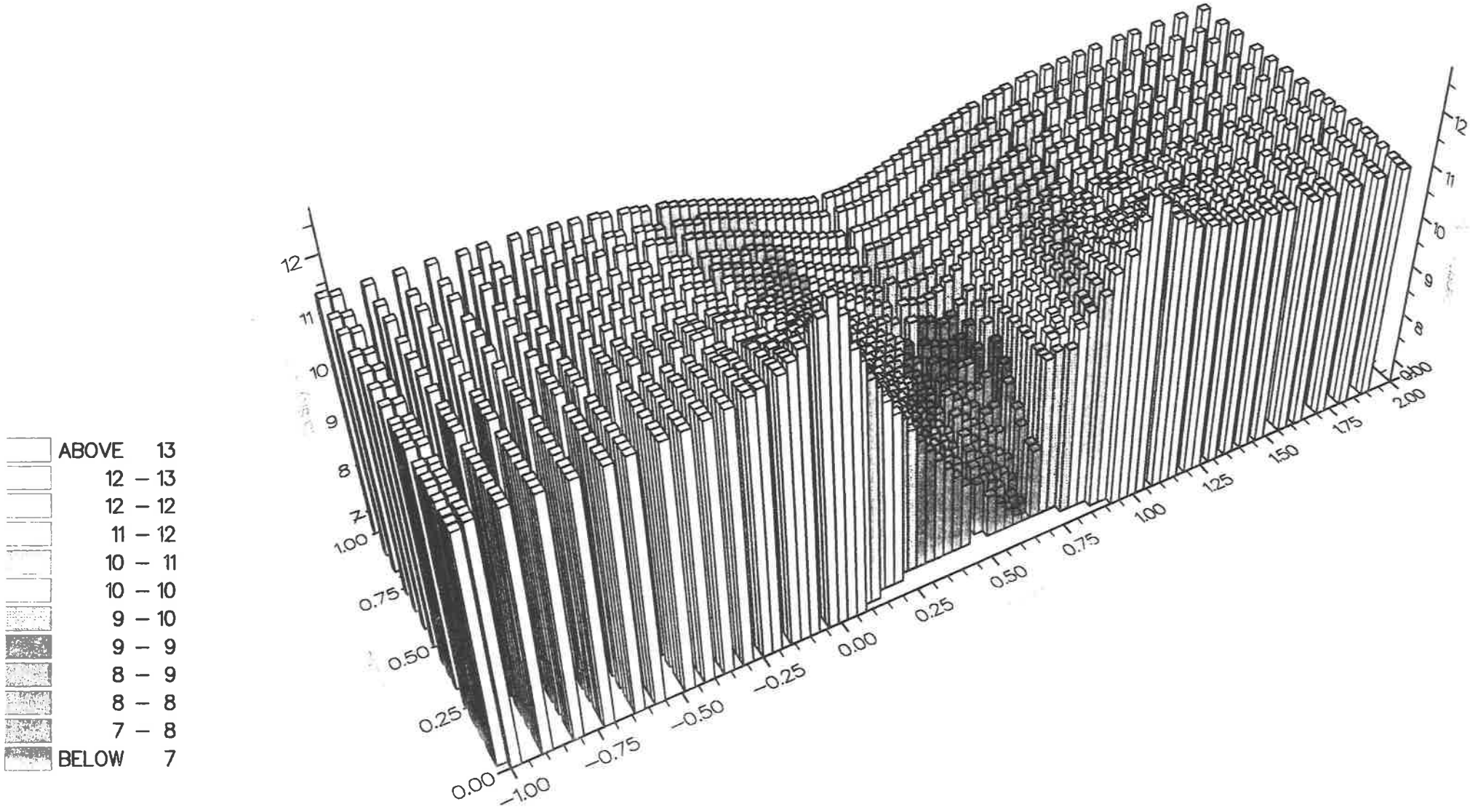

Shock Captured, pressure x 10

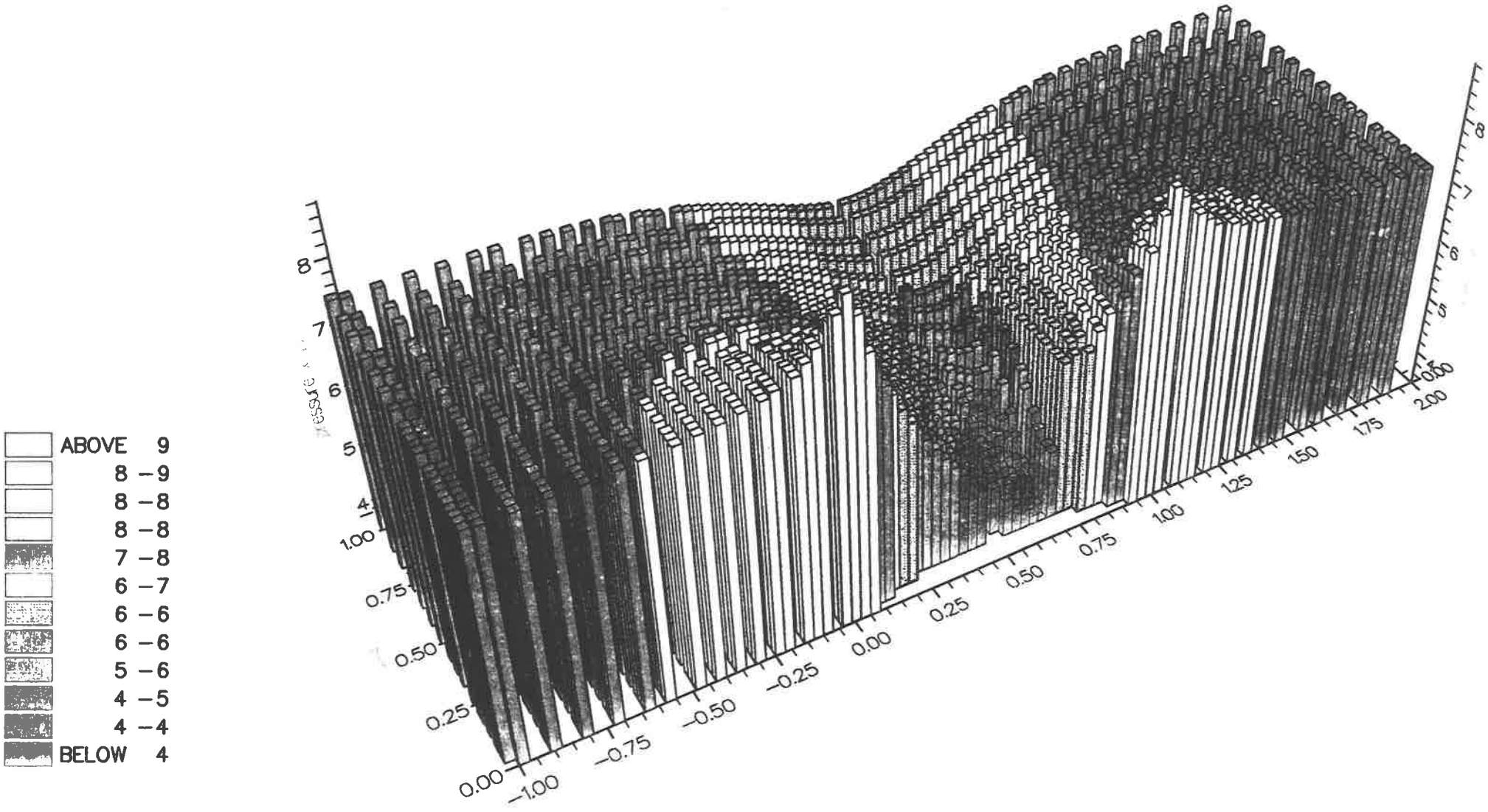

Shock Captured, mach no. x 10

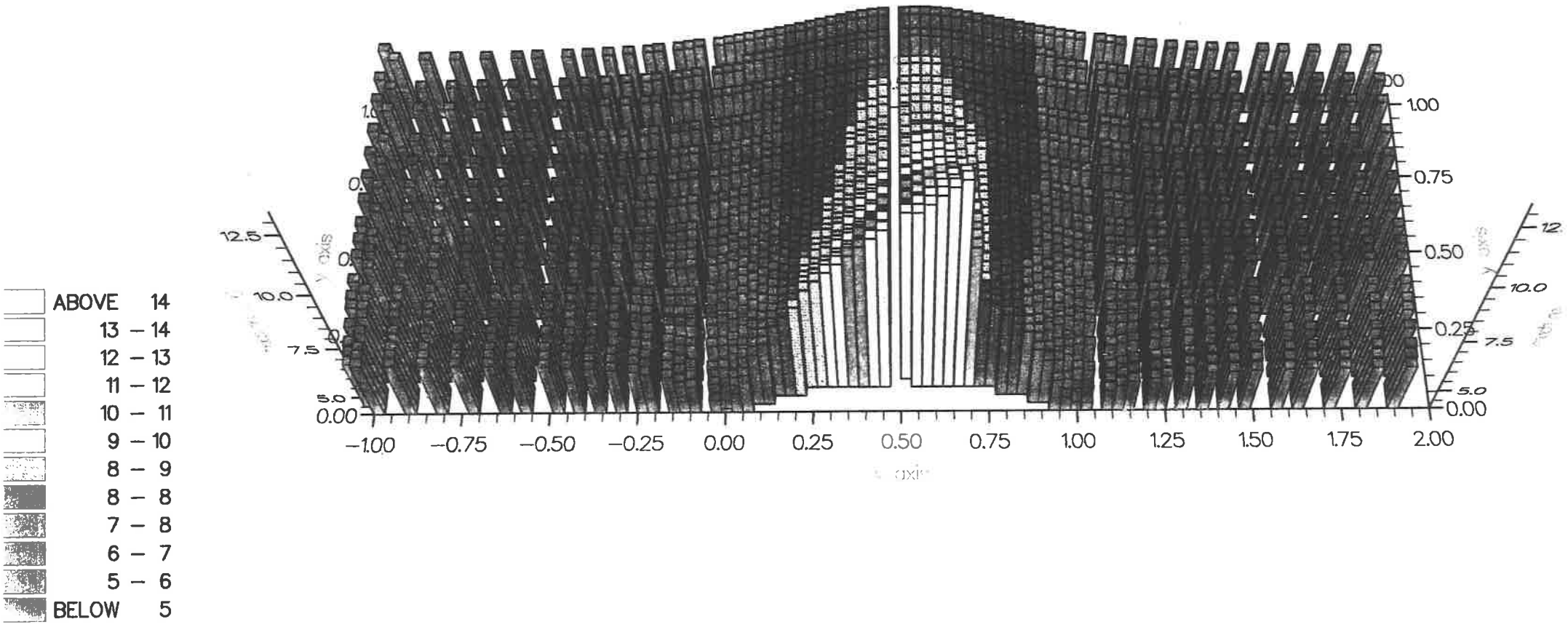

Shock Captured, Density Residual, 65 x 17 Grid.

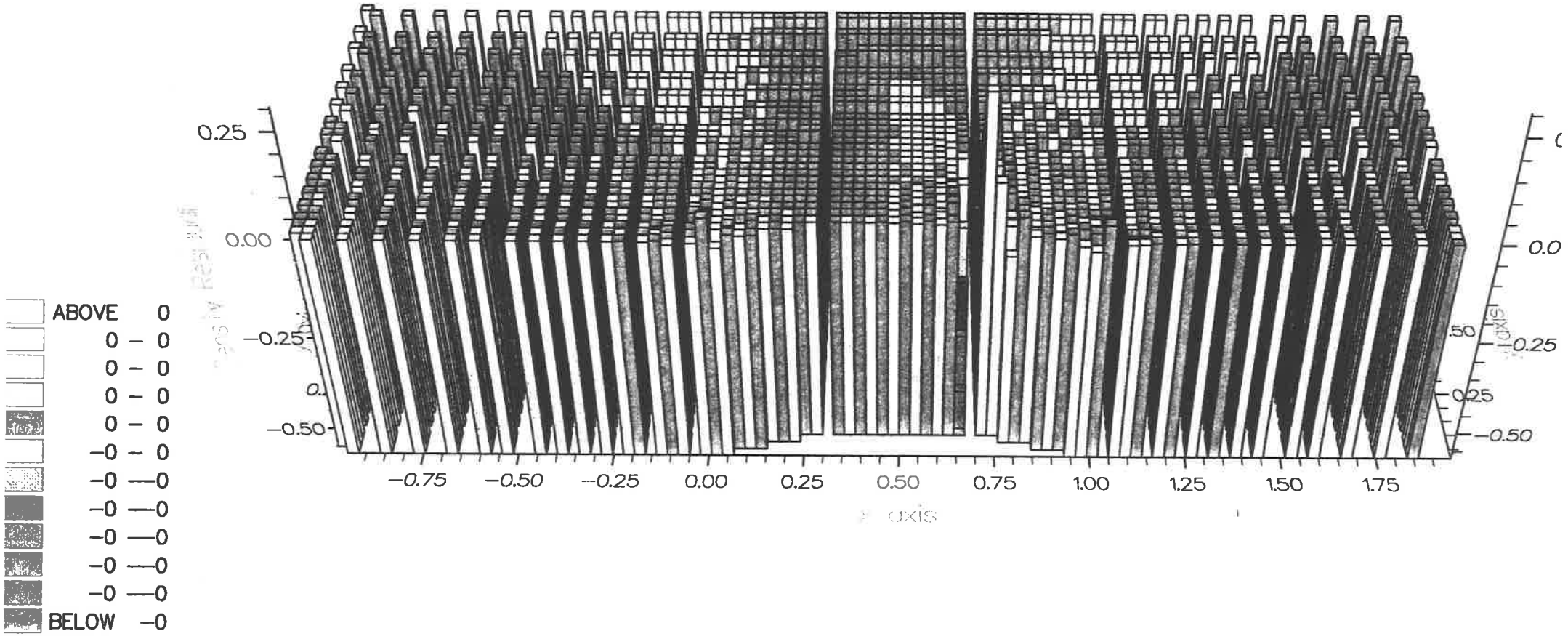

Shock Captured, X Momentum Residual, 65 x 17 Grid.

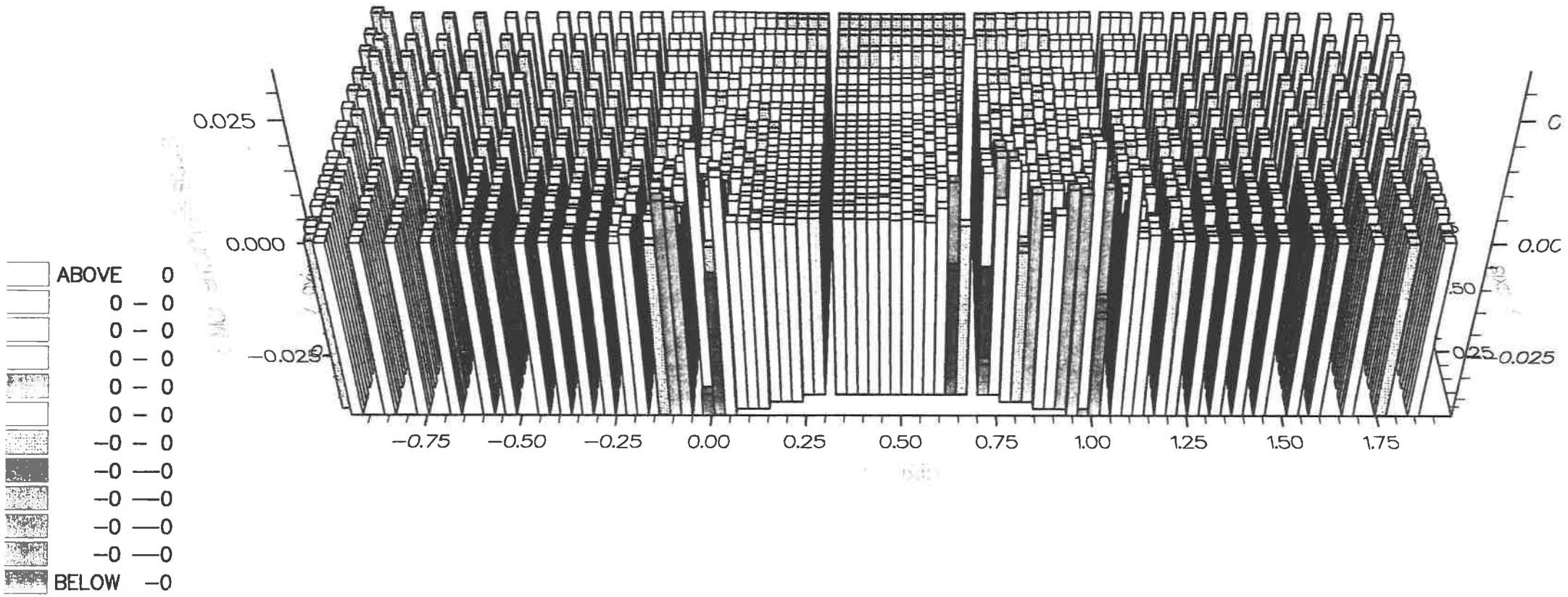

Shock Captured, Y Momentum Residual,65 x 17 Grid.

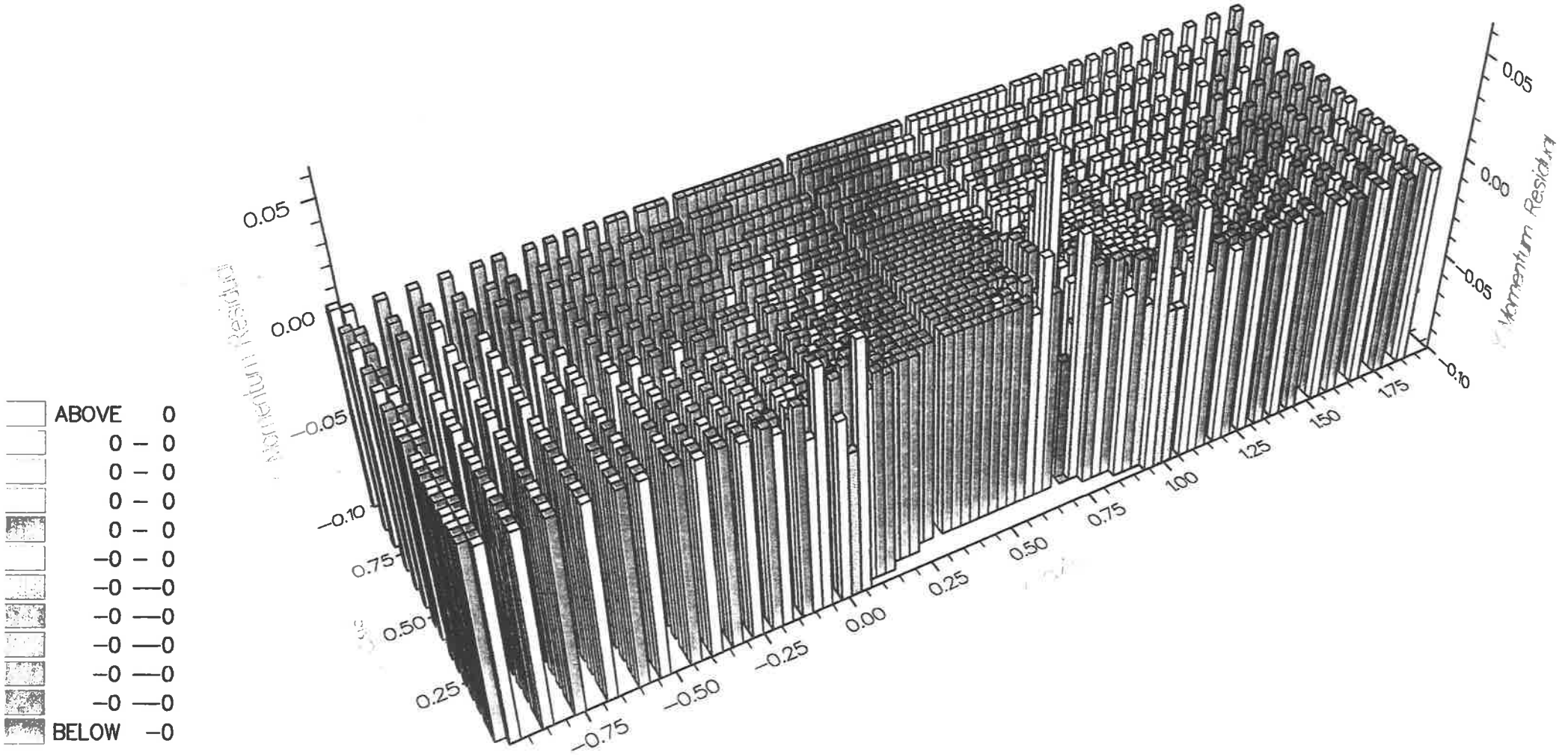

Shock Captured, abs(Density residuals),65 x 17 Grid

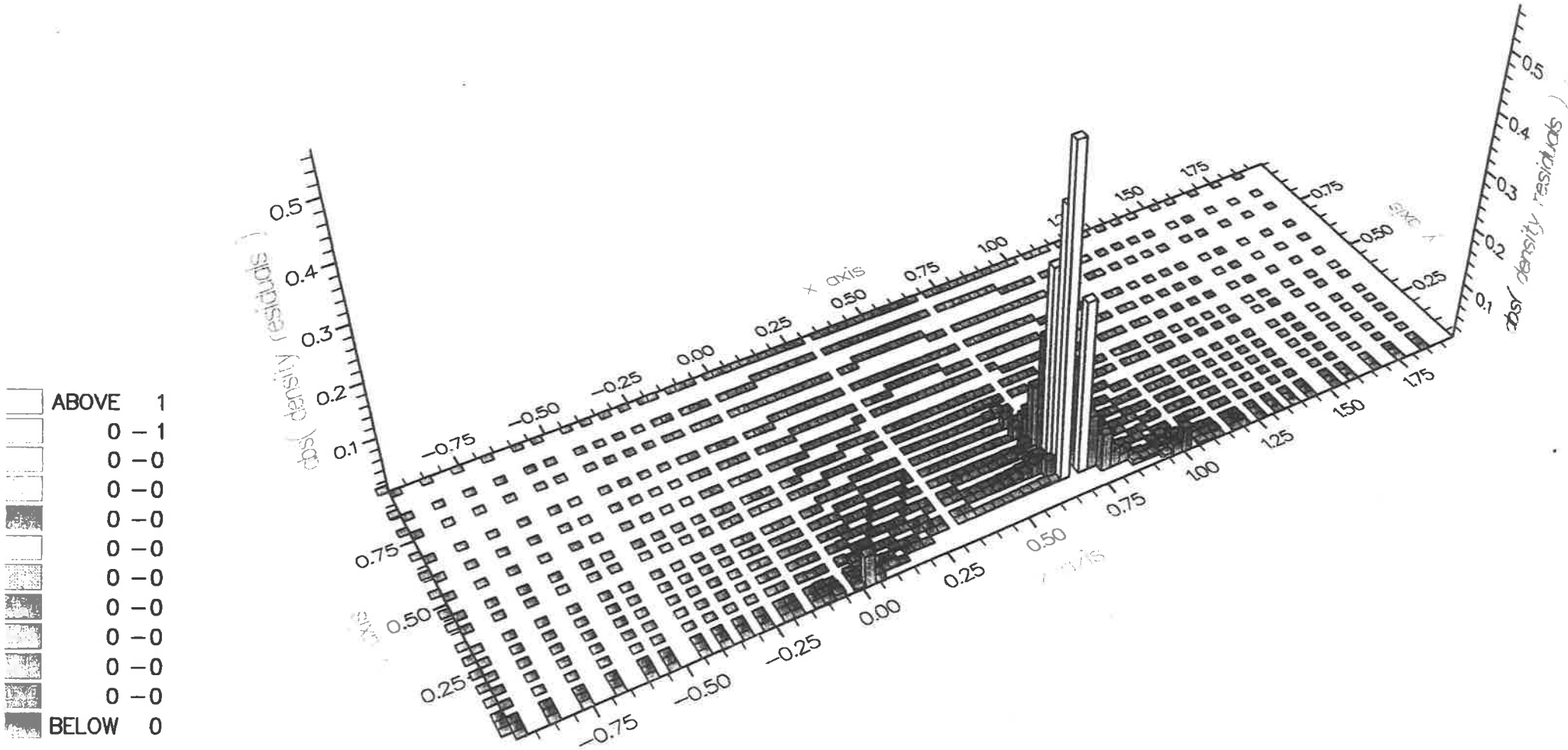

Shock Captured,abs(x momentum residuals),65 x 17 Gr

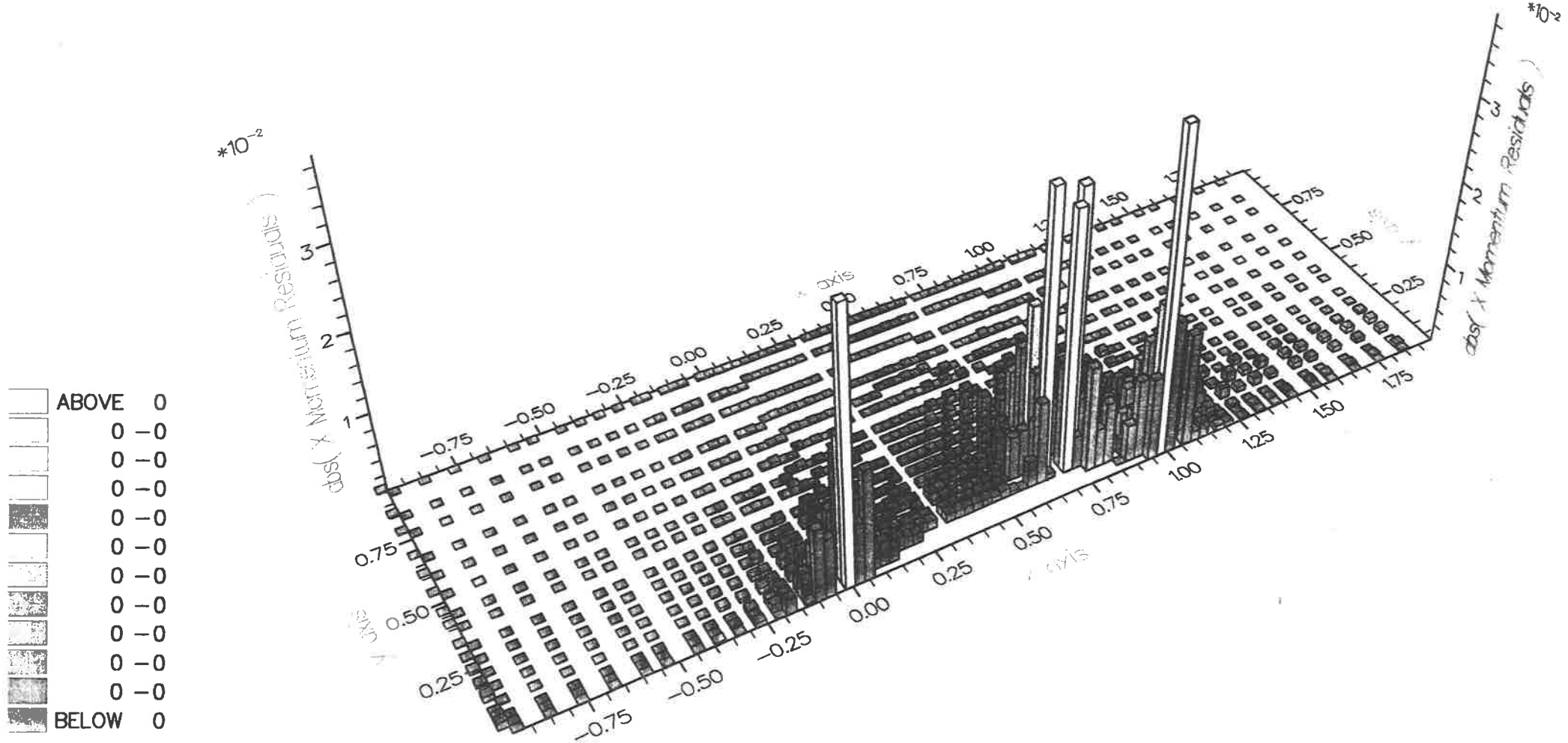

Shock Captured,abs(y momentum residuals),65 x 17 Gr

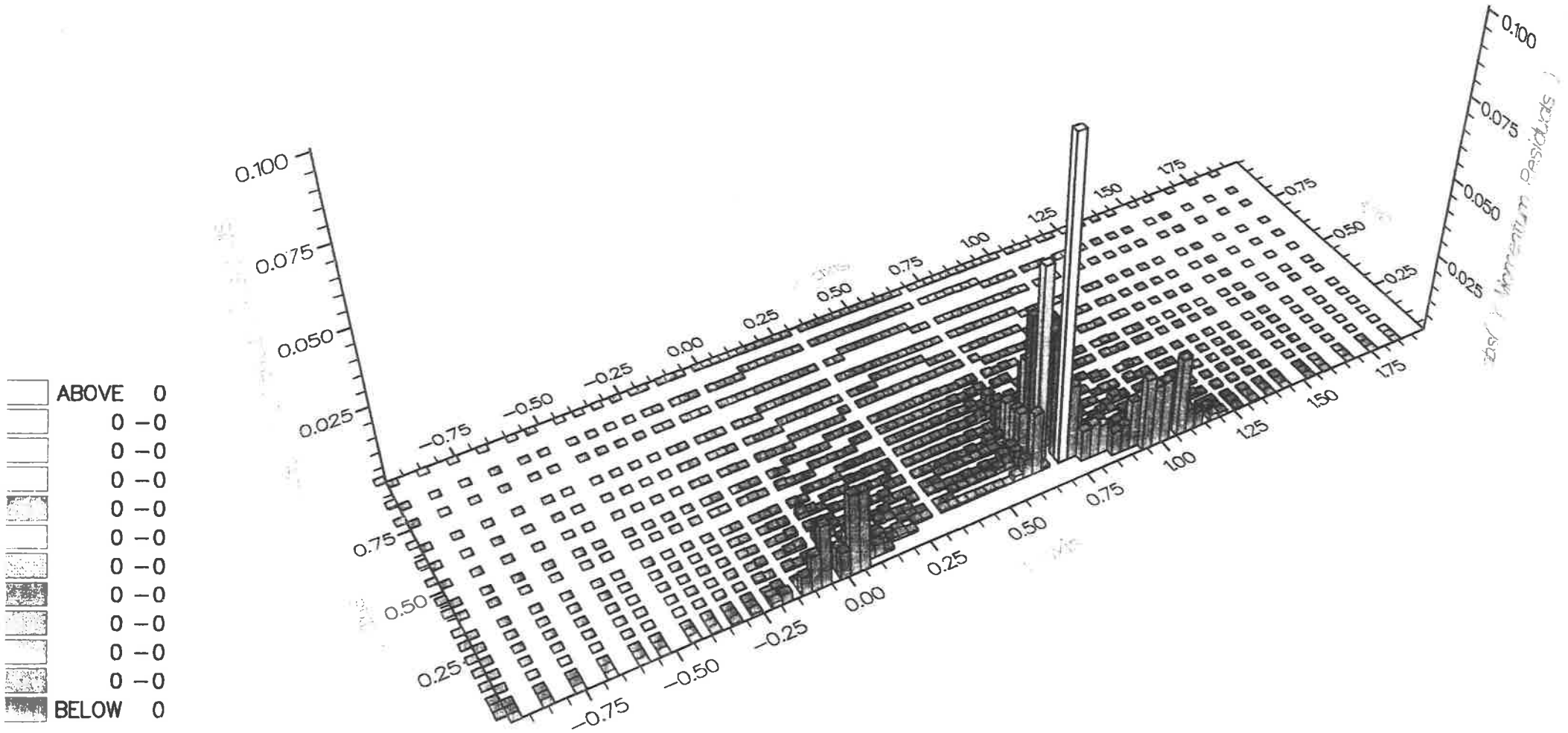

65X17, shock captured, log10(abs density cell residuals)

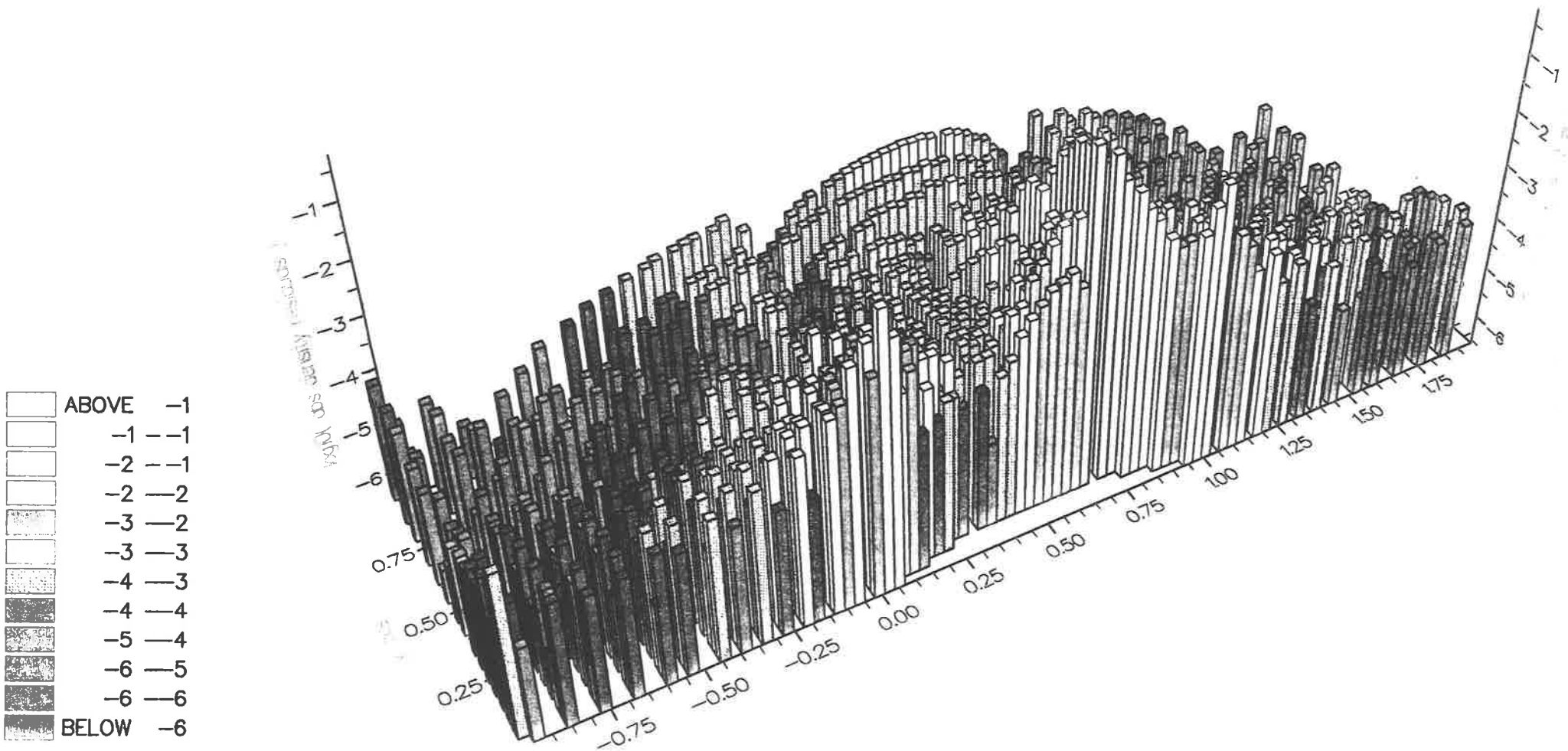

55X17,

Shock Captured, log10(abs x momentum cell residuals

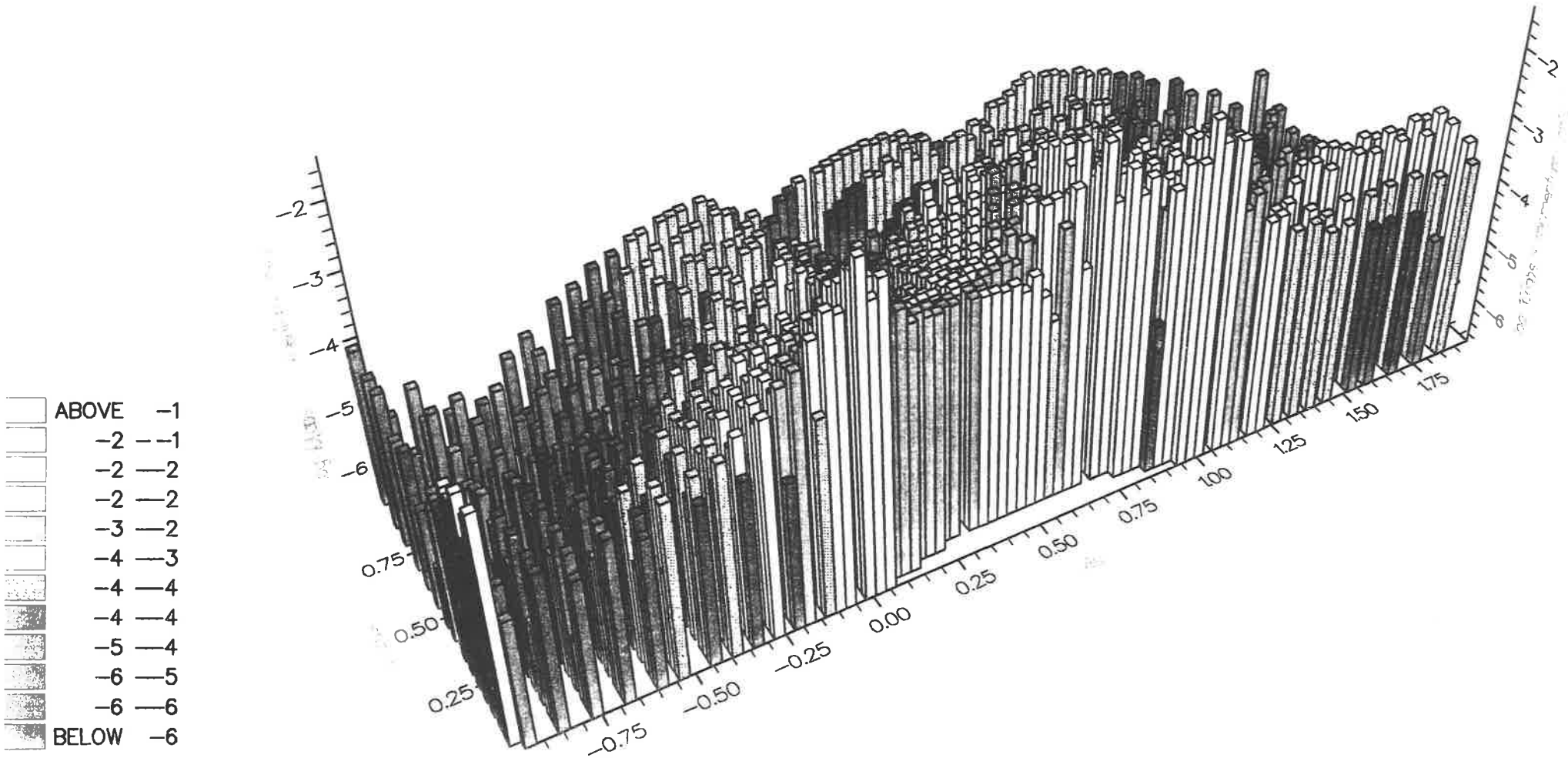

65 X 17,

Shock Captured, log10(abs y momentum residuals)

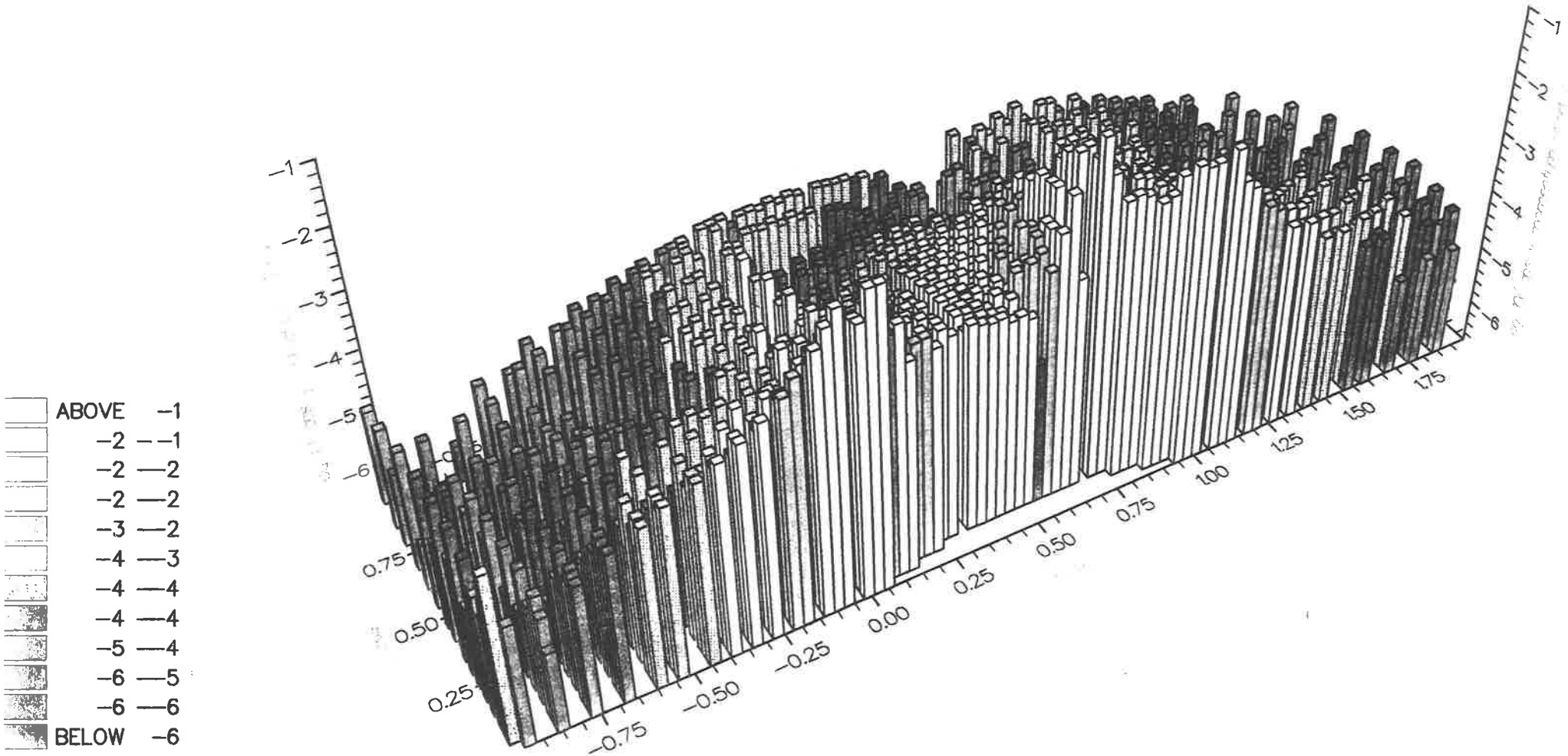

Shock Captured, Density Residuals,129 x 33 Grid.

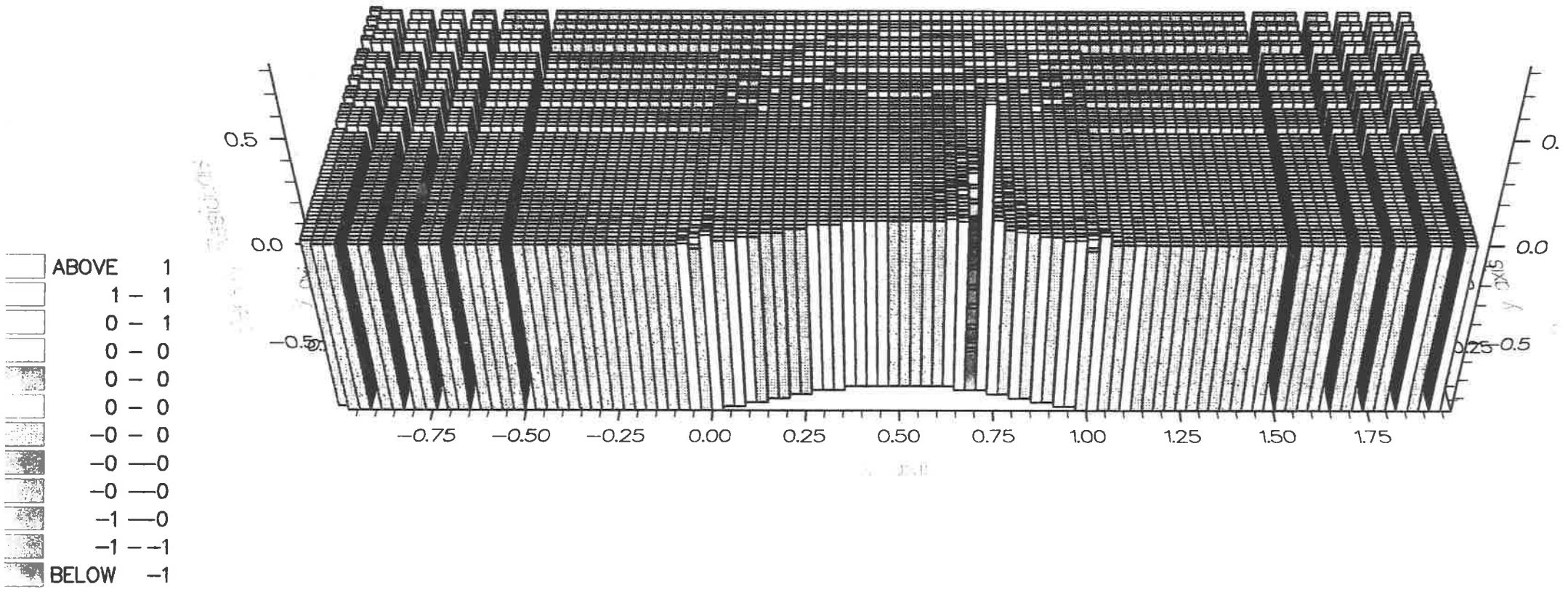

Shock Captured, X Momentum Residuals,129 x 33 Grid

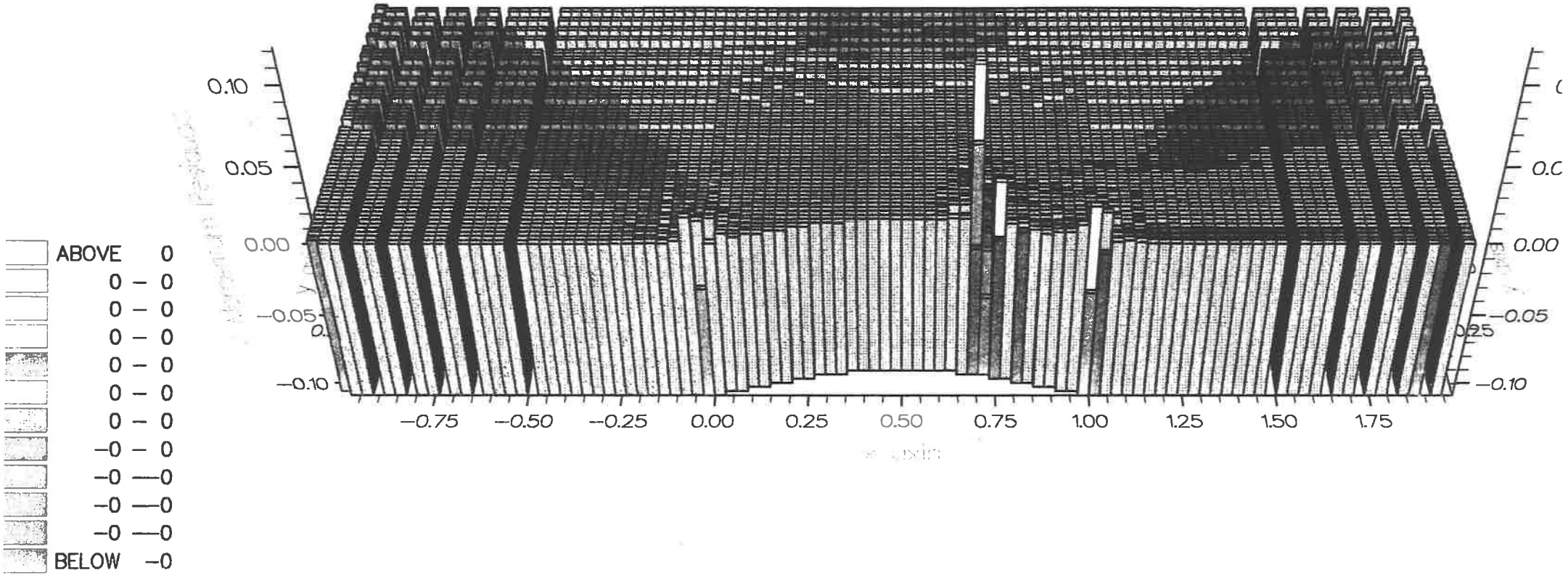

Shock Captured, Y Momentum Residuals,129 x 33 Grid

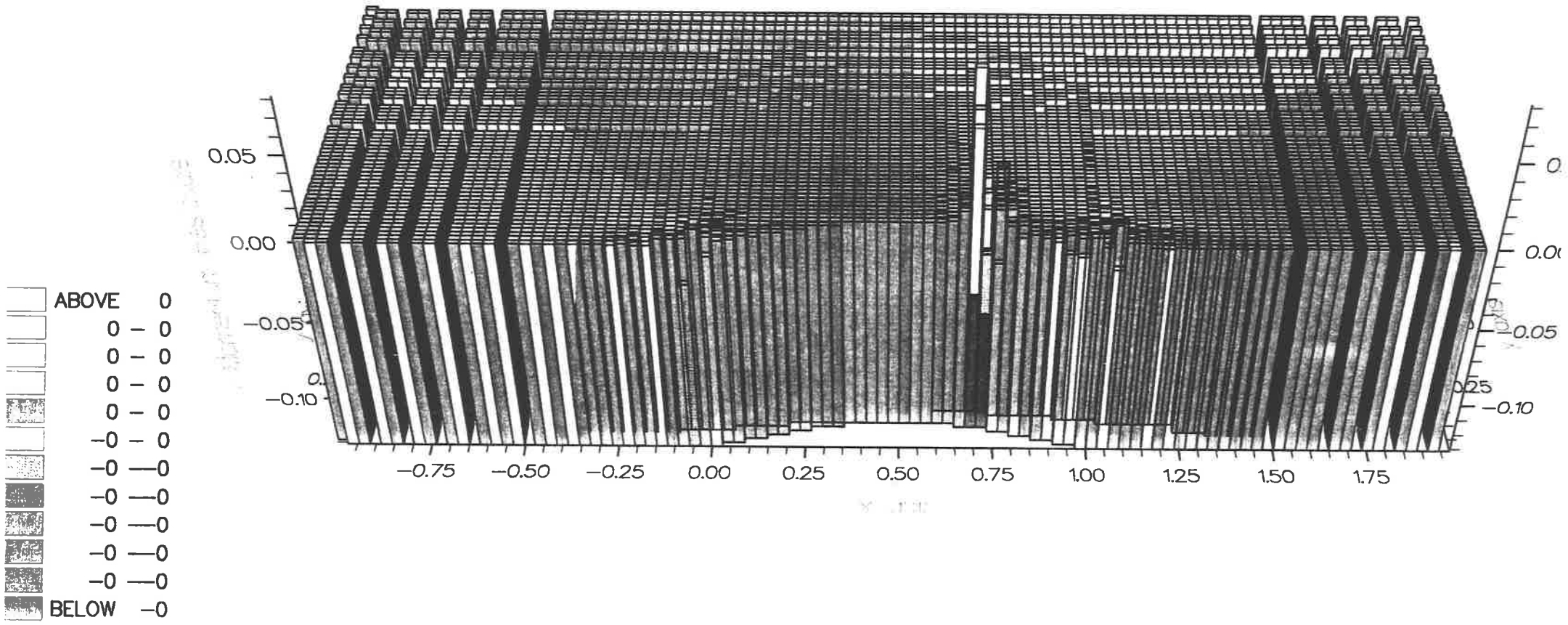

Shock Captured,abs(density Residuals) 129 x 33 Grid.

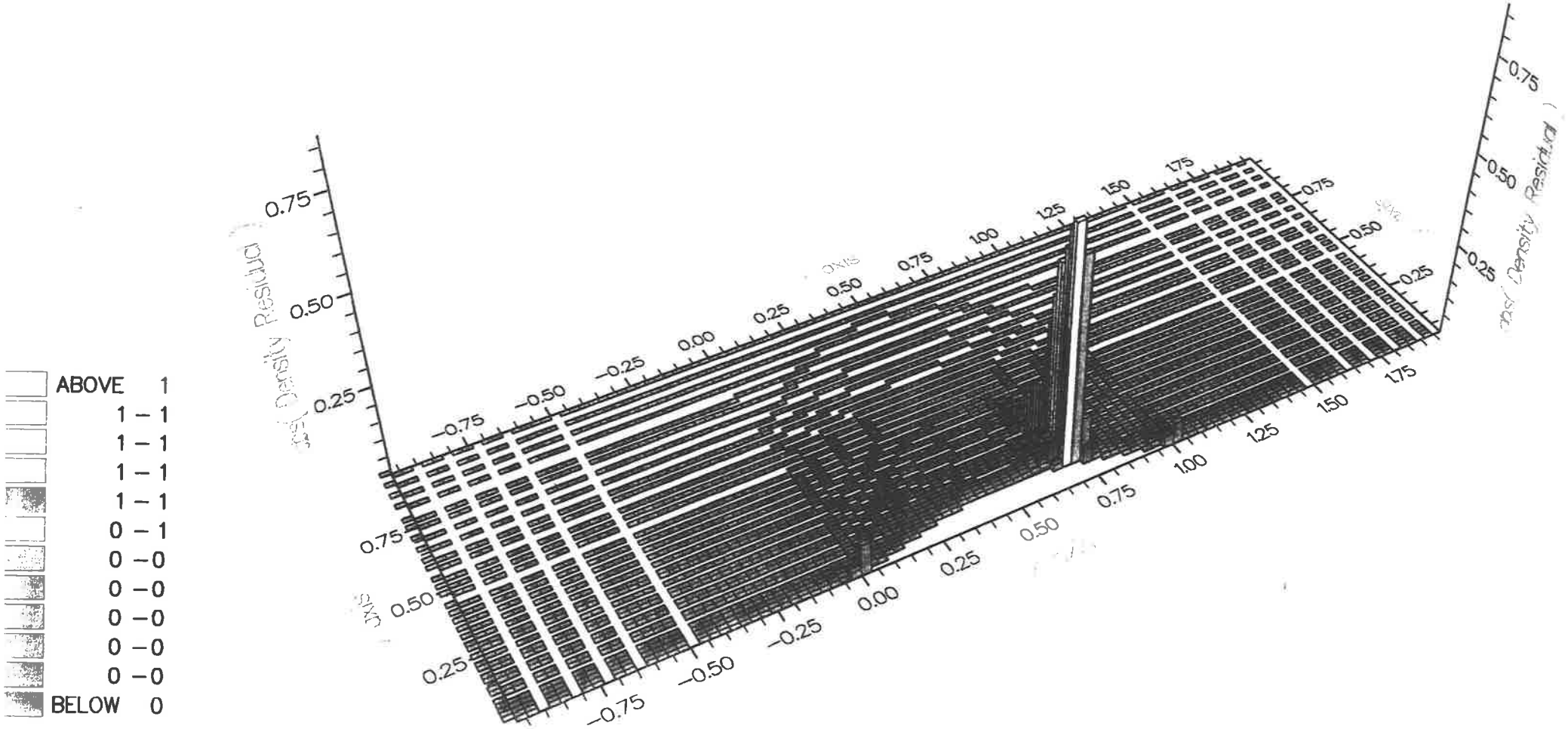

Shock Captured,abs(X Momentum Residuals),129 x 33 (

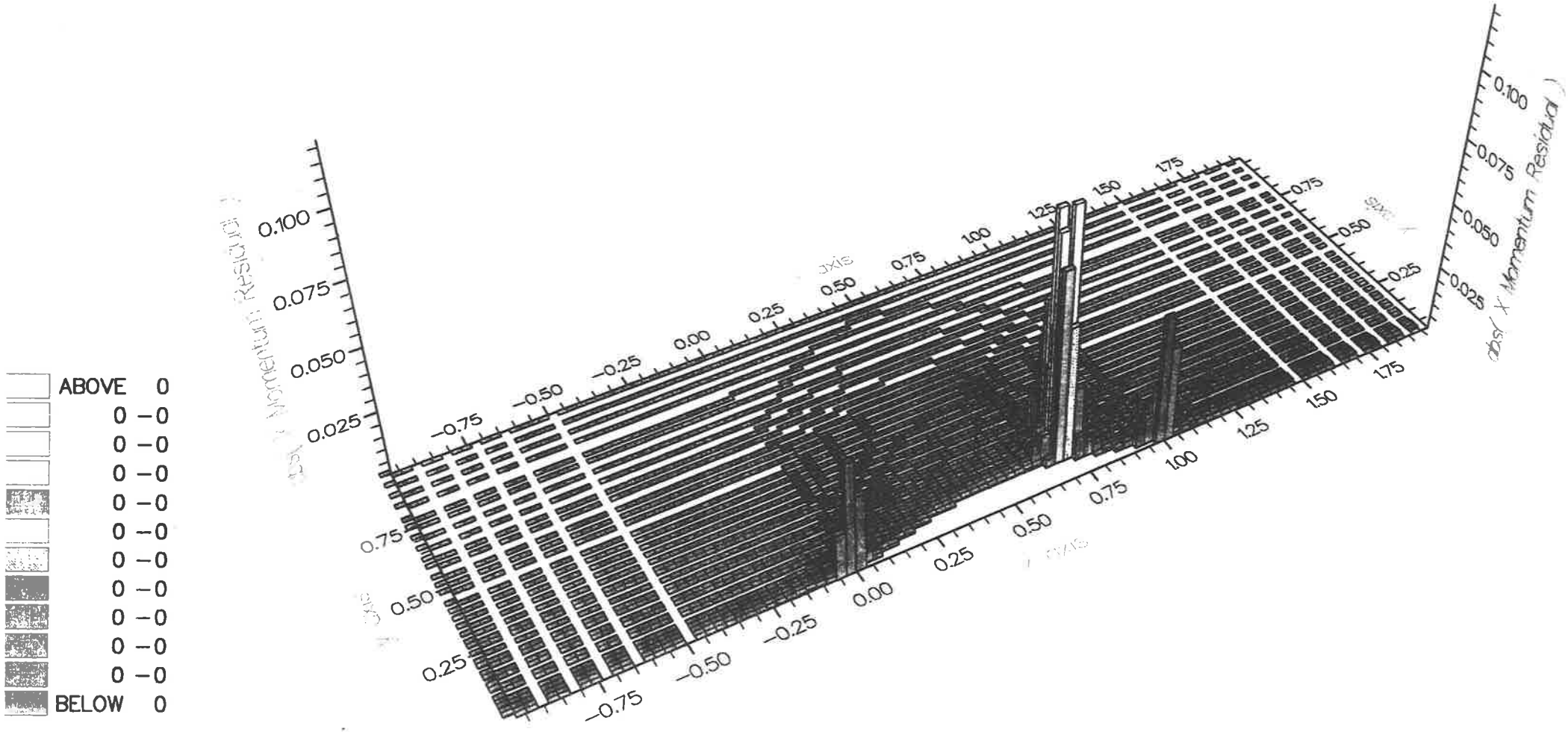

Shock Captured abs(y Momentum Residual) 129 x 33 (

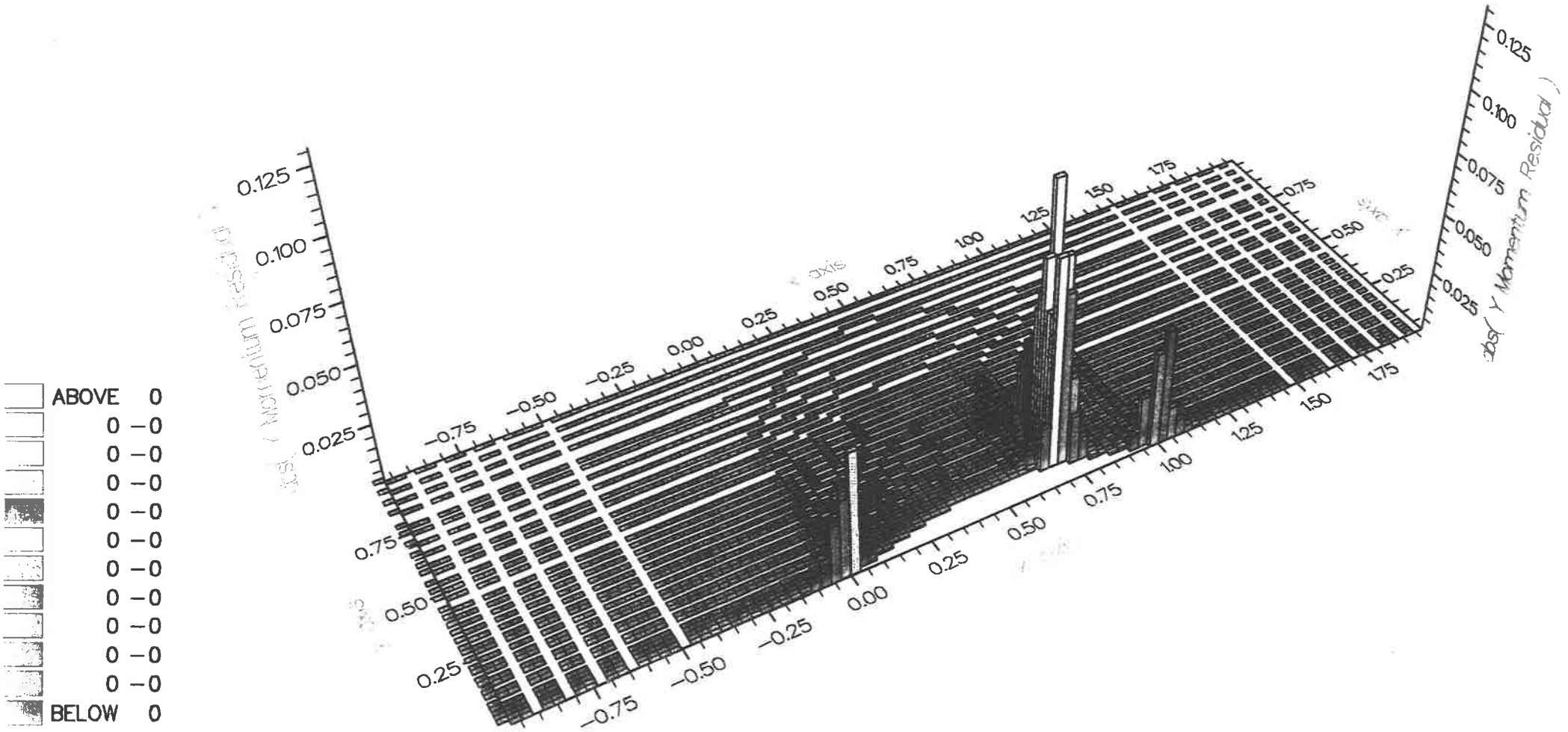

Shock Captured ,log10(abs Density residuals) 129 x 33 G

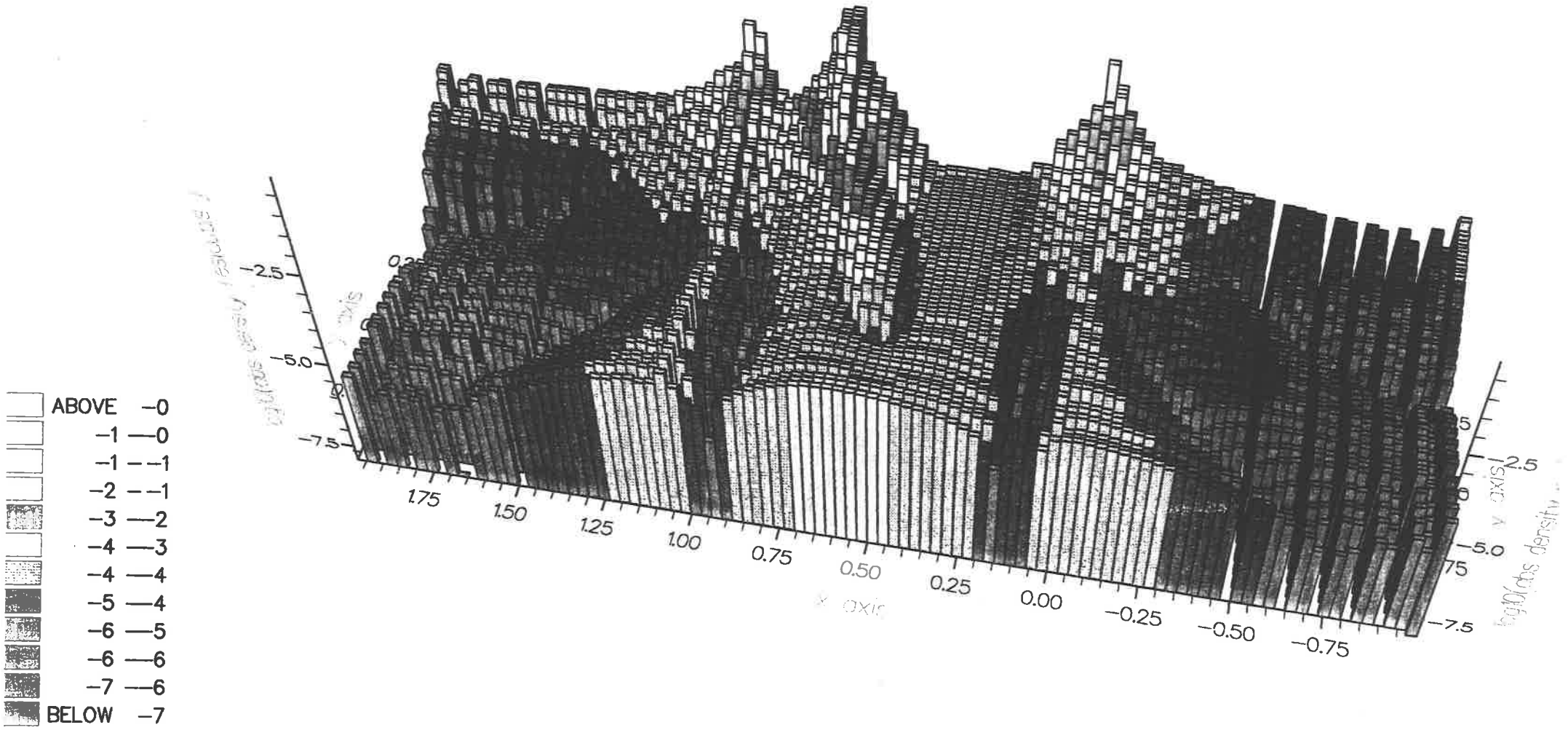

Shock Captured,log10(abs X Momentum Residuals) 129x33

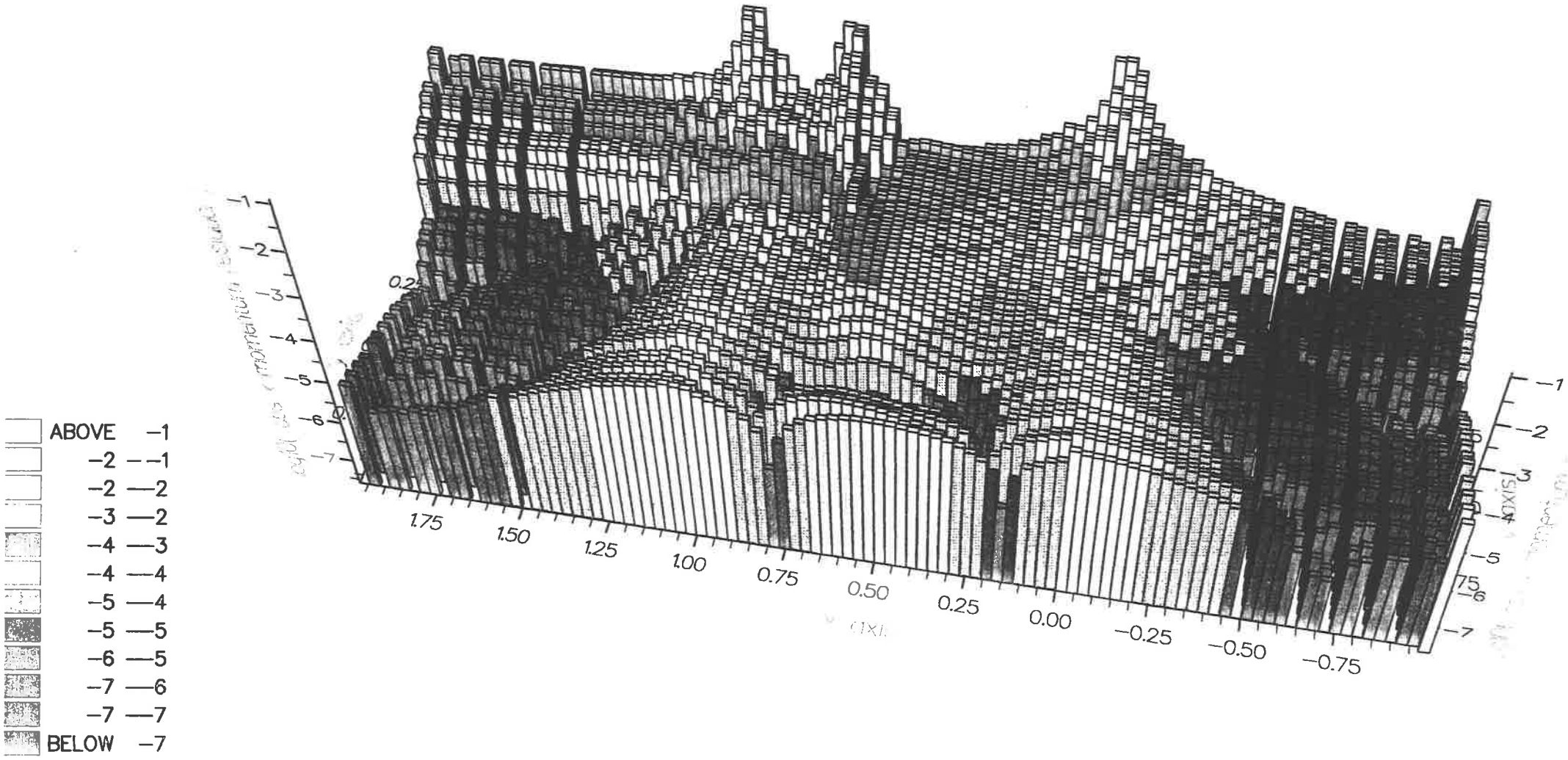

Shock Captured,log10(abs Y Momentum Residuals),129x33

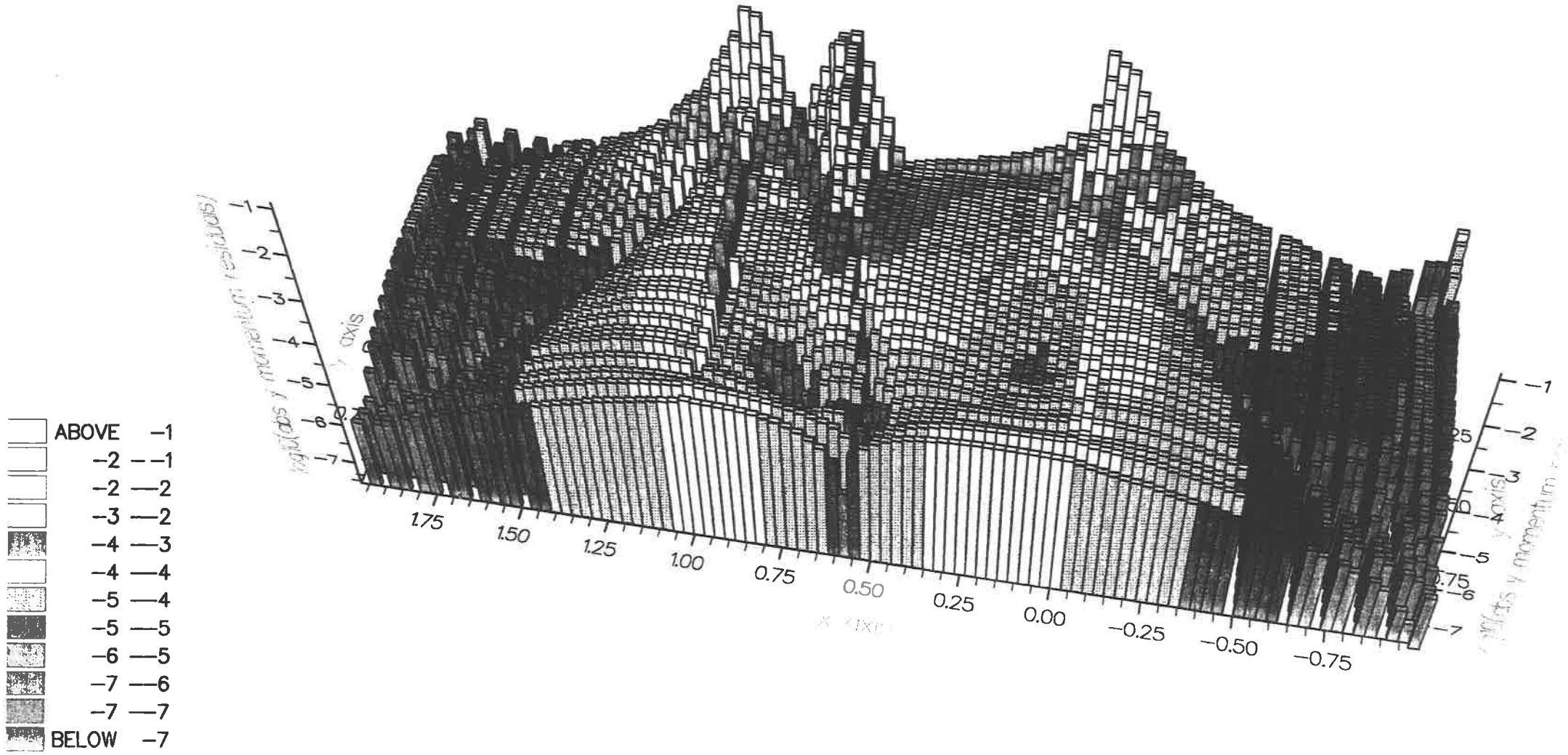

Shock Captured, abs(Density Residual) 257 x 65 Grid.

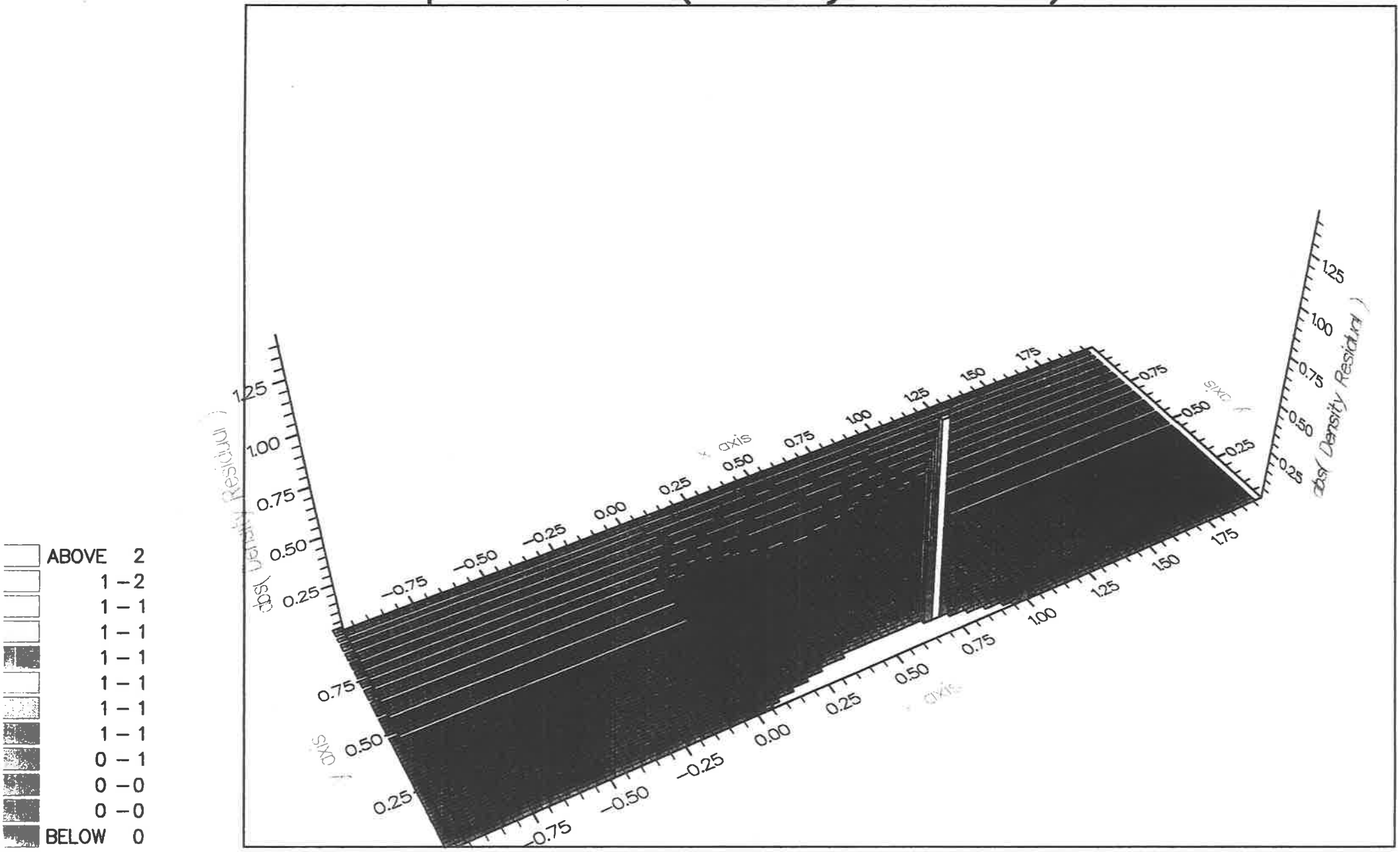

Shock Captured,abs(X Momentum Residual),257 x 65 G

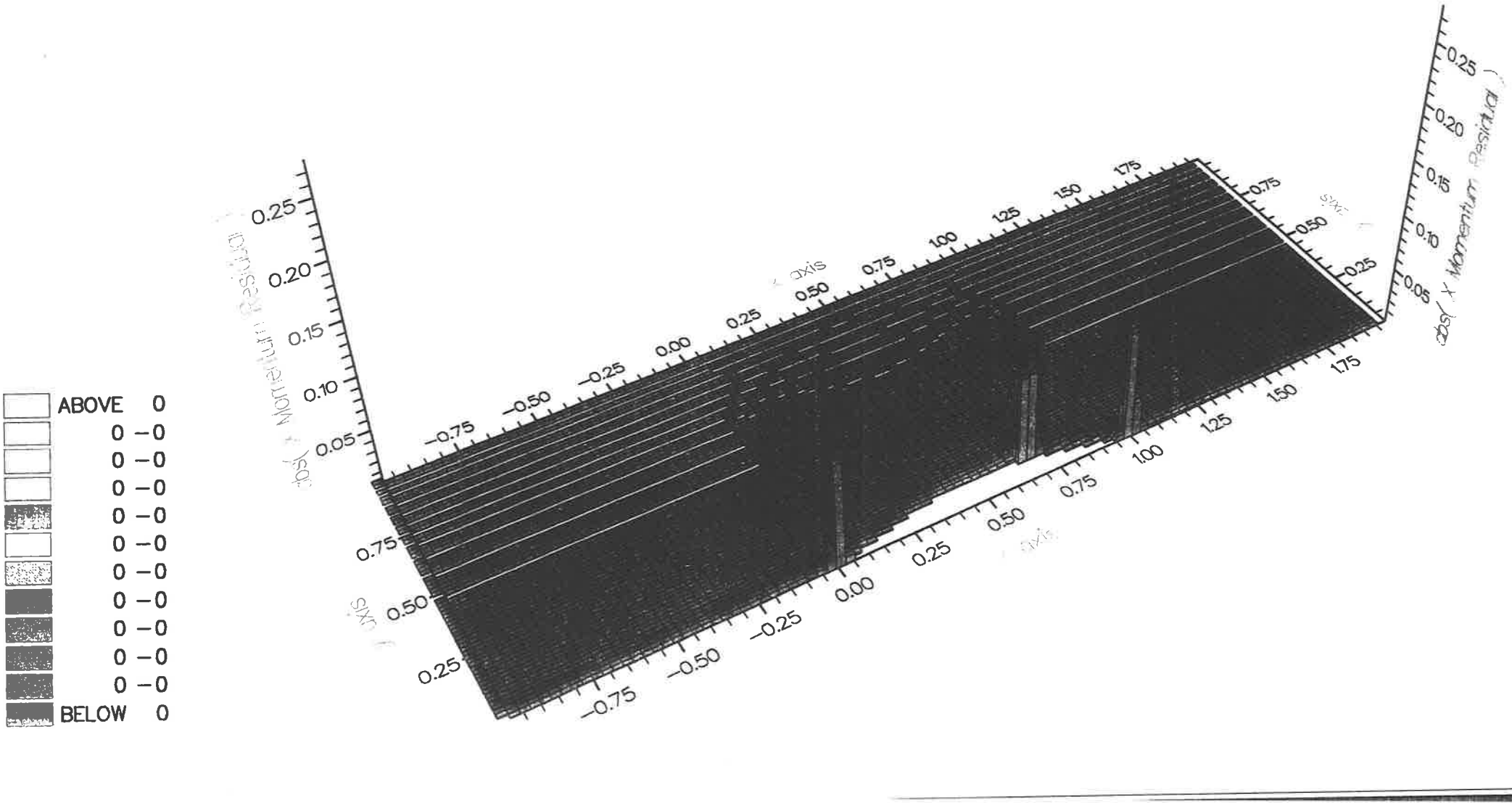

Shock Captured ,abs(Y Momentum Residual),257 x 65 Grid

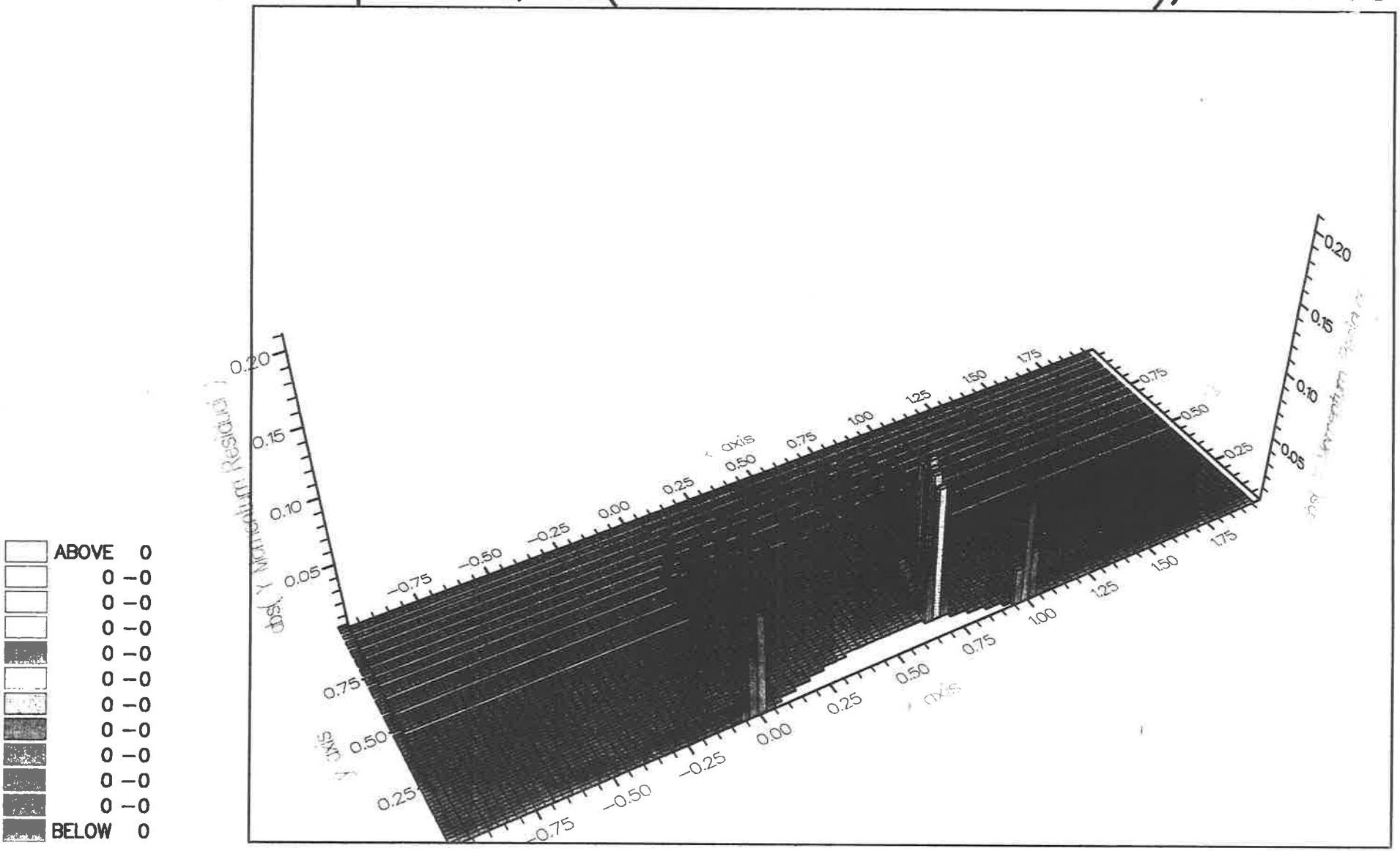

Shock Fitted,Density Residual, 65 x 17 Grid.

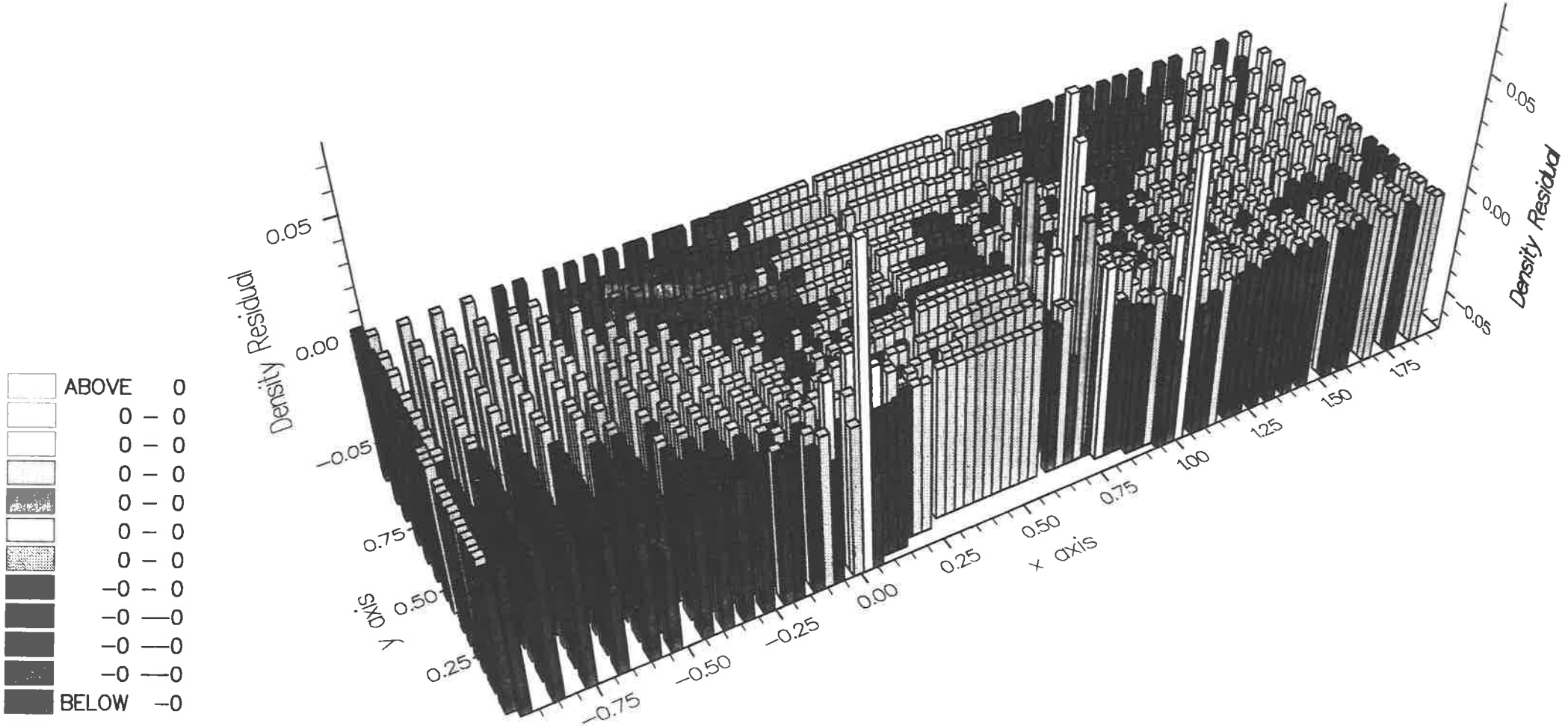

Shock Fitted, X Momentum Residual, 65 x 17 Grid.

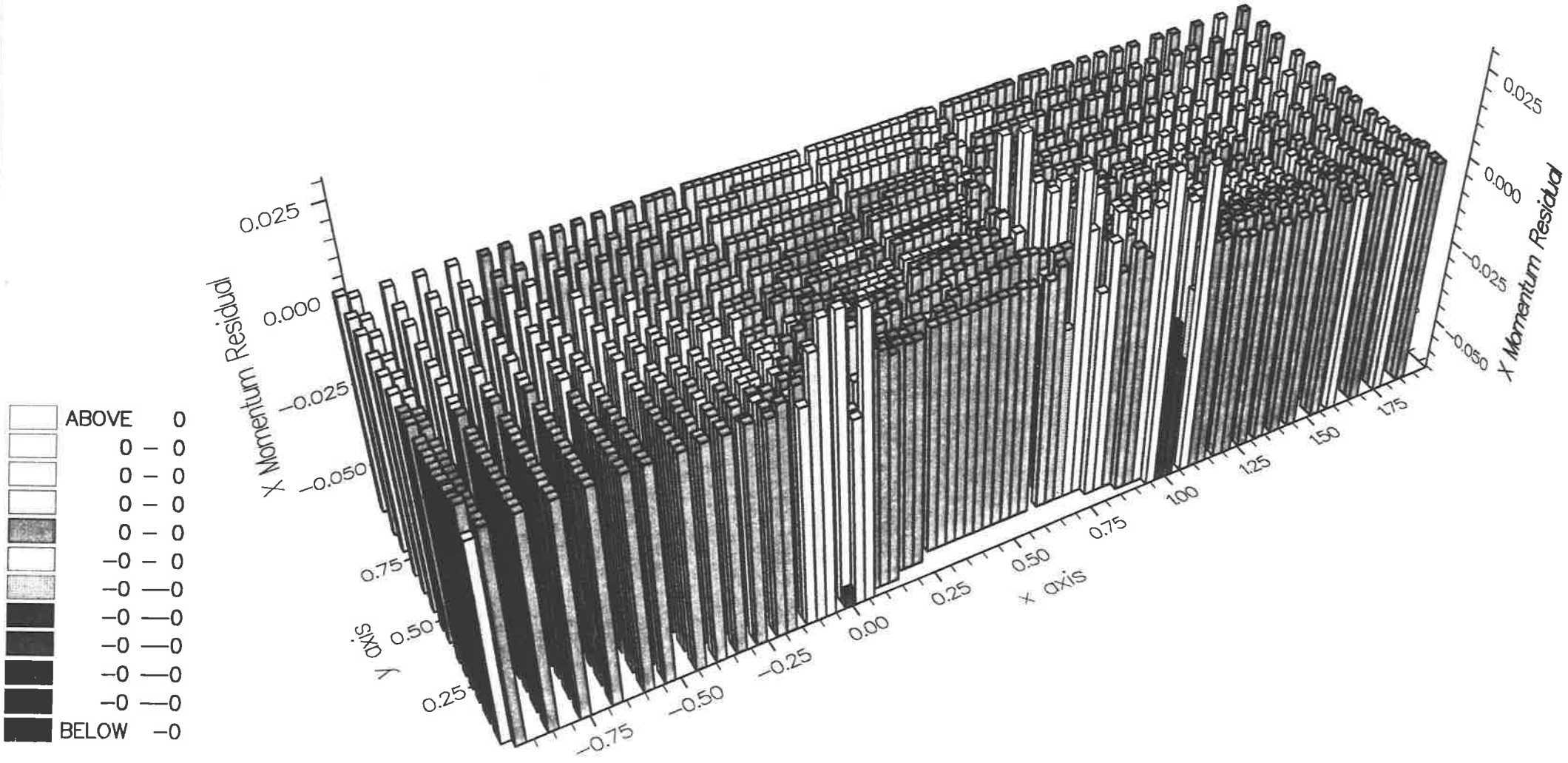

Shock Fitted, Y Momentum Residual, 65 x 17 Grid.

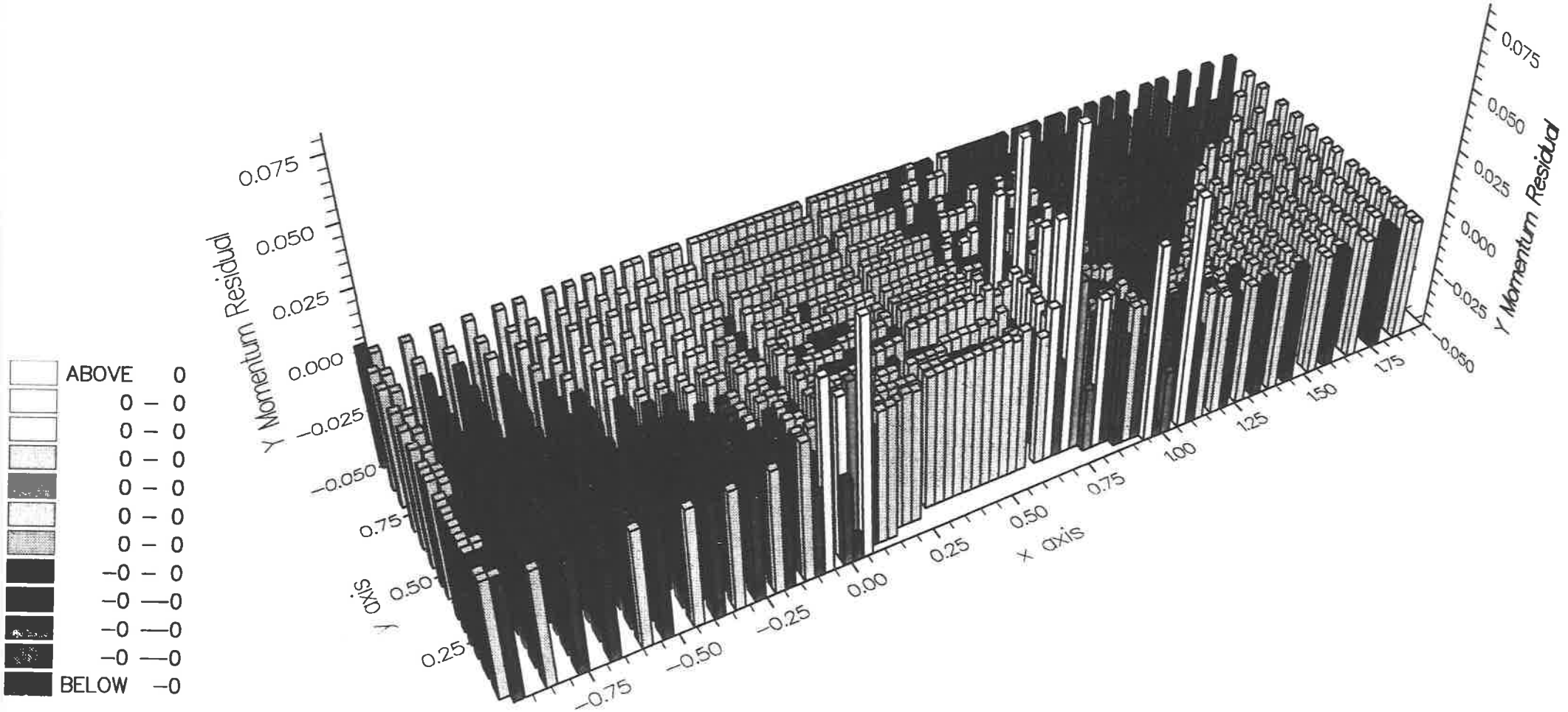

Shock Fitted, abs(Density Residual),65 x 17 Grid.

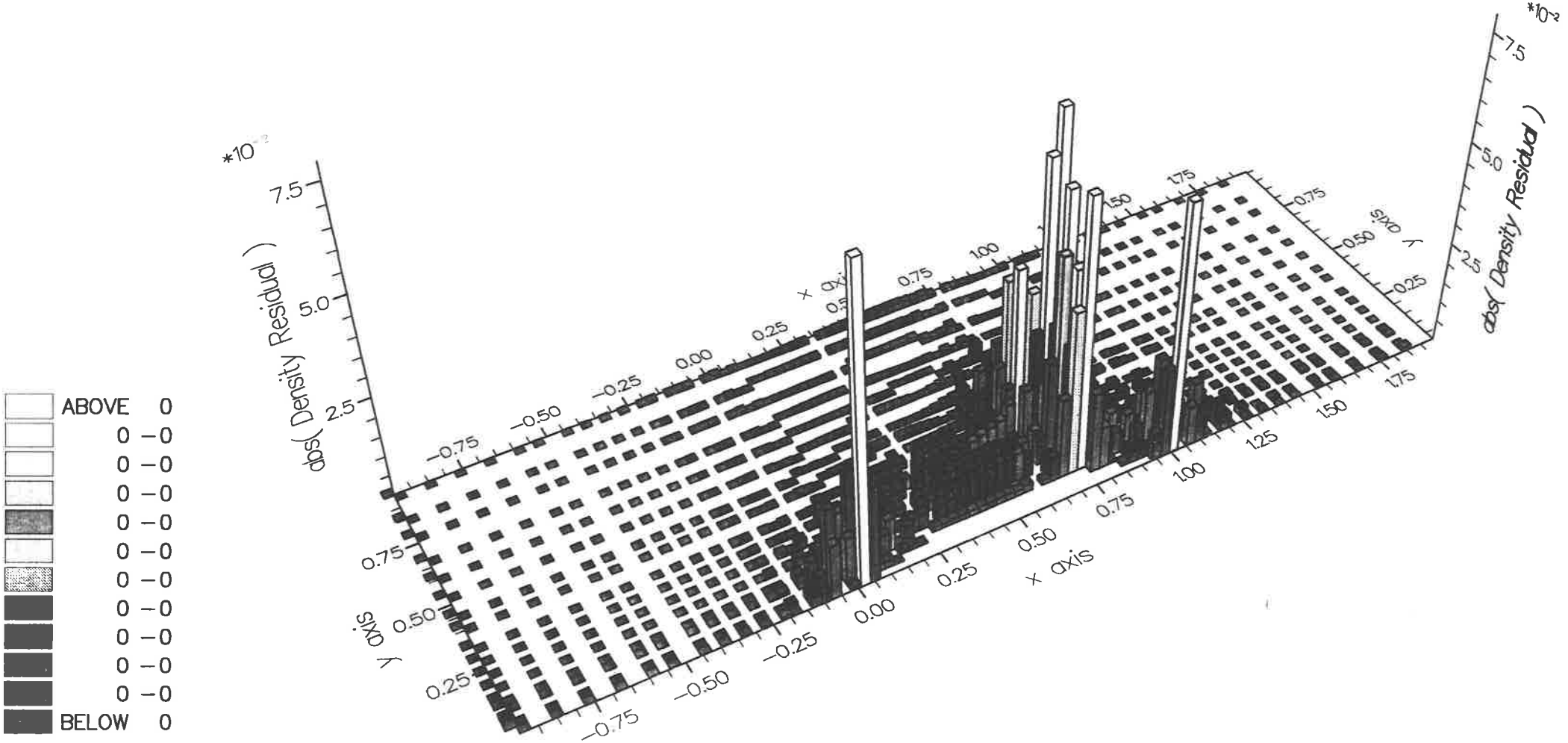

Shock Fitted, abs(X Momentum Residual),65 x 17 Gri

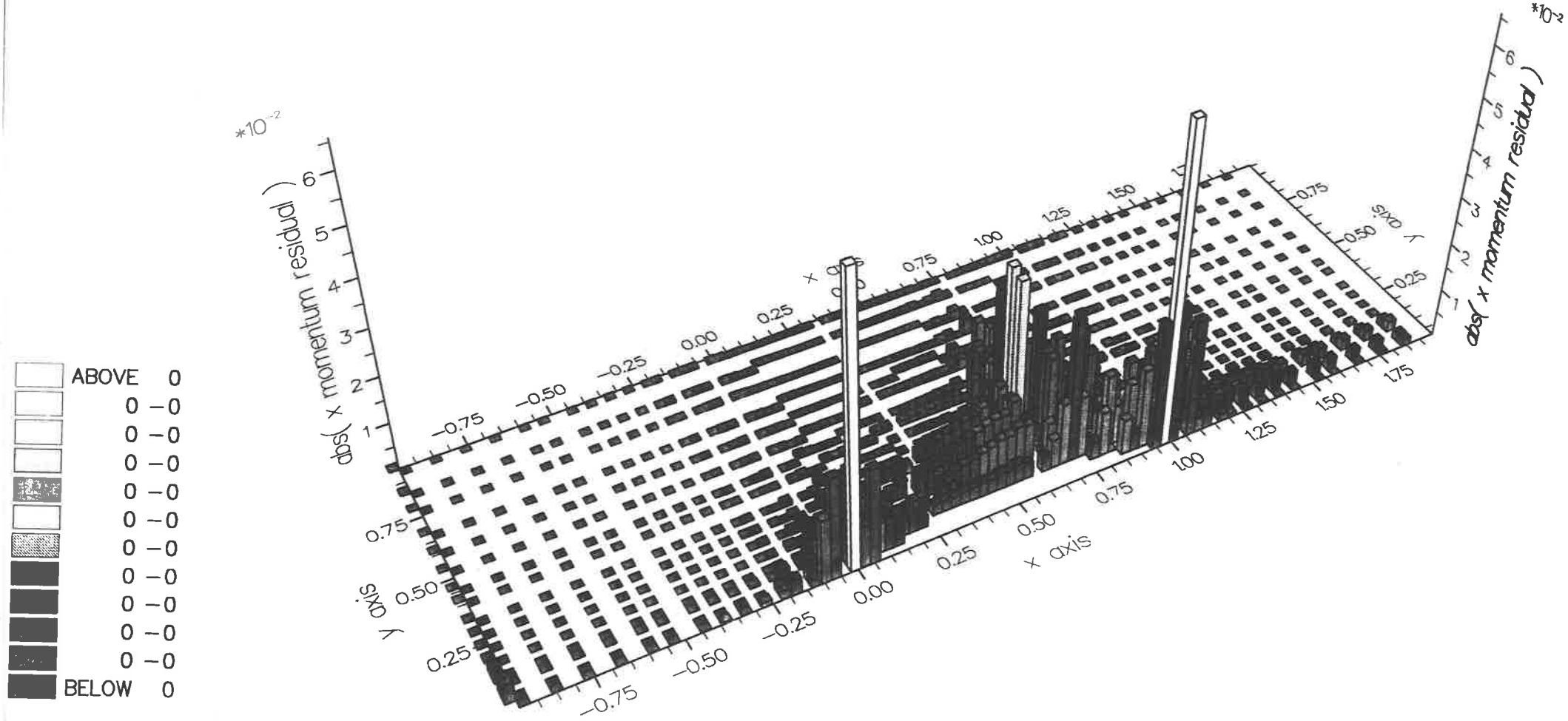

65X17,

Shock Fitted, abs(Y Momentum Residual)

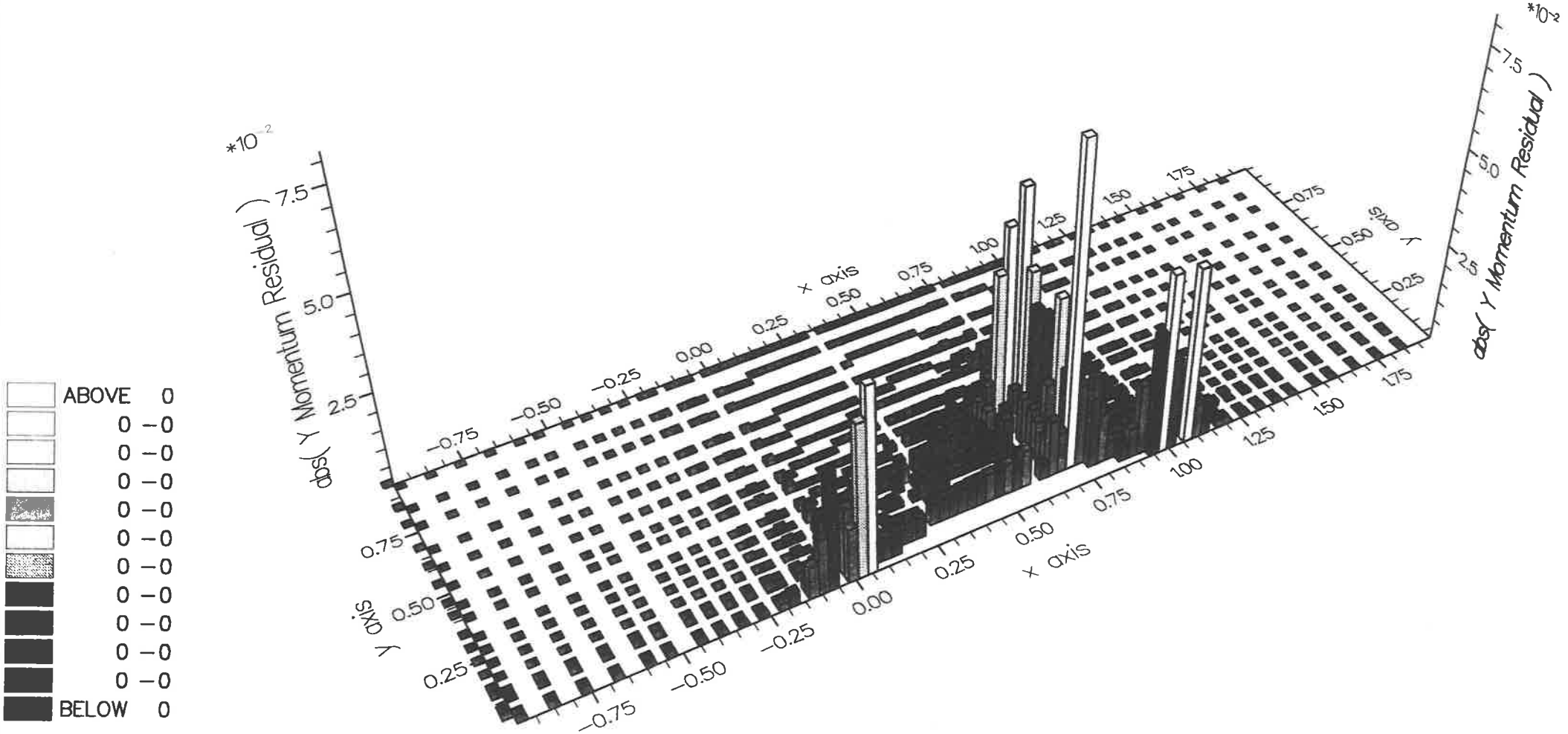

Shock Fitted, log10(abs Density Residual),65 x 17 Gric

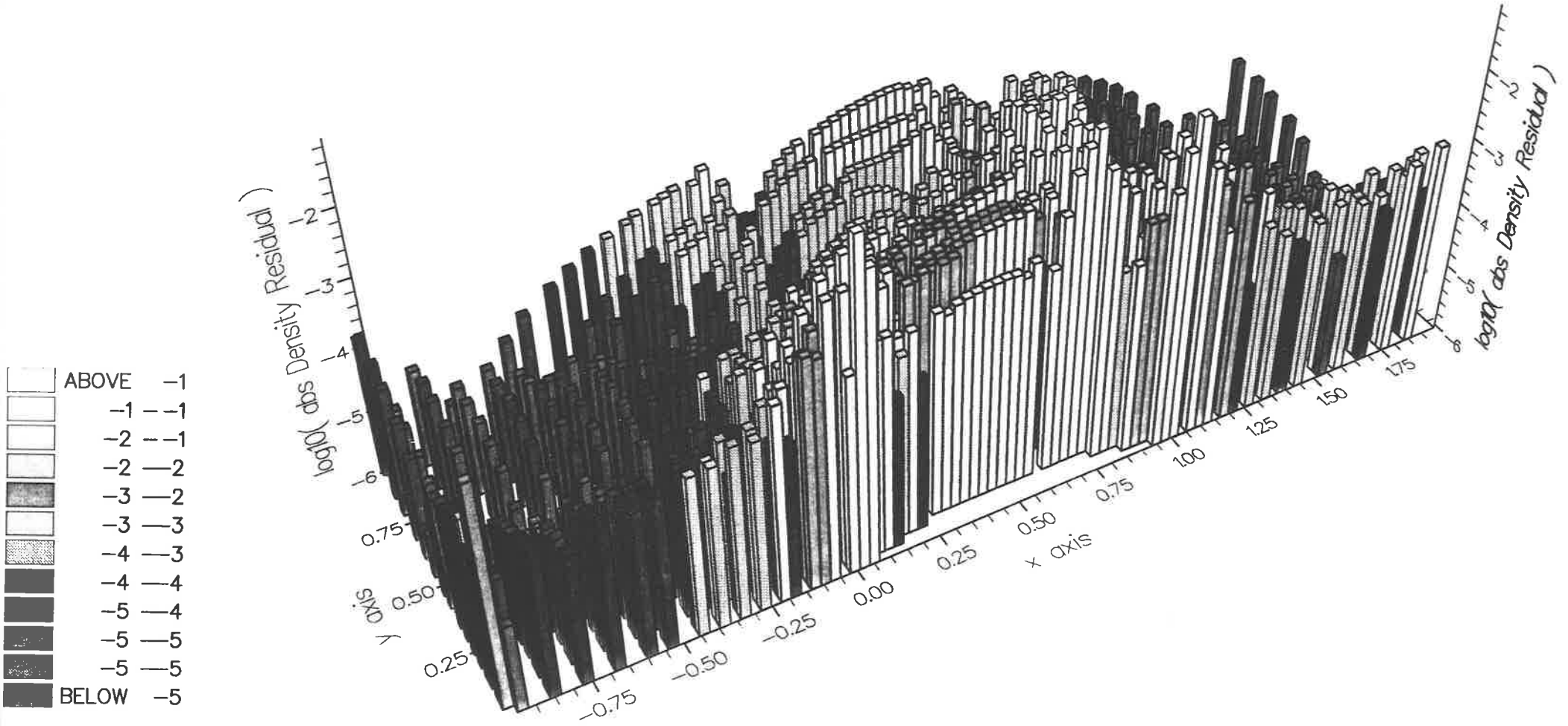

Shock Fitted,log10(abs X Momentum Residual),65 x 17 g

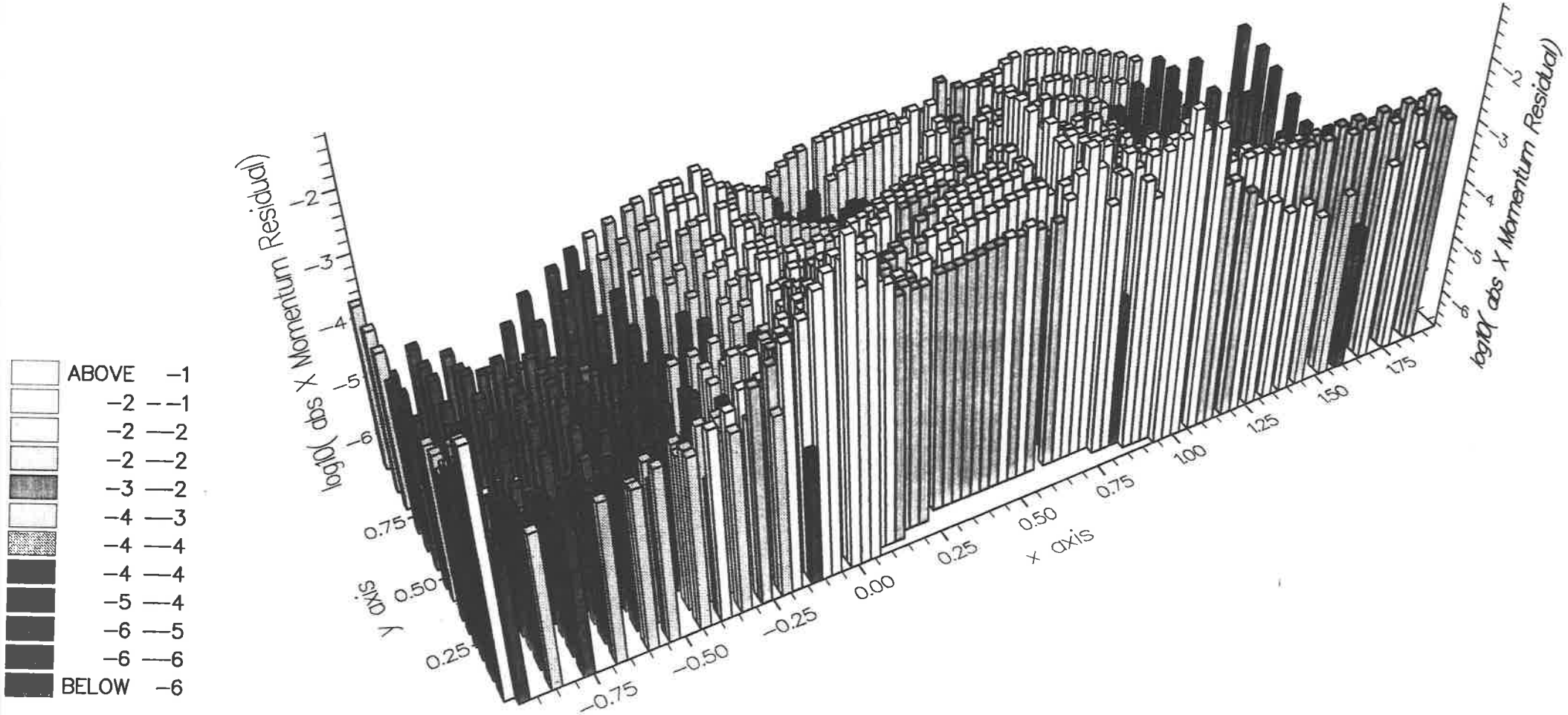

Shock Fitted, log10(abs Y momentum Residual),65 x 17 G

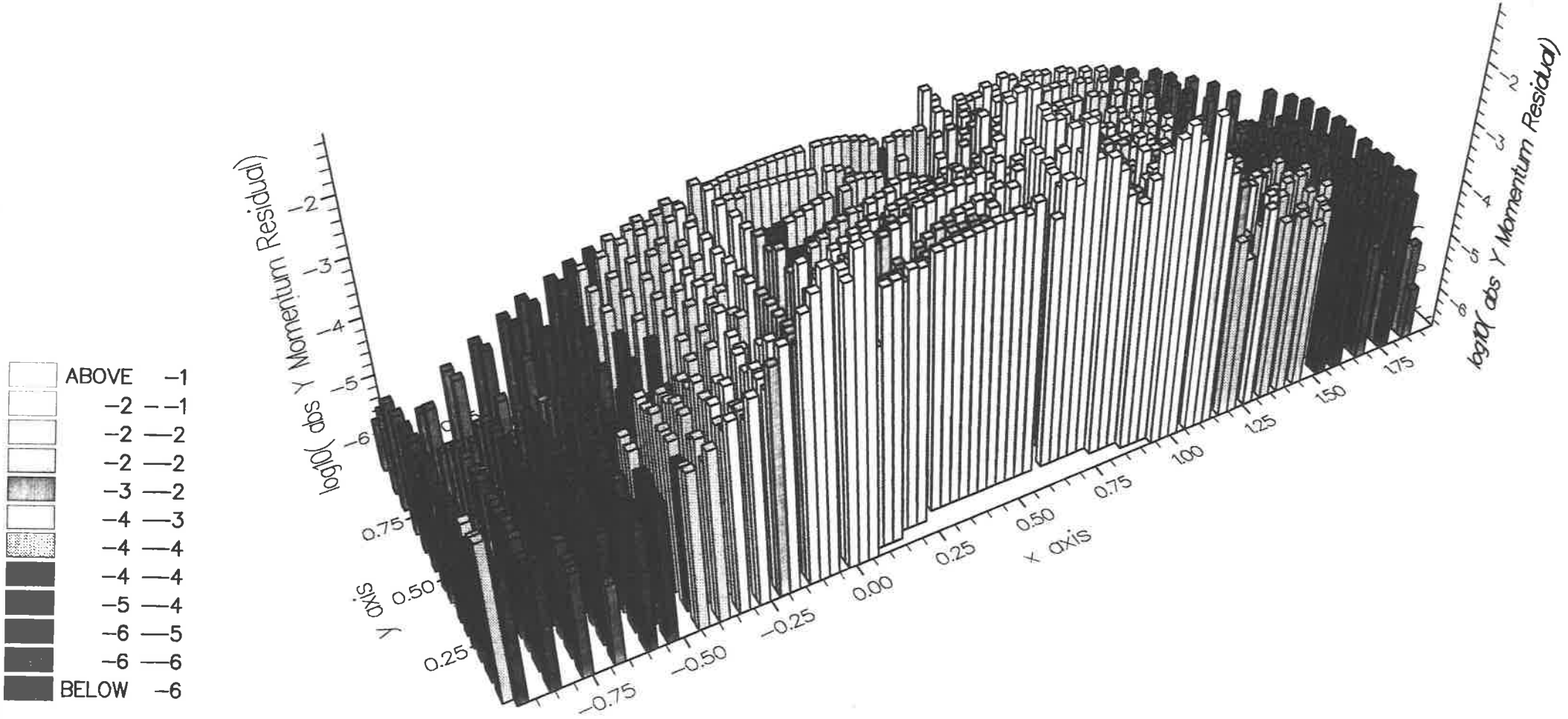

Shock Fitted, Density Residual, 129 x 33 Grid.

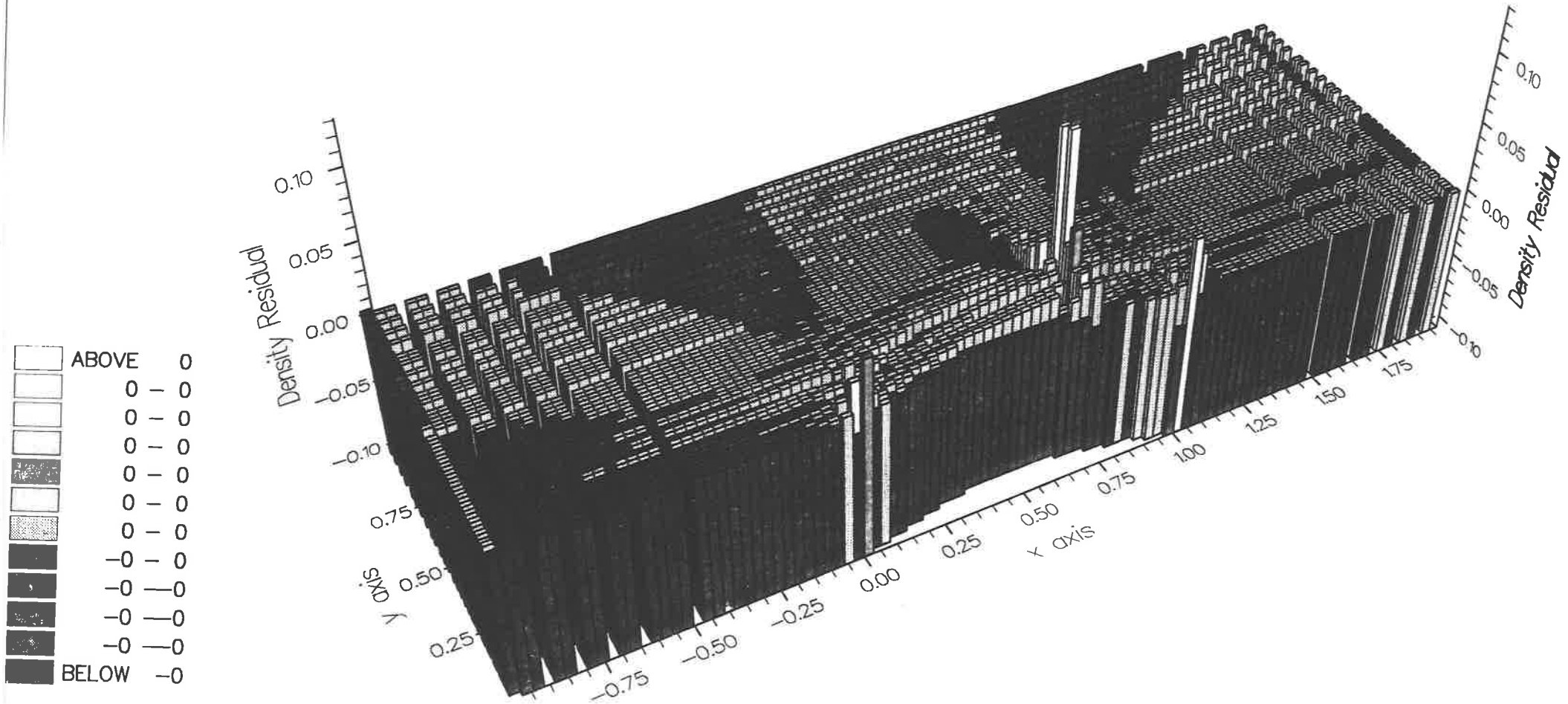

Shock Fitted, X Momentum Residual, 129 x 33 Grid.

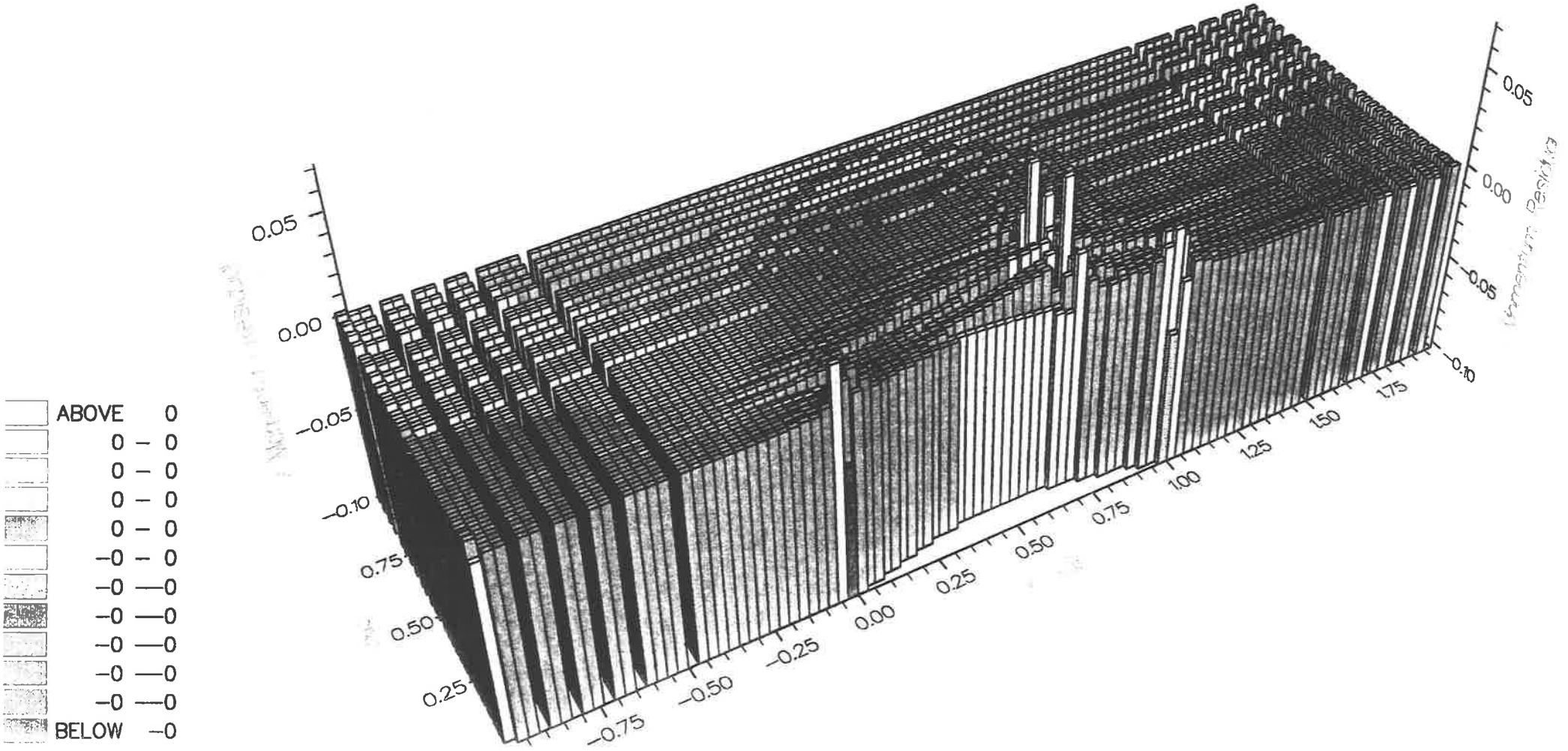

Shock Fitted, Y Momentum Residual, 129 x 33 Grid.

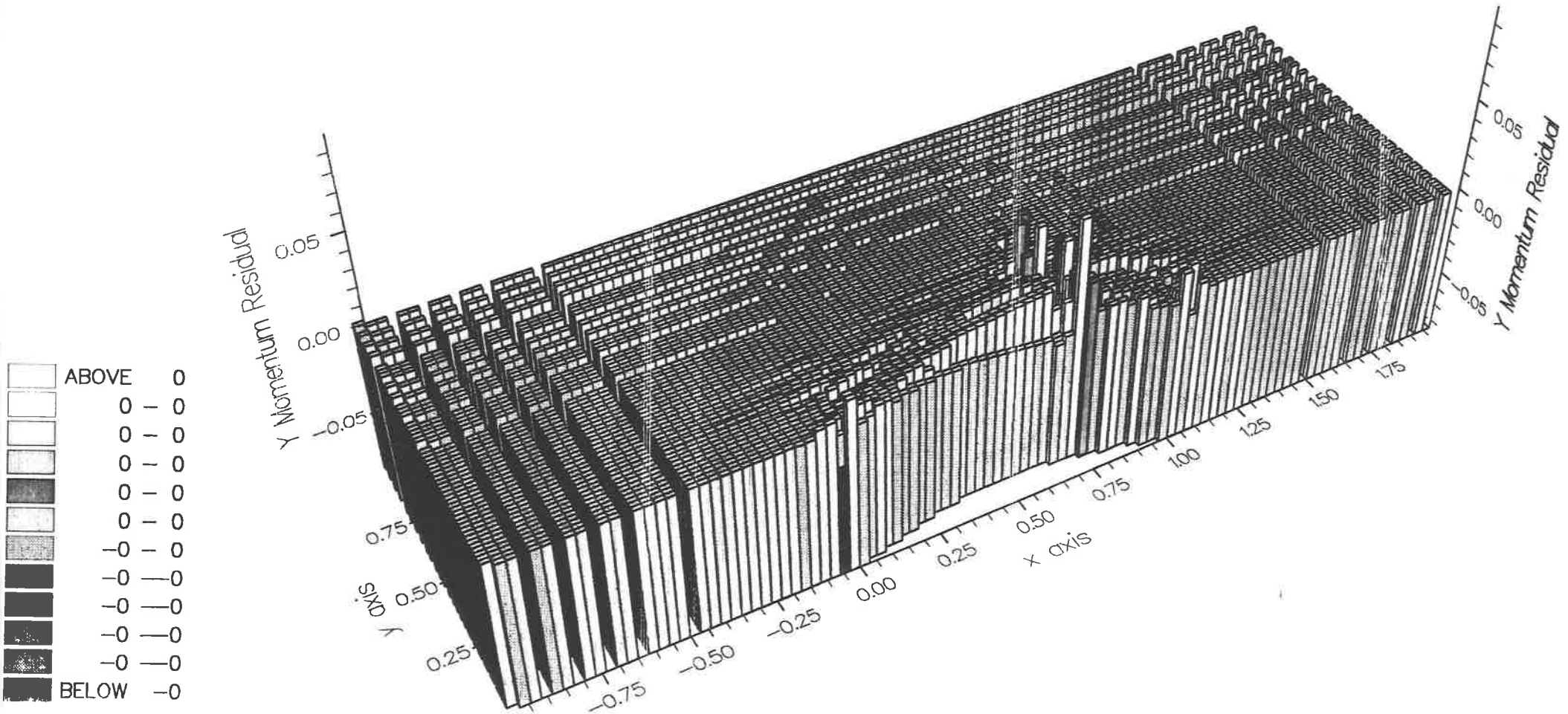

Shock Fitted,abs(Density Residual),129 x 33 Grid.

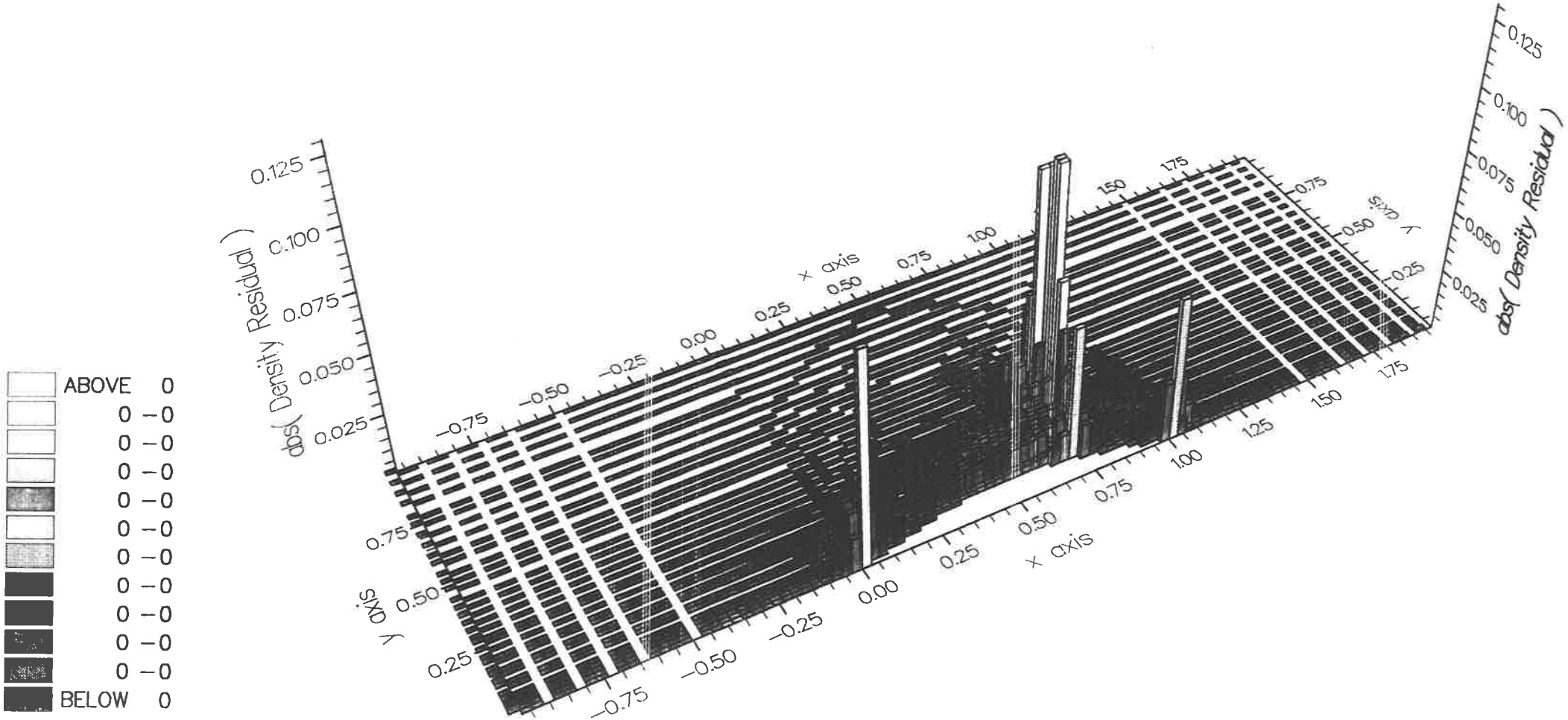

Shock Fitted,abs(X Momentum Residual),129 x 33 Gri

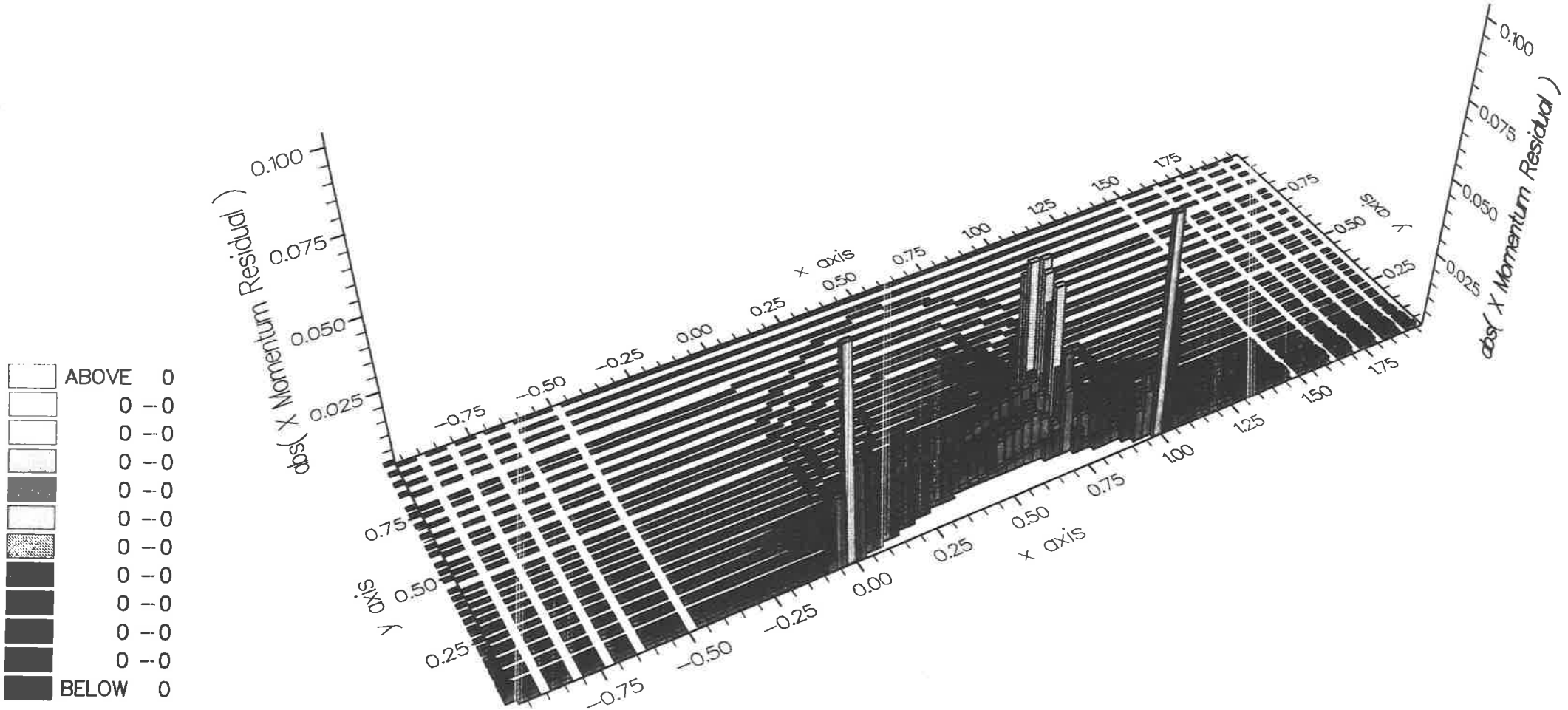

Shock Fitted,abs(Y momentum Residual),129 x 33 Gri

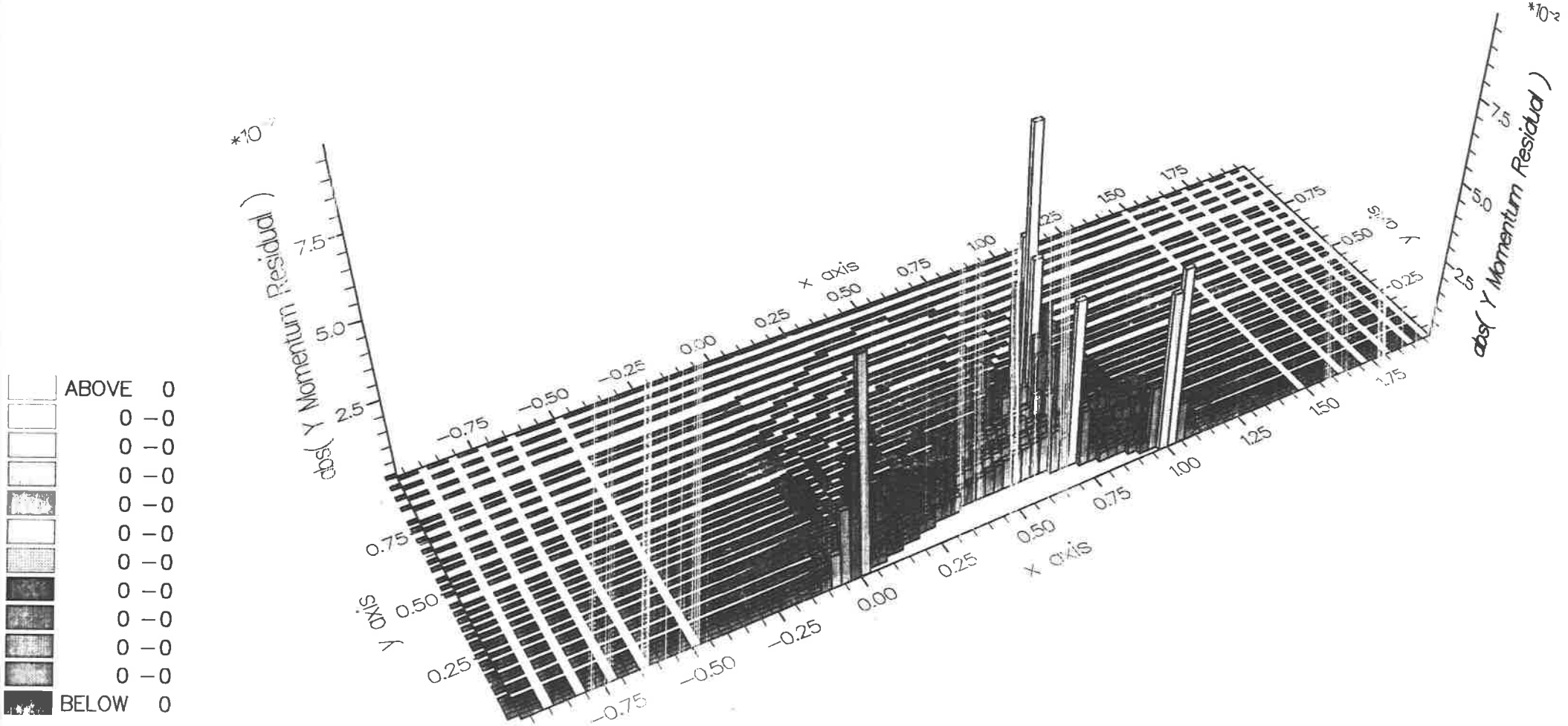

Shock Fitted,log10(abs Density Residual),129 x 33 Grid